Republic of Iraq
Ministry of Higher Education and Scientific Research
University of Kerbala-College of Science
Chemistry Department

Preparation and Characterization of ZnS/Doped ZnS Nanoparticles for Dyes Photodegradation

A thesis
Submitted to the Council of the College of Science/ University of Kerbala as a Partial Fulfillment of the Requirements for The Degree of Master of Science in Chemistry

By

Bedour Ali Mohammed AL-Samawi

B.Sc of Kerbala University / 2005

Supervisor

Asst.prof.Dr. Luma Majeed Ahmed

2018AD   *1439AH*

Dedication

To my mother…

To my family who make my dreams possible

To my husband, who supported me
along the way

To my friends…

Who helped me all the time

Bedour Ali / 2018

Acknowledge

First of all, I want to thank the almighty Allah who enabled me   the power during this work in particular.

I would like to extend my deep thanks, gratitude, and appreciation to my superisor Asst*. **Prof. Dr. Luma Majeed Ahmed** for their continuous support and invaluable suggestions and great contributions since the very beginning of this work.

Also, I want to thank all faculty members of department of chemistry in college of science in university of kerbala, for their worthless support of the work.

Finally, I want to thank my family and friend for their continual support throughout this journey. They were my source of encouragement along the way.

Bedour

<center>**Supervisor Certification**</center>

I certify that this thesis**(Preparation and Characterization of ZnS/Doped ZnS Nanoparticles for Dyes Photodegradation)** was conducted under my supervision at the Department of chemistry , College of science, University of kerbala , as apartial fulfillment of the requirements for the degree of Master in chemistry.

Signature:

Name: Asst.Prof .Dr .Luma Majeed Ahmed

Address:Kerbala University / College of science /Department of chemistry

<center>**Date: / / 2018**</center>

Report of the head of Chemistry Department

Chairman of Postgraduates Studies Committee

According to the recommendation presented by the chairman of the postgraduate studies committee, I forward this thesis**(Preparation and Characterization of ZnS/Doped ZnS Nanoparticles for Dyes Photodegradation)** for discussion   .

.

Sigature:

Head of Chemistry Dept : Asst. Prof. Dr. Haitham Dalol A- Shably

Address:Kerbala University / College of science /Department of chemistry

Date: /   / 2018

Committee Certification

We are the examination committee, certify that we have read the thesis entitled **(Preparation and Characterization of ZnS/Doped ZnS Nanoparticles for Dyes Photodegradation)** and examined the student **(Bedour Ali Mohammed)** in its content and that in our opinion it is adequate as a thesis for the degree of master of science in chemistry.

(Chairman)

Signature:

Assistant Professor Dr.Abdulkareem

Alsammarraie

(Member)   **(Member)**

Signature: Signature:

Assistant Professor Dr. Muhsen   Assistant Professor Dr.Hayder

Abood Muhsen Al-ibadi   Hamid Al-Hmedawi

Date: / / 2018   Date: / /2018

(Member and Supervisor)

Signature:

Assistant Prefessor Dr. Luma Majeed Ahmed

Kerbala University College of science

Department of Chemistry

Date: / /2018

Approved by the College Committee of Graduate Studies

Signature:

Professor

Dr. Amir Abd AL-Ameer Mohammed Ali

(Dean of College)

Report of Linguistic Evaluator

I certify that the linguistic evaluator of this thesis **(Preparation and Characterization of ZnS/Doped ZnS Nanoparticles for Dyes Photodegradation)** was carried out by me and it is linguistically sound.

Signature:

Name: Asst.Prof. Dr.Tafeeq Majeed

Address: Department of English /College of Education / University of Kerbala

Date: /   / 2018

Report of Scientific Evaluator

I certify that the Scientific evaluator of this thesis**(Preparation and Characterization of ZnS/Doped ZnS Nanoparticles for Dyes Photodegradation)** was carried out by me and it is accepted scientifically.

Signature:

Name: Asst.Prof. Dr.Abbas Jassim Attieh

Address: Babylon University / College of science /Department of chemistry

Date: /   / 2018

Abstract

In this work, the practical part consists of three parts, the **first part** deals with the preparation of ZnS as nanopowder and then loaded metals (Cr & Mn) on this surface by using co-precipitation method.

The **second part** is concerned with investigated the characteristics of prepared samples and a commercial ZnS. The atomic absorption analysis was used to estimate if the used metals loaded or not loaded on prepared ZnS. XRD data were useful to calculate the mean crystal size by Scherer equation. The mean crystal sizes for all samples are sequence:

Commercial ZnS > prepared ZnS > Mn:ZnS:Cr$_{(1)}$ > Mn:ZnS:Cr$_{(2)}$ > Cr:ZnS> Mn:ZnS.

The AFM images indicated that the shapes for all samples are semispherical and the no.of particles sizes for them contain (2.5-6) crystals. The fluorescence technique was employed to measure the Bg for all samples. The Bg values for most samples decreases with increasing the mean crystal sizes and the ranges of Bg for all studied were ranged (3.260-3.577) eV.

The **third part** focused on studying the effect of different parameters on photodecolorization of RB5 dye from aqueous solution on studied photocatalyst samples. The parameters include: type of metals, mass of catalyst, initial of pH of solution, temperature and oxidation agent ($K_2S_2O_8$).

The best metallization on prepared ZnS are produced for Cr: ZnS, Mn: ZnS: Cr $_{(2),}$ hence, in this work these samples were studied and compared with prepared ZnS. The optimum dose of studied photo-catalysts such as commercial ZnS, prepared ZnS, prepared Cr:ZnS and prepared Mn:ZnS:Cr$_{(2)}$, that found equal to 2.5g, 1g, 1g, and 1.5 g respectively . The effect of initial pH is played a vital role to improve the photoreaction, and the maximum rates of reaction for commercial ZnS, prepared ZnS, prepared Cr:ZnS and prepared Mn:ZnS:Cr $_{(2)}$ was 4.1, 6.3, 4.1, and 6.3 respectively.

The effect of temperature was investigated at temperature range (283.15-303.15) K. The results were indicated that the activation energies for all studied samples are ranged (13.420-42.35) kJ mol^{-1}. Moreover, the thermodynamics parameter such as $\Delta H^{\#}$, $\Delta S^{\#}$ and $\Delta G^{\#}$ for all studied samples were calculated and found that the photoreaction is exothermic with using commercial ZnS, and prepared Cr: ZnS as photocatalyst. But the photoreaction is endothermic with using prepared ZnS and Mn:ZnS:Cr$_{(2)}$ as photocatalysts.

The oxidation agent such as $K_2S_2O_8$ is very important to raise the rate of reaction and to decrease the illumination times, hence, the optimum concentration of $K_2S_2O_8$ is ranged (7-8) mmoles/L with using all the studied samples

Content	page
Acknowledgement	
Abstract	I-II
Contents	III-V
List of tables	VI-VIII
List of figures and schemes	IX-XIII
List of abbreviations and symbols	XVI - XV

List of abbreviations and symbols	The Meaning
Δk	The total wavevector of the electrons in filled band is zero
AFM	Atomic Force Microscopy
AOPs	Advanced Oxidation Processes
CB	Conduction Band
C_o	Initial Concentration
C_t	Concentration of substrate at time t of irradiation.
VB	Valance Band
CWAO	Catalytic wet air oxidation
e^-	Negative Electron
E_{fermi}	Fermi Energy
E_a	Activation Energy
E_g	band gap energy
E^o	Standard potential energy
eV	Electron Volt
E_{vacum}	Potential energy at vacuum
Evs NHE	Normal hydrogen electrod
FCC	Face –Centered Cubic
FWHM	Full width half –maximum
G	Gram
h^+	Positive Hole
H^+	Hydronium ion
Hcp	Hexagonal Close -Packed
I_o	Light intensity
K	Kelvin
k_{app}	Rate of constant
kJ	Kilo Joule
L	Mean Crystallite Size
mL	milli liter
mmole	Millimole
Mol	Mole

Nm	Nanometer
PDE	Photo decolourization efficiency
PEG	Poly ethylene glycol
RB5	Reactive black 5
rpm	Root per min
t	Time of irradiation
T	Temperature
UV-A	Ultra violet light in the range from 315 to 380nm
V	Volt
V_{ac}	vacum energy
VS	Verse
WAO	Wet air oxidation
XRD	X-Ray Diffraction
ZB	Zinc blend
Λ	Wavelength
ΦM	working function of the metal

CHAPTER ONE

INTRODUCTION

1. Introduction

1.1 General Introduction

Large amounts of wastewaters are generated during processes involved dyes in the manufacture, utilization from them particularly that employed in textile, paper, leather, printing and carpet industries, and in disposal of dyes[1,2].

The major sources of water contamination [3] in the last years; textile industry was regarded as a higher impact to produce polluted water by discharging their effluents into different receiving groups including ponds, rivers and other public sewer. The textile industries can also be ordered into two groups via dry and wet fabric industry. Solid wastes are generated in dry fabric industry whereas liquid wastes are formed in wet fabric industries. This effluent wastewater contains chemicals like acids, alkalis, dyes, hydrogen peroxide, starch, surfactants dispersing agents and soaps of metals. Major sources of pollutants that load from the textile industries are produced from the several of their wet processing operations such as scouring, bleaching, mercerizing and dyeing [4,5].

In view of the fact that the dyeing process normally uses large amount of water for dyeing, fixing and washing processes. In recent times, the recovery and reuse of wastewater has received considerable attention because of the scarcity of water. The interest today is not in technologies for color removal but in technologies that can generate reusable water, removed toxicity, mineralizes aromatic compounds or recover the dyes, recover the salt, do not produce toxic sludge, possibly do not yield sludge at all [6-8]. The disposal of wastewater leads to damages the environment via containing on carcinogenic and toxic compounds which destroy the aquatic life [2], and can explain the effect of textile waste water in table (1-1) below in:

Table 1-1: Effects of textile wastewater into the environment [9].

Textile Wastewater Discharge of the Environment	
Direct Effects	Indirect Effects
• Changed of color.	• Damaged of aquatic life such as Fishes, mammals and plants.
• Very low sunlight penetration that reach to water which causes a damage flora and fauna of ecosystem.	.Eutrophication.
•The pollution of ground water due to filtering of contaminants via soil.	•Coloured allergen accelerates Genotoxicity and micro toxicity.
• Doing of depressing of receiving Water. Suppression in the streams re-oxygenation capacity.	• Suppression of immune system of human beings

Hence, the decolourization process of dye from wastewater is very important subject to remove the organic or inorganic substances that appearance color in water [6, 10].

Many techniques were used to treat wastewater such as adsorption [11,12], bio-removal [13], extraction [14], photocatalytic decolorization [15,16], coagulation [17,18] photo fenton and fenton-like [19,20] and using dielectric barrier discharge [21].The summarized method for treatment of wastewater can be explained in the scheme (1-1).

Treatment of textile waste water

Physical Methods   **Oxidation Methods**

Biological Methods

| Filtration |
| Coagulation |
| Adsorption |

| Advanced Oxidation |
| Oxidation Chemical |

| Enzymes |

| Microorganism |
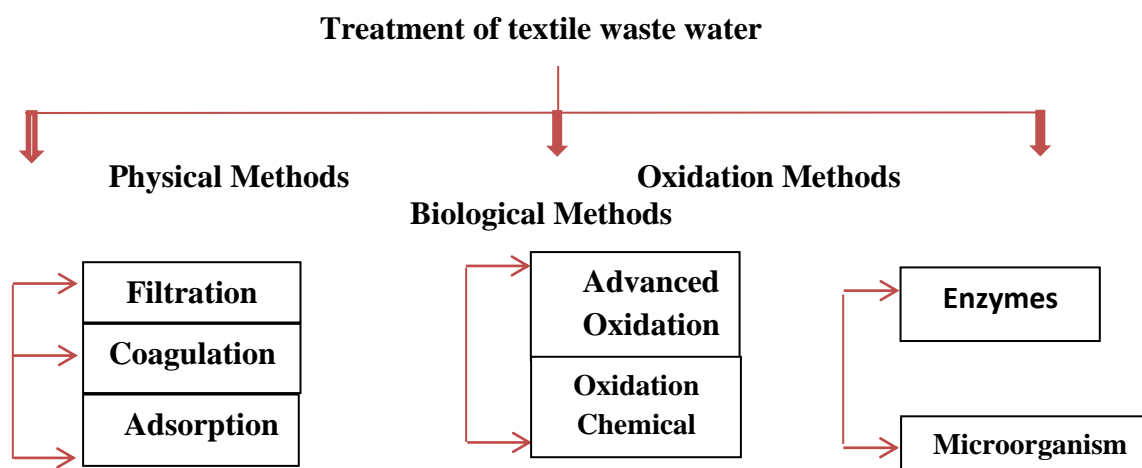
Scheme 1-1: Treatment methods for the degradation of dyes in textile wastewater
[7, 22, 23].

1.2 Advanced Oxidation processes

Advanced oxidation processes (AOPs) are vital processes that have two stages: the 1st Stage uses strong oxidants, that leads to mainly formed a hydroxyl radicals, the 2nd Stage is performed by reacting these oxidants with organic contaminants in water[24,25]. Because of the AOPs are versatility, thereby they enhanced by different possible ways for hydroxyl radical production, which allow to obtain a better compliance with specific treatment requirements. The produced hydroxyl radicals acted as a powerful oxidizing agent. These oxidizing agents have an oxidation potential equal to 2.8V and gives faster rates of oxidation reactions as compared with conventional oxidants such as hydrogen peroxide or potassium permanganate.

In fact, the hydroxyl radicals react with most dyes with high rate reaction constants; hence, they easily attack the most part of organic molecules. This process is regarded as a little selectivity which is a useful attribute for an oxidant used in wastewater treatment and for solving the pollution problems [26, 27]. Photo oxidation can take place at any temperature and pressure, but does not yield any secondary components.

The essential mechanism of advanced oxidation processes is the generation of $^{.}$OH ions [24, 27]. These processes can appearein the scheme (1-2) and Scheme (1-3).

Homogeneous Process	
Non- Photochemical	**Photochemical**

- Ozonation in alkaline media (O_3/HO⁻)
- Ozonation with hydrogen peroxide (O_3/H_2O_2)
- Fenton (Fe^{2+} or Fe^{3+}/H_2O_2)
  - Electro chemical-oxidation
  - Wet air oxidation (WAO)

- Photolysis
- UV/O_3
- UV/O_3/H_2O_2
  - UV /H_2O_2
  - Photo Fenton (Fe^{2+}/ H_2O_2/UV).
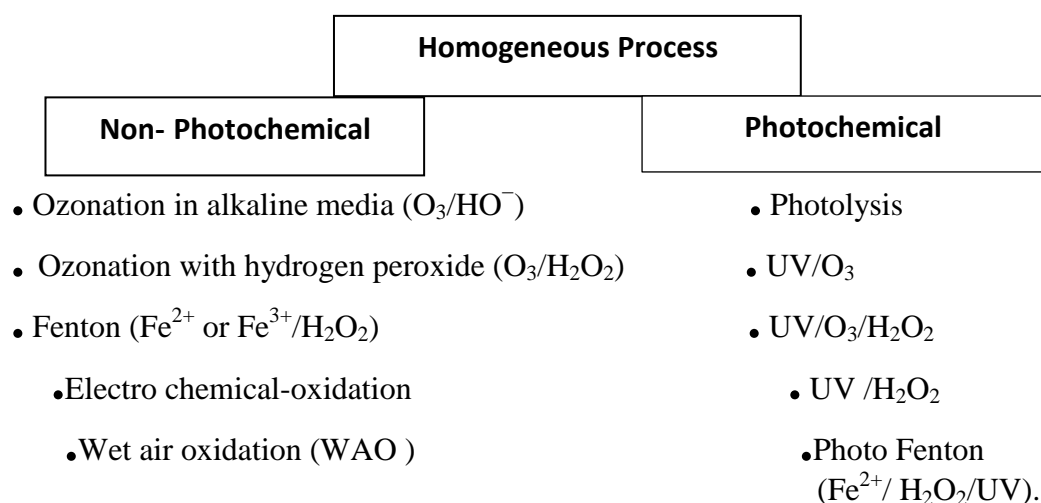
Scheme 1-2: Types and classification of advanced oxidation processes (Homogeneous process) [28], [29].

Heterogeneous Process	
Non- Photochemical	Photochemical
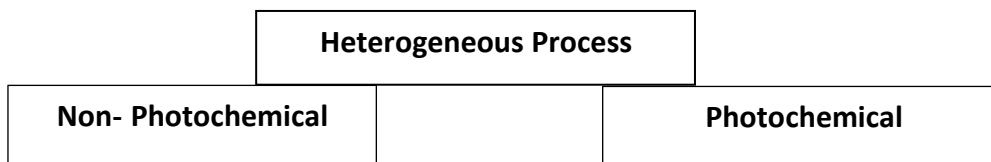
•Catalytic wet air oxidation (CWAO).   •Heterogeneous photocatalysis

•Fenton catalytic ozonation.

Scheme 1-3: Types and classification of advanced oxidation processes (heterogeneous process) [28], [29].

1.3 Photocatalysis

It is a Greek word, which consists of combination of two words: the 1st word is photo ("phos" means lights) and the 2nd word is catalysis ("katalyo" means to break apart, decompose). Generally, the term photocatalysis is employed to describe process that used light to stimulate a photocatalyst and accelerated the rate of chemical reaction [9]. In other words, photocatalysis is defined as a process that used a semiconductor to absorb the light energy which must be greater than or equal to its band gap that leads to generate an excitations of valence band electrons in the conduction band. Hence, the charge separation leads to the creation of electron-hole pairs which can further generate free radicals such as (•OH) in the system for redox of the substrate. The resulting hydroxyl radicals are given a high efficient for oxidizing and degrading of organic pollutants [30]. There are two types of photocatalysis [28, 31]:

a. Homogeneous photocatalysis:

This process occurs when the reactant and photocatalyst exist in the same phase, such as used coordination compound, or dyes, or natural pigments with light and O_2 or O_3.

b. Heterogeneous photocatalysis:

In this type, the reactant and photocatalyst will be found in different phases. The principle of heterogeneous photocatalysis is based on the activation of a semiconductor like (TiO_2, CdS, ZnO, ZnS *etc.*) by using appropriate wavelengths from radiation [28,31].Heterogeneous photocatalysis is deemed as one of the advanced oxidation processes (AOPs), which have a cost-effective

treatment method for removing of toxic pollutants from industrial waste water and formed end products such as CO_2, H_2O and mineral acids [32].

1.4 Photocatalyst

Photocatalysts are photo-active catalysts which play a vital role in the improvement of the rates of photochemical reactions. The ideal photocatalyst must be stable, highly photoactive, inexpensive and non-toxic. From the other hand, photocatalysts have the ability to initiate redox processes with enhancing of incident light on the catalyst surface that due to find of a band gap in the semiconductor [33, 34]. The primary principle for the degradation of organic compounds is recognized on the redox potential of the $H_2O/^{\cdot}OH$ couple, whereas, OH^- is generated $^{\cdot}OH$ at $E^o = -2.8V$, that lies within the band gap of the semiconductor [34]. Figure (1-1) explains several photo semiconductors that have enough band gap energies for catalyzing a wide range of chemical reactions.
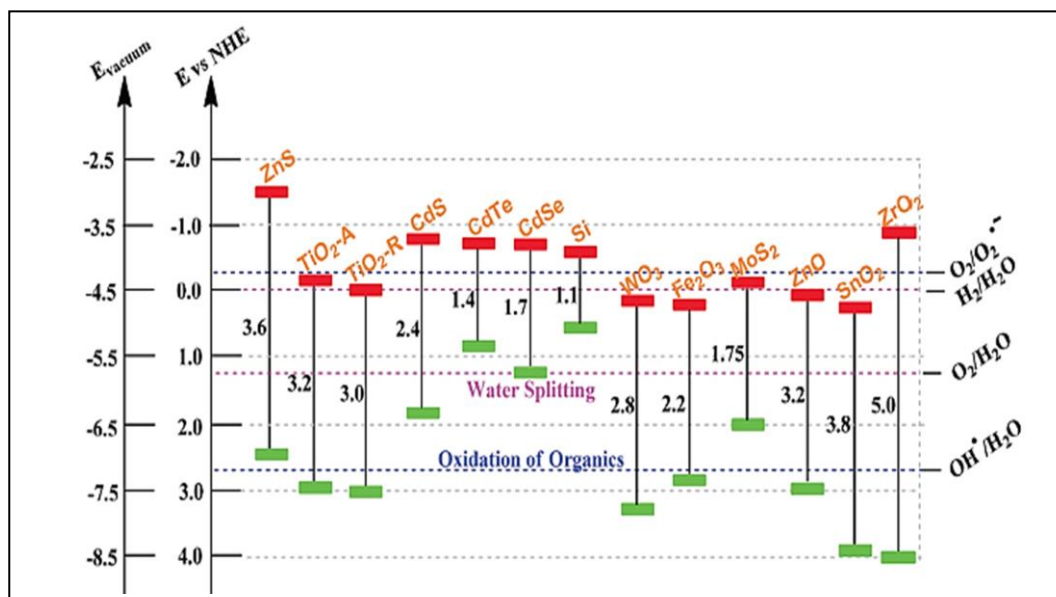
Figure 1-1: Band gap energy and band edge positions of varies photo semiconductor [35].

In general, the characterized of any bulk semiconductors are dependent on the band gap energy (Eg), which is defined as the minimum energy required to excite an electron from the ground state (valence energy band) into the vacant conduction energy band[36].

There are two types of band gap in semiconductors:
Direct band gap and (b) Indirect band gap.

A direct band gap means that the minimum of the conduction band lies directly above the maximum of the valence band in momentum space. Thereby no momentum transfer is required to takeoff the electron from the

valence band into the conduction band ($\Delta k = 0$). But indirect band-gap semiconductors do not have the lowest conduction band energy at the point. Thereby the fast electron has to transfer momentum to an electron in the valence band in order to excite it into the conduction band ($\Delta k \neq 0$) [37]. Figure (1-2) explained the direct and indirect band gap of photo semiconductors.
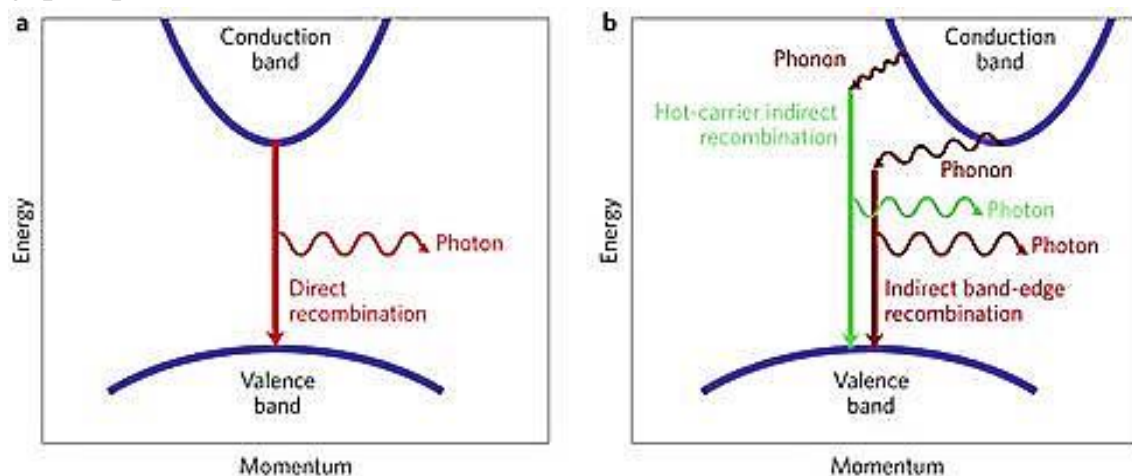
Figure 1-2: Simplified optical transition of semiconductor. (a) Direct band gap (b) Indirect band gap [38].

When a semiconductor catalyst such as (ZnS) is illuminated with photons whose energy is equal to or greater than their band-gap energy [39] that will lead to the generated a positive hole (+) in the valence band and an electron (e−) in the conduction band (CB). The positive hole oxidizes either pollutant directly or water to produce ·OH radicals, but the electron in the conduction band reduces the oxygen adsorbed on the catalyst as soon as in figure (1-3), and can explain in five steps[40, 41]:

(1) Absorption of light-UV by a semiconductor to create electron–hole pairs (exciton).

(2) Charge separation and migration to the surface of the semiconductor.

(3), (4) steps, the converted of O_2 and H_2O to $^.OH$ radical.

(5)Return electron from conduction band to valance band by recombination process.
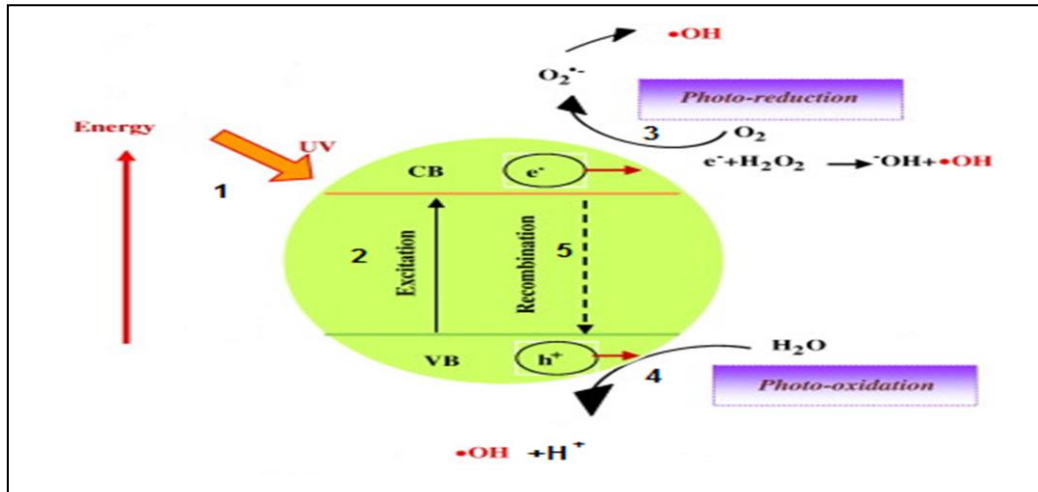
Figure 1-3: schematic of photocatalytic reaction on photocatalyst surface [40].

The electron-hole pair which encourages the reduction and oxidation of species that adsorbed on the semiconductor surface [42]. The photo efficiency of any photo reaction can be reduced by the electron-hole recombination, which tallies to the degradation of the photoelectric energy into heat.

$$e^- + h^+ \rightarrow N + E \qquad \qquad \textbf{... (1-1)}$$

Where: N is the neutral center and E is the energy released under the form of light ($h\bar{v} \leq hv$) or of heat [39].

In order to decrease the recombination process and increase life time of photohole must perform that through modification of photocatalyst surface, which can be represented as follows scheme (1-4).

```
                    ┌─────────────────────────────────┐
                    │   Modification of Photocatalyst  │
                    └─────────────────────────────────┘
            ┌──────────────────────┼──────────────────────┐
            ↓                      ↓                      ↓
Surface Sensitization                              Composite Modification
Semiconductor              Metal-Semiconductor
```
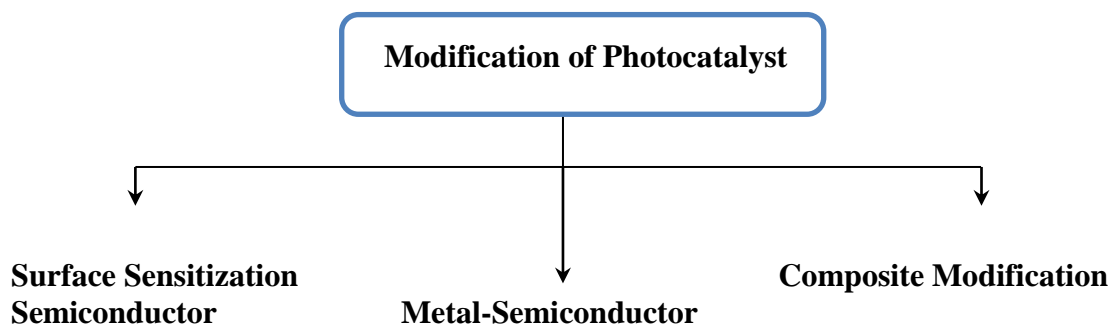
Scheme 1-4: Modification of Photocatalyst on surface [43].

The modification type in this study was done by metal-Semiconductor modification. So, when any metal such as (Mn, Cr) is loaded on photocatalyst surface, for instance; ZnS and then irradiated, the atom utilizes the photon energy (hυ) and reduces a crystal size. Briefly, it can be clarified role of loaded metal which results in addition charge carriers in presence of light and increase the surface area, which rise the decolonization efficiency of dye[44].Several studies have designated that the photocatalytic rate increases with catalyst loading with metal, but at high concentrations of metal load that will lose the efficiency, because of light scattering and screening effects happened [45].

From the other side, the agglomeration (particle–particle interaction) also increases at high solids concentration that leads to reduce the surface area available for light absorption. Although the number of active sites in solution will increase with catalyst loading while photocatalytic degradation rate decrease light penetration because of excessive particle concentration. The compromise between these two opposing phenomena results and so on optimum catalyst loading for the photocatalytic reaction [40].When such an n-type semiconductor is contacted in an electrolyte solution, electrons in the donor levels go out to the electrolyte since the donor level in an *n*-type semiconductor that may be more cathodic than the electrode potential of electrolyte solutions. This flow of electrons in the donor level to an electrolyte results in the formation of a so-called Schottky-type [46].

The loaded of metal on semiconductor leads to formation of Schottky barrier, that takes place between an n-type semiconductor like (ZnS, ZnO, TiO$_2$…etc) and a metal interface. In fact, when the metals have lower Fermi energies (E Fermi) compared to semiconductors then the metal and semiconductor must link. This flow electron from the semiconductor to the metal continued until the Fermi of the semiconductor reaches to equilibrium with that of the metal, hence, that will guide to a constant value of E Fermi for both of the devices. Moreover, that will be due to this deformation band structure between the semiconductor and the metal [33,47]. Figure (1-4) explains how Schottky barrier generates.
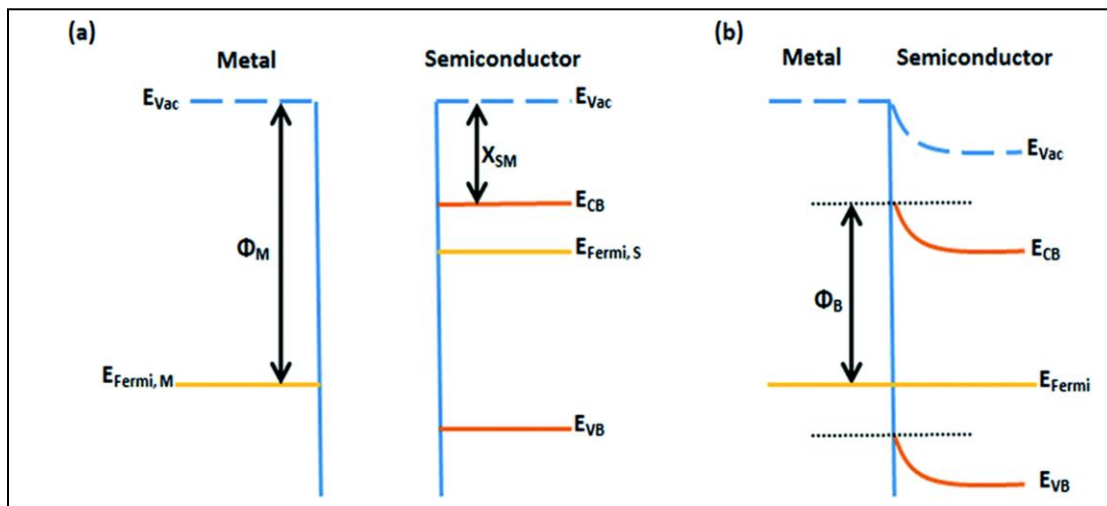
Figure 1-4: Formation of the Schottky barrier between n-type semiconductors and metals (a) before interaction and (b) after interaction[33].
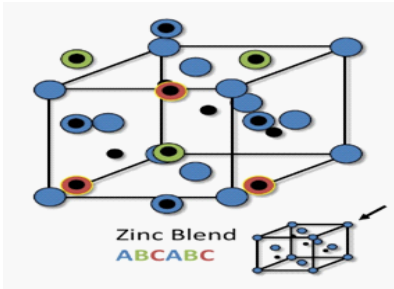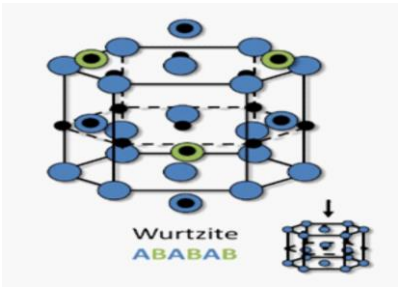
Where, Φ M is the working function of the metal, which is defined as the energy necessary to carry an electron from the metallic Fermi energy to the vacuum. XSM is the electron affinity, the energy difference between the minimum conduction band (CB) and the vacuum (Vac) energy.

1.5 ZnS Bulk

Zinc sulphide is one of the very important   II-VI group of compound semiconductors with have energy band gap about (3.72-3.77) eV in the bulk form, so, it is deemed as ideal for short wavelength optoelectronic applications [48-51]. ZnS is a non-toxic, abundant and eco-friendly and good chemical stability against

oxidation and hydrolysis. It is high stable in a large pH range and can be synthesized from earth-abundant components ,in addition ,it is widely employed in many fields of application such as electronics, solar cells, light emitting diodes, catalyst, including lasers, active sensors and waste water treatment [52-55]. In general, ZnS is a polymorphous material that has two crystalline forms namely: Zinc Blend (sphalerite) and Wurtzite. In both forms the co-ordination geometry at Zn and S is tetrahedral. Both structures have similar closest neighbor connections, but the distances and angles to furthermore neighbor's quietly differ. Table (1-2) explains the differences between the two crystal structures of ZnS phases.

Table 1-2: differences of crystal structure of ZnS phases [53, 56].

Zinc blend(ZB)	Wurtzite Zinc(WZ)
1. Cubic form (fcc).	1. Hexagonal form (hcp).
2. It is more stable than (WZ).	2. Less stable than (ZB).
3. Band gap of (ZB) approximately 3.72 eV.	3. Band gap is 3.77 eV.
4. Zinc blend has four asymmetric units in its unit cell.	4. wurtzite has 2 units in itself.

1.6 ZnS Nano powder

Semiconductor nanocrystals are tiny crystalline particles. In fact, the nano powder has a size-dependent on the optical and electronic property and the ideal dimensions are in the range of (1-100) nm. So, the size of nanocrystals regard as bridge of the gap at range between small molecules and large crystals, displaying discrete electronic transitions of isolated atoms and molecules, as well as enabling the

exploitation of the useful properties of crystalline materials. Semiconducting nanoparticles involved in photo conversion systems present a temperately wide energy gap between the conduction band (CB) and the valence band (VB) [36]. ZnS nano powder is considered as a good photo catalyst due to fast generation of the electron-hole pairs (exciton) by photo-excitation and highly negative reduction potentials of excited electrons; as if conduction band position of ZnS in aqueous solution is higher than that of other semiconductors such as TiO$_2$ and ZnO. Since, a larger ratio of surface to volume of a catalyst would facilitate to give a better catalytic activity [9,50].The enhanced surface to volume ratio will reason to increase of surface states, which change the activity of electrons and holes will effect on the chemical reaction dynamics. However, the size quantization increases the band gap of photo catalysts to enhance the redox potential of conduction band electrons and valence band holes [57,58].

The manner, ZnS nanopowder keeps unusual physical and chemical properties compared with the ZnS Bulk like: enhanced surface to volume ratio, the quantum size

effect, surface and volume effect, macroscopic quantum tunneling effect, more optical absorption, chemical activity and thermal resistance, catalysis, and the low melting point [53].

1.7 Co-precipitate method

Co-precipitation method is a wide chemical method (Bottom-Up approach) that used to prepare nanomaterials. It is involved several stages: nucleation, growth and secondary process such as agglomeration, attrition and breakage. The particles obtained with a convention co-precipitation process are relatively larger with a broad size distribution, due to a difficulty to avoid the nucleation during the subsequent growth of nuclei [59]. Although co-precipitation is the most widely employed method but the nanoparticles are prepared by this method tends to be rather poly disperses and the control process on their shapes is very difficult [60].

Nanoparticles also attracted magnetically the synthesized nanoparticles that must be protected through surface modification. Hence, in this method, it can use that organic additives or stabilizers such as 1% poly vinyl alcohol (PVA), poly ethylene glycol (PEG) that used to be an

important factor in preparing mono-disperse magnetite particles of varying sizes, and in addition to the usual flocculation. In fact, the effect of the parameters such as pH, salt type, the ionic strength of the precipitation medium, and temperature of the reaction, allows one controlled on the crystal and particle sizes, shape, and composition of the resultant magnetic nanoparticles. Other parameters are affected the size and mono disperse of nanoparticles that involve the amount of stabilizing ions, the found of other ions, chelation and adsorption of additives on the nuclei and growing crystals [60].

Advantage: This method is characterized by being simple, effective and fast preparative method; easy control of particle size and arrangement, very powerful for synthesis the particles that are loaded on the surface.

Disadvantage: The particles deposited on the surface that is easy to aggregate and difficult to control the shapes [61-63].

8 Adsorption

Adsorption is a process that takes place when a gas or liquid solute as adsorptive, which accumulate on the surface of a solid (adsorbent), and then forming a molecular, ionic, or atomic film. The species like: molecules, atoms and ions of the adsorptive will adhere to the adsorbent are called adsorbate, it is possible to find the difference between adsorption of the gas phase and the liquid phase as a multilayer for the gas phase adsorption and a monolayer for the liquid phase [64].

Adsorption technique proved an efficient and an economical process for the treatment of dyes effluents. The efficiency of the technique lies in choosing the suitable adsorbent. Hence, the chosen adsorbent should be easily available, cheap and should have no economic value [65].

Generally, adsorption of Liquid-Solid interface can take place in solution. This interface is decidedly heterogeneous, so that most solids used as adsorbents, but characterized surfaces by being poorly [66].The classification of adsorption depends on the strength of the binding forces is more common, to physical adsorption (physisorption) and chemical adsorption (chemisorption). The type of forces for physical adsorption involve Vander Waal's forces, hydrogen bonding and ion-exchange processes, whereas the electrostatic, covalent and Co-

ordinate displacements are the main factors in chemical adsorption [67,68].

1.8.1 Adsorption on Catalyst Surface

The Adsorption process on catalyst surface is considered the important phenomena of catalysis that occur on the surface. The role of using catalyst for increasing the rate of reaction can be explained in term of adsorption of the reactants on the surface of the catalyst. So, adsorption helps the reactions by leading to concentrate of the reactant molecules on the surface of the catalyst. since the adsorption is an exothermic process, thereby, the heat of adsorption shall exist the reactants via activated of reactant molecules, and then leads to chemical reaction, that depends upon lowering the activation energy of the reaction. This behavior will enhance rate of reaction and changing in oriented for the reaction (mechanism). At last, the adsorbed molecules separate from catalyst surface and yield of reactive atoms or free radicals that employed to eliminate the pollutants from the waste water [69].

The essential mechanism of using catalysts to start the reaction, can be explained by the following steps [70]:

1. **Diffusion of reactants** on the surface of the catalyst.
2. **Adsorption** of reactants on the surface of the solid catalyst. The catalyst surface is unbalanced attractive forces, since the presence of these unsatisfied forces or free valences.
3. The adsorbed reactant molecules undergo a **chemical reaction** to form an intermediate activated complex. This complex is highly unstable.
4. The activated complex breakdowns to form the products. Hence, the products separate from catalyst surface, this is called **desorption.**

5. **Diffusion of product** molecules away from catalyst surface.

1.8.2 Dyes adsorption

Photo catalysis through excitation of adsorbed dyes when light with energy are less than the band gap of the irradiated semiconductor will

be absorbed by the adsorbed dye molecules. Dye molecules will be decolorized by a photosensitization process, at energy of light less, the excited (dye*) is recognized to inject an electron to the conduction band of the semiconductor. The following equations can be explained the process in this pathway [71,72] :

$$Dye + h\nu \rightarrow {}^1Dye^* \text{ or } {}^3Dye^* \qquad \text{... (1-2)}$$

$$^1Dye^{\cdot} \text{ or } {}^3Dye^{\cdot} + Semiconductor \rightarrow Dye^{\cdot+} + e^-_{semiconductor} \qquad \text{... (1-3)}$$

$$e^-_{semiconductor} + O_2 \rightarrow O_2^{\cdot-} + Semiconductor \qquad \text{... (1-4)}$$

$$Dye^{\cdot+} + O_2^{\cdot-} \rightarrow DyeO_2 \rightarrow degradation\ products \qquad \text{... (1-5)}$$

$$Dye^{\cdot+} + HO_2^{\cdot} \text{ (or } HO^{\cdot}) \rightarrow degradation\ p \qquad \text{... (1-6)}$$

$$Dye^{\cdot+} + 2\ HO^{\cdot} \rightarrow H_2O + products\ oxidation \qquad \text{... (1-7)}$$

$$Dye^{\cdot+} + HO^- \rightarrow Dye + HO^{\cdot} \qquad \text{... (1-8)}$$

$$Dye^{\cdot+} + H_2O \rightarrow Dye + HO^{\cdot} + H^+ \qquad \text{... (1-9)}$$

1.8.3 Adsorption of Oxygen and water

The activity of any catalyst depends upon the ability for many metals; metal sulfides and metal oxides on produced surface hydroxyl groups [73]. Oxygen reduction reaction (ORR) depends on oxygen adsorbed on catalyst surface and produces a several intermediates ($O_2^{\cdot-}$, $\cdot OH$, and $\cdot OOH$), according to the following mechanism [74].

In outset, dissolved oxygen in solution is reduced by e^- of conductive band on catalyst surface, and the super oxide anion ($O_2^{\cdot-}$) will generate.

$$O_2 + e^- \rightarrow O_2^{\cdot-} \qquad \text{... (1-10)}$$

The superoxide anion radical may be gone in other reduced process to generate hydrogen peroxide.

$$O_2^{\cdot-} + H^+ \rightarrow HO_2^{\cdot} \qquad \text{... (1-11)}$$

$$HO_2^{\cdot} + HO_2^{\cdot} \rightarrow H_2O_2 + O_2 \qquad \text{... (1-12)}$$

$$O_2^{\cdot-} + HO_2^{\cdot} \rightarrow HO_2^- + O_2 \qquad \text{... (1-13)}$$

$$HO_2^- + H^+ \rightarrow H_2O_2 \qquad \text{... (1-14)}$$

The H_2O_2 is either split under light or reacted with super oxide anion that will produce hydroxyl radical, which is contributed for dye degradation [15].

$$H_2O_2 + O_2^{\cdot-} \rightarrow HO^{\cdot} + HO^- + O_2 \qquad \text{... (1-15)}$$
$$H_2O_2 \rightarrow 2OH^{\cdot} \qquad \text{... (1-16)}$$

In general, the surface of any catalyst can be coverage by oxygen, is independent on temperature and oxygen pressure. However, the ratio of adsorption concentration increases with the oxygen pressure [75]. From the other hand, the water oxidation ($2H_2O \rightarrow O_2 + 4e^- + 4H^+$) is a vital key step in both natural and artificial photosynthesis [76].

Water is oxidized by a positive hole to produce a hydroxyl radical ($^{\cdot}OH$) which in turn oxidizes of organic dye pollutants [15]. This behavior can be applied, according to following equations.

$$H_2O + h^+ \rightarrow HO^{\cdot} + H^+ \qquad \text{... (1-17)}$$
$$HO^{\cdot} + Dye \rightarrow Products \qquad \text{... (1-18)}$$

1.9 Dye

Azo dyes are recognized as a wide common classification of dyes, that consist of approximately 60-70% of the available dyes. The most communal colors of azo dye are deemed on found azo bonds (–N=N–) in the molecule of dye to prepare the monoazo, diazo, triazo,…etc, in different colors such as red, orange and yellow [77].

1.9.1 Classification of Dyes

There are different ways for classification of dye molecules. It can be classified in terms of chemical structure, colour and application methods. However, the classification that based on application is often favorable, like: direct, disperse, developed, acidic, reactive…etc as shown in scheme 1-5. The other classification based on chemical structure for the common class of the dyes is presented such as azo,

xanthene, triaryl methane, diphenyl methane, quinioline ….etc. Other than the above, dyes are also classified based on their particle charge upon dissolution in aqueous medium like cationic (all basic dyes), anionic (direct, acid, and reactive dyes), and non-ionic (dispersed dyes) [78].

Classification of dye according to their application

Vat	Sulfur	Reactive	Disperse	Direct	Basic	Acid
Water -insoluble Oldest dye More chemically complex	Organic compounds containing sulfur or sodium sulfide	Water – soluble Anionic compound Largest dye class	Water-insoluble	Water -soluble Anionic compound Can be applied directly to cellulosic without metals like chromium	Water – soluble Applied in weakly acidic dye baths very bright dyes	Water - soluble Anionic compound

Scheme 1-5: Classification of dye according to their application [79].

Reactive black 5 dye

The reactive dyes are a most consumed in the dye market, that attitude to high ability for producing strong covalent bonds with cellulosic fibers by the hydroxyl groups in highly alkaline medium. This behavior leads to a high fastness [80,81]. In addition, they have a low cost, highly soluble in water as anionic electrophiles, since they contain one or more reactive groups, which are linked a covalent bond with hydroxyl group of cellulosic fibers and becomes a part of it [82]. Reactive dye is having a wide range of color can be given bright colors fastness to washing [15] [83-86] that due to the natural chromophoric groups (like azo, metallized azo, phthalocyanine, anthraquinone, formazane and oxazine group) and the bridging groups (like ether or ester linkage as a covalent chemical bond) that linkage obtains between the dye and the fibers [15].These dye had many kinds,

so, they have a general formula structure S-F-T-X, where, S is solubilizing group like- SO_3 group, F is chromophore groups like azo or aromatic ring groups, T is abridge group such as sulphide, imino, oxide, ethyl & methyl groups and X is active group such as vinyl sulfone and dichlorotriazine that accountable to bound with cellulosic fibers [80,86]. In general, the chromophore groups in these dyes are determined the kind of the absorbed light area, hence, the azo bond has absorption in a visible light area, while, in the UV light area the aromatic ring has absorption [87]. Reactive Black 5 (RB5) is one of the reactive azo dye that used in textile industries and caused a pollution of river water. When this dye is extremely contacted it may cause allergic reactions of breathing and hardly skin irritation. The chemical formula of RB5 is $C_{26}H_{21}N_5Na_4O_{19}S_6$, with weight 991.82 g/mol [11].The chromophore of RB5 molecule absorbs the visible light at 596 nm [88]. The structure of this dye can be explained in figure (1-6).
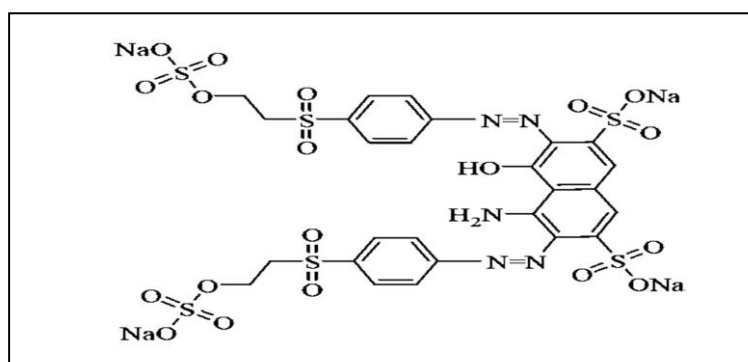
Figure1-6: Structural formula of reactive black 5 dye [19,89].

When UV-light focus on RB5 dye solution in presence photocatalyst , the series of redox reactions were obtained and leaded to formed ahydroxyl radical.
In outset, azo bond is oxidative cleavage either C-N or N-N cleavage by attaching the hydroxyl radical that generated via photocatalysis process [81,90] in presence the prepared photocatalysts. The intermediate I and intermediate II were produced with liberated N_2. After that the C-S bond is cleavage in series steps to generate CO_2 and H_2O and inorganic anions [81], as notice in scheme (1-6).
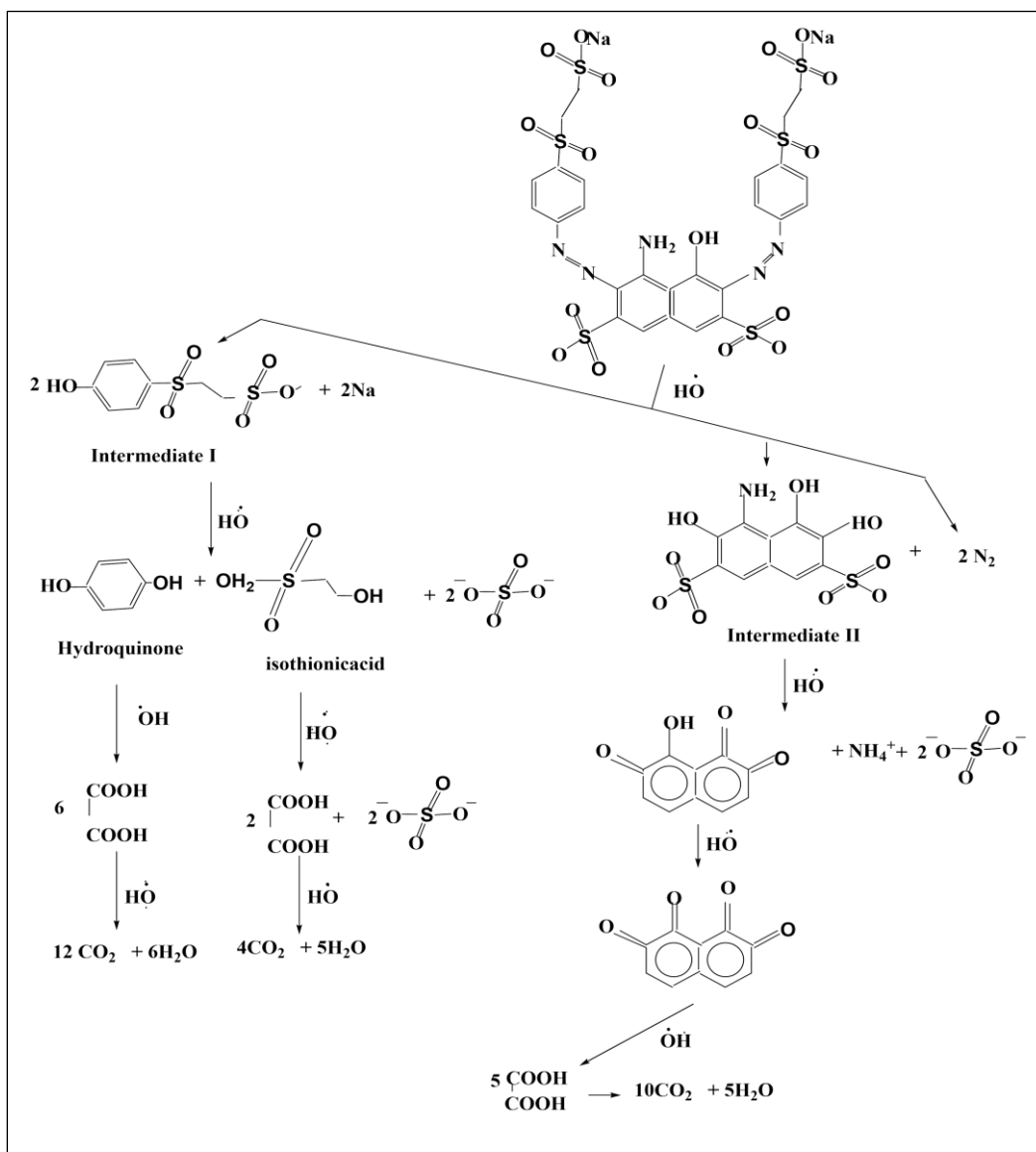
Scheme 1 -6: Summarized of photo degradation mechanism for RB5 dye

(Modified from ref.[81, 91]).

1.10 Literature Review

ZnS nanoparticles have been prepared by different ways. Parvaneh and coworkers [92] prepared ZnS nanoparticles by Co- precipitation method using EDTA as stabilizer and capping agent, wherase, Ayodhya and coworkers [58] used the same method with various capping agent like PVP(poly vinyl pyrrolidone , PVA (poly vinyl alcohol, and PEG-4000(poly ethylene glycol).

Pathak and coworkers [93] synthesized ZnS nanoparticles by the mechanochemical route and measured the crystallite size of as prepared nanoparticles are found to be in the range (4–7 nm).

Chandran and coworkers [94] prepared bare ZnS nanoparticles by hydrothermal method and then calculated the average crystallite size of the sample using Scherrer equation, which found to be 20.036 nm.

Bera and coworkers [95] found the sizes of the prepared crystals for ZnS and Mn doped ZnS nanoparticles are increased with doped.

Shanmugam and coworkers [96] noticed the prepared cerium-doped zinc sulfide nanorods are had a flower-shaped morphology,that indicated to successfully synthesize under air atmosphere through simple chemical precipitation method.

Silvaa and coworkers [97] employed the sonochemical method to prepare ZnS nanoparticles as a nanocrystalline powder with crystallite size around 2 nm.

Mahammed and Ahmed [17] proved that the prepared bare zinc sulfide and chromium (1:1)% doped on bare zinc sulfide via Precipitation method are sucssusfuly synthesis by measured XRD data, AFM analysis and Fluorescence spectra, these prepared photocatalyst were applied in decolorization of reactive black 5 dye and changed the Efficiency percentage from 59% to 94% with Cr doped on ZnS nanopowder.

Goharshadi and coworkers [3] successfully synthesized ZnS nanoparticles with an average particle size of 2 nm under using ultrasonic with irradiation, without any surfactant and high temperature treatment. They found that the photocatalytic activity of semiconducting sulfide quantum dots for degradation of reactive black 5 was investigated in little time (10 min) using 0.2 g ZnS NPs in a neutral pH .

1.11 The Aim of the Present Work

In this work there are many aims as that following:
1. Preparation of ZnS nanoparticle.
2. Metalized of ZnS nanoparticle by different types of metals (Mn, Cr).
3. Study the characterizations of all samples by employing XRD and AFM analysis, atomic absorption analysis and fluorescence then it compares the characterizations of prepared (bare and metalized ZnS) with the commercial ZnS.
4. Study the effects of the followings on photocatalytic activity on decolorization of reactive black 5 dye:
a. Type of metal.
b. Weight of catalyst.
c. Initial pH of solution.
d. Temperature.
e. Amount of $K_2S_2O_8$.

5.Suggested a suitable mechanism for decolorization of reactive black dye.

CHAPTER TWO
EXPERIMENTAL

This chapter displays the used chemicals, instruments, methods of preparation of bare and metalized ZnS nanoparticles, characterized of prepared materials with a vital equations.

2.1 Chemicals

Table 2-1 lists the chemicals used in this work. All the chemicals were obtained without further purification.

Table 2-1: Chemicals and their commercial sources

NO	Chemicals	Company supplied
1	Absolut ethanol (99.98) % (C_2H_5OH).	J. K. Baker, Netherlands.
2	Hydrochloric acid (36.5-38.0) % (HCl).	J. K. Baker, Netherlands.
3	Sulphuric acid (99.00) % (H_2SO_4).	CDH, India.
4	Sodium hydroxide 99.00% (NaOH).	Panareac, Spain.
5	1, 10- Phenanthroline ($C_{12}H_8N_2$).	Riedel-De-Haen AG, Seelze, Hannover, Germany.
6	Potassium oxalate ($K_2C_2O_4$).	Riedel-De-Haen AG, Seelze,Hannover, German
7	Iron (III) sulfate ($Fe_2(SO_4)_3$).	Panareac, Spain.
8	Zinc sulfate hepta-hydrate ($ZnSO_4.7H_2O$).	Labochemie, India.
9	Reactive black 5 ($C_{26}H_{21}N_5Na_4O_{19}S_6$).	Hilla textile factory.
10	Zinc sulfide commercial (ZnS).	Thomas baker, India.
11	Persulphate potassium ($K_2S_2O_8$).	Maknur Laboratories, Canada.
12	Thiourea (NH_2CSNH_2)	Fluka –Garantie,Switzerland.
13	Poly (ethylene glycol) (PEG) $H(OCH_2CH_2)_nO_4$	CDH, India.
14	Manganese (II) Chloride -tetra hydrate ($MnCl_2.4H_2O$).	Riedel-De-Haen AG, Seelze, Hannover, Germany
15	Chromium (III) Chloride ($CrCl_3$).	BDH Limited Poole England General Purpose reagent.
16	Ammonia (NH_4OH).	Sinopharm Chemical Reagent,China.

2.2 Instruments

Different instruments were used in this study. Types of instruments and the suppliers companies are listed in table 2-2.

Table 2-2: Utilized Instruments.

No.	Instrument	Company
1	Sensitive balance.	BL 210 S, Sartorius, Germany.
2	UV-Visible spectrophotometer.	Cary 100Bio, Shimadzu (Varian), Germany
3	Ultrasonic.	FALC,Italy.
4	High Pressure Mercury Lamp UV A (400W).	Rudium, China.
5	Oven.	Memmert, Germany.
6	Centrifuge.	Hettich- Universall II, Germany.
7	Hot plate Stirrer.	Heido-MrHei-Standard, Germany
8	Atomic absorption spectrophotometer.	AA-6300, Shimadzu, Japan.
9	Fluorescence Spectrometer.	FS-2, Scinco, Korea.
10	X-Ray Diffraction Spectroscopy.	Lab X- XRD 6000, Shimadzu, Japan.
11	pH meter.	Hanna Instruments- Mauritius, India.
12	Scan Probe Microscope	AFM model, AA 3000, Advanced Angstrom Inc.,USA.
13	UV- Visible spectrophotometer.	AA-1800, Shimadzu, Japan.

2.3 Preparation of Bare and Metallized ZnS

Co-precipitation method was done to prepare bare ZnS and (Cr, Mn) loaded ZnS nanopartilces. The metals loaded method was performed as a single form of meal and as mixture of two metals (Cr and Mn) in colloidal solution [98].

2.3.1 Preparation of Cr: ZnS

The prepared solutions were dissolved in distill water then shaking by ultrasonic (FALC) for 10 min to ensure getting for homogenous solution. The metal loaded Zinc sulfide procedure was modified from procedure in reference [51]. 0.05 M (7.188gm) from $ZnSO_4$ was used as starting material. The equal volume from 0.05M (3.740 gm) thiourea was taken in a burette and added drop by drop into $ZnSO_4$ solution with vigorous stirring (Labtech-magnetic stirrer) for about 25 minutes to get ZnS solution, and simultaneously 0.05M (0.307gm) from $CrCl_3$ was added to this solution as drop -drop using burette for 25 min to create the Cr loaded ZnS. This final formed solution was followed by drop wise addition of 1% of poly ethylene glycol - 4000 (PEG- 4000) in 100 ml D.W as neutral capping agent solution under vigorous stirring for 1 hour. Afterwards, 0.1M from ammonia solution was added slowly to solution of metal until the pH reached to range between 10 and 12 that is necessary to generate the metal complex. The produced material is shown in figure 2-1. Finally, the metal complex solution was filtrated under vacuum using Büchner's funnel. The precipitate was washed twice by using distill water until the solution becomes the output of washing neutral (**pH**=7), then used absolute ethanol to remove the impurities. The produced precipitate for Cr/ZnS was grey color as seen in figure 2-2. This catalyst was dried overnight by silica gel powder in desiccator then dried in oven at less 100 ^{o}C for 2h to obtain powder sample.
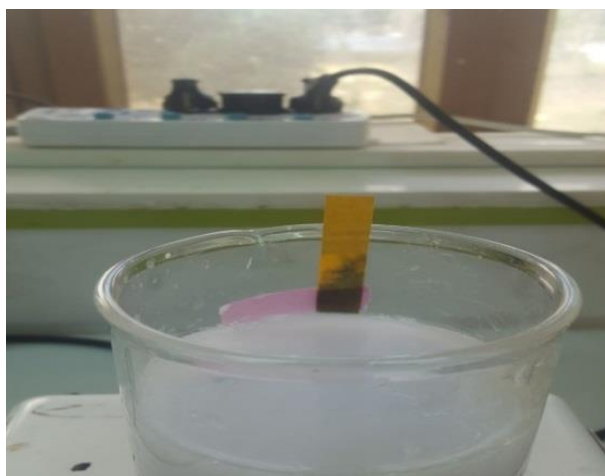
figure2-1: The resulting solution at pH=10-12

via preparation prosess.

2.3.2 Preparation of Mn: ZnS and Cr: ZnS: Mn (1), (2)

The precipitates of (Mn: ZnS) and Cr:ZnS:Mn are prepared in the same way as the chromium loaded on ZnS, whereas all prepared solutions were dissolved in distill water, then the solutions are mixed with the same concentrations [46]. After that, add 0.05 M (0.494gm) of $MnCl_2.4H_2O$ at loaded Mn on ZnS, while the addition of mixture solutions from 0.05M (0.247gm) of $MnCl_2.4H_2O$ and 0.05 M (0.153gm) $CrCl_3$) were applied either in the addition process is consecutive where Mn solution was firstly added then Cr solution to form Cr:ZnS:Mn(1) or the addition was perform at the same time to prepare Cr:ZnS:Mn(2) Subsequently. For all prepared catalysts must precipitate by slowly adding 0.1M from ammonia solution to solutions until the pH touched to (10-12). Finally the metal complex solutions were filtrated. The precipitates were twice times by using distill water then used absolute ethanol to remove the impurities. The precipitates are dried overnight by silica gel powder in desiccator, and then dried in oven at less 100 ^{o}C for 2h to obtain powder sample.
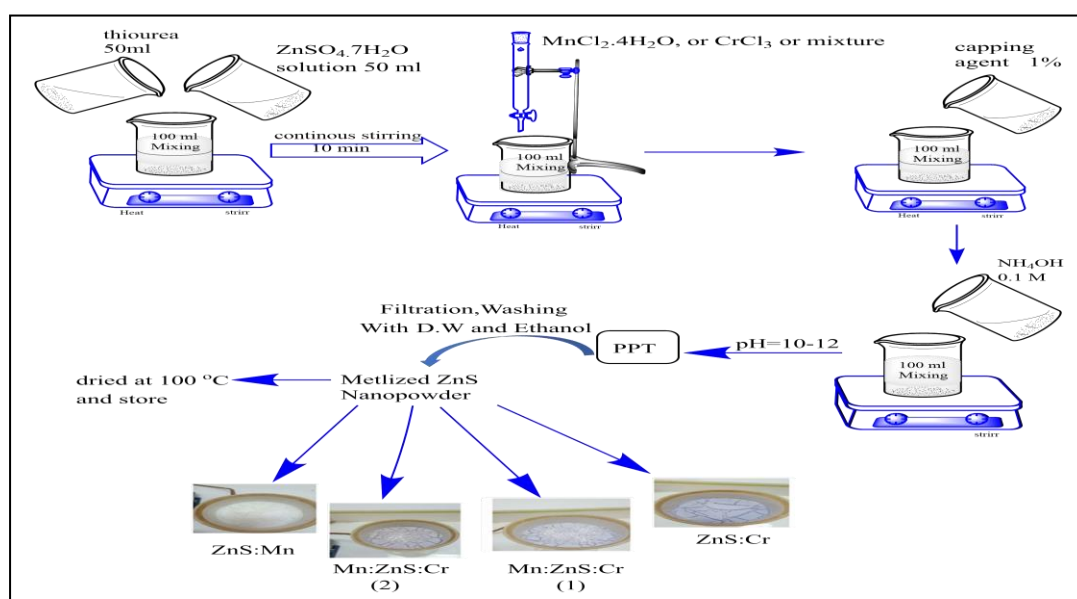
Figure2-2: Schematic diagram for prepared of metalized ZnS nanoparticle.

2.3.3 Preparation of ZnS nanoparticle

It is prepared with the same steps and materials that used for metallized ZnS, but without addition of any solution of metals. At last, the white nanopowder was generated, according to the following steps in figure 2-3.
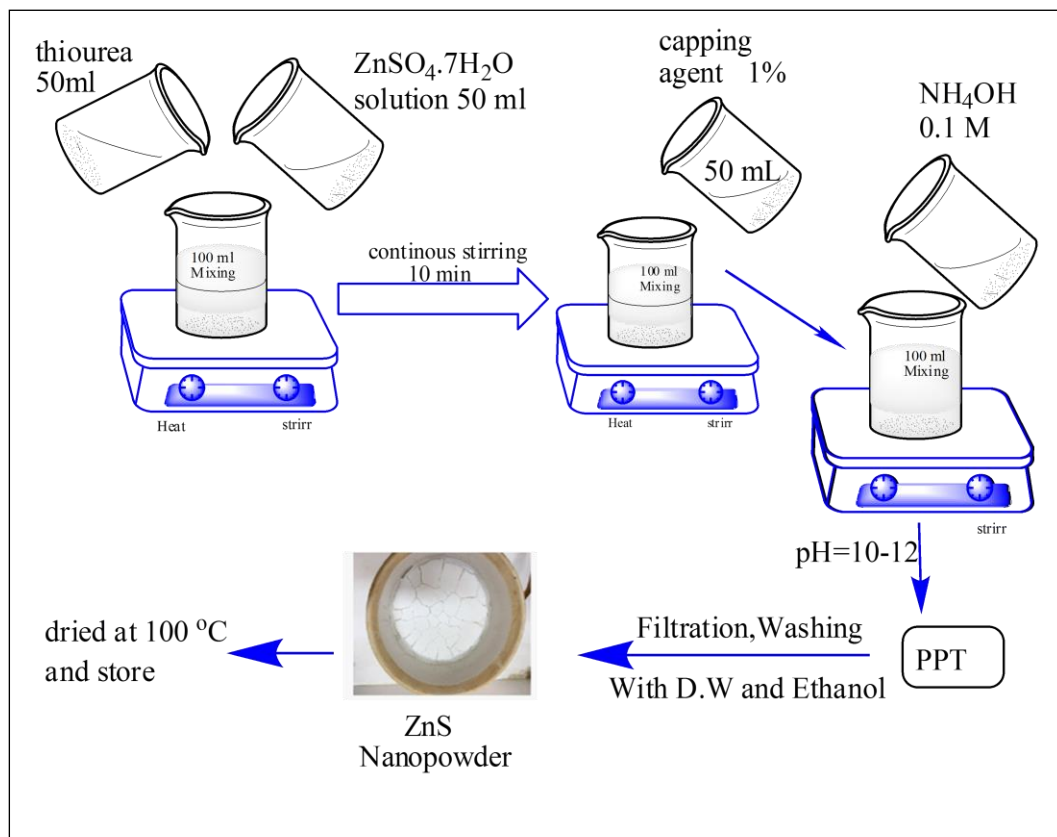
Figure 2-3: Schematic diagram of prepared of ZnS nanoparticle

2.4 Characterization

2.4.1 X-Ray Diffraction Spectroscopy (XRD)

The characterization of the crystal morphology and the size of the commercial and prepared bare and metalized of ZnS were employed by XRD measurements. The average crystallite sizes in nm, were calculated for all samples by Debye-Scherrer formula [99].

$$L = \frac{K\lambda}{\beta \cos\theta} \qquad \text{...(2-1)}$$

Where L is the average crystallite size, k is the constant crystal lattice (0.90), $\lambda = 0.154$ nm which is the wavelength of the radiation, β is the full width at half maximum in radians and θ is the angle of diffraction.

2.4.2 Atomic Force Microscopy (AFM)

The AFM images as two and three dimensions were noted with instrument (SPM AA-3000, USA). This technique was taken to find the particle sizes (D_p) for all studied samples. Very slight amount of each sample was suspended in absolute ethanol and treated by ultrasonic instrument for 10 min in power of 25 kHz. One drop of each of the obtained colloidal solutions was dropped on (1×2 cm) glass slides. The crystallinity index was calculated by depending upon the mean crystal size and practical size via the following equation [100]:

$$\text{Crystallinity Index} = \frac{D_p}{L} \qquad \qquad \textbf{...(2-2)}$$

Where: D_p is the particle size which is measured by the AFM analysis and L is the average crystallite size that calculated by Scherrer equation (equation 2-8).

2.4.3 Atomic Absorption Spectrophotometry.

Atomic absorption instrument was estimated to measure the residue amount of Cr or Mn in filter solutions after loading them on prepared ZnS. This analysis was done with passing mixture of air and acetylene via the flame using (Shimadzu-AA-6300) instrument. The analyzed samples were determined after using a calibration curve for these metals at wavelength of Mn and Cr equal to 279.5 nm and 357.9 nm respectively. These results note in figure 2-4 and figure 2-5. From other hand, the amount of Mn and Cr in solutions were listed before and after loaded on prepared ZnS surface, that is explained in the table 2-3.

Table 2- 3: Calibration Curve of Mn and Cr standard Concentrations.

Intensity	C/ppm (Mn)	Intensity	C/ppm(Cr)
0.000	0.000	0.000	0.000
0.021	1.000	0.014	0.610
0.061	3.000	0.024	1.061
0.100	5.000	0.046	2.000
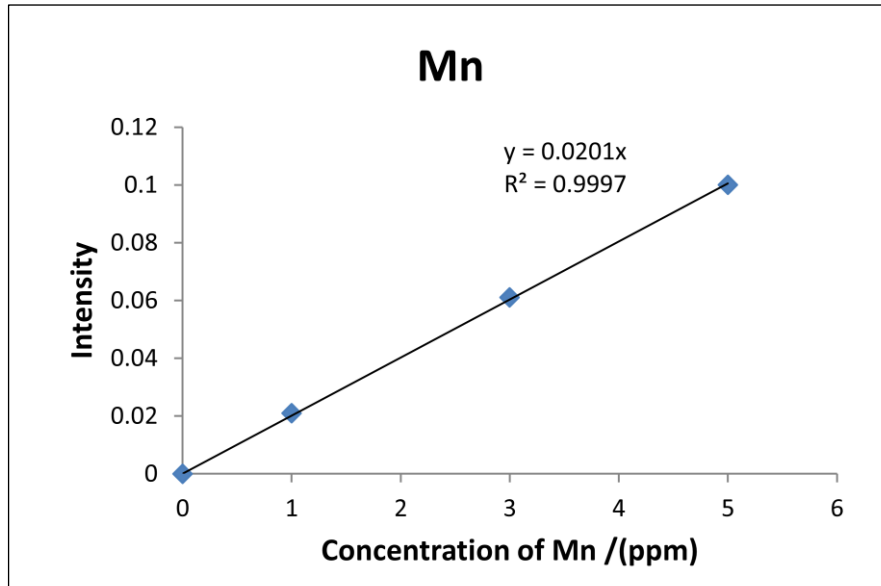
Figure 2- 4: Calibration curve at different Concentrations of Manganese.
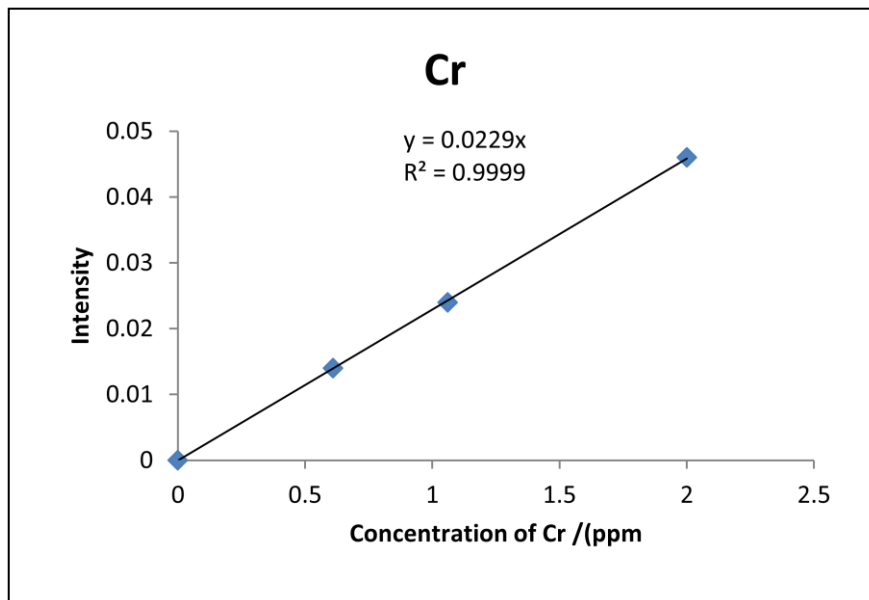
Figure 2- 5: Calibration curve at different concentrations of Chromium.

2.4.4 Band gap energy measurements

In order to calculate the band gap energy in (eV) for all studied samples, the fluorescence spectroscopy was employed, and then applied the produced wavelength (λ) in equation (2-10) at the maximum intensity in the fluorescence spectra of all studied samples [101].

$$\text{Band gap (eV)} \quad = \frac{1240}{\lambda_{(nm)}} \qquad \textbf{... (2-3)}$$

2. 5 Photocatalytic decolorization Reaction of reactive black 5 (RB5)

In this work, all experimental for photocatalytic decolorization of dye was done inside a homemade photo reactor. The rector has been irradiated from outside using a high pressure mercury lamp UV-A (400 Watt), which was employed as a source of radiation in figure 2-6. This lamp of incident light is having a wavelength about 365 nm. All solutions were prepared from appropriate grams of photocatalyst samples were added to 100 mL of 25 ppm from reactive black 5 dye solution. The produced suspension solutions were subjected to UV-A light flux at intensity equal to 1.47×10^{-6} Einstein s^{-1}. The light intensity was calculated by chemical actinometer [102] according to item 2.6. At different time intervals, about 3.5 mL was taken out with using syringe, and then carried out double separated processes by using centrifuge at 10 min and 4000 rpm. The formed filters were studied by reading the absorption at 595 nm to find the residue concentrations of dye after irradiation.
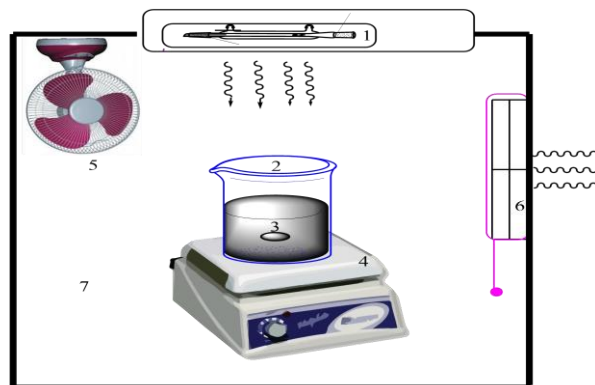
Figure 2-6: Schematic diagram of photoreactor.

Where: High pressure mercury lamp(400W)(1), 400 cm^3 Pyrex glass beaker (2), Teflon bar (3), magnetic stirrer (4), fan (5), vacuum fan (6) and wooden box(7).

2.5.1 Calibration Curve of reactive Black 5 dye

The calibration curve was obtained by using series of standard RB5 dye in aqueous solutions, which explained in table 2-4 and figure 2-7. The absorbance of all prepared standard solution was applied at wavelength equal to 595 nm.

Table 2-4: Relationship between absorbance and different concentrations of RB5.

Conc. of RB5 dye (ppm)	Abs at 595 nm
0	0.000
1	0.025
5	0.142
10	0.264
20	0.469
30	0.691
40	0.895
50	1.099
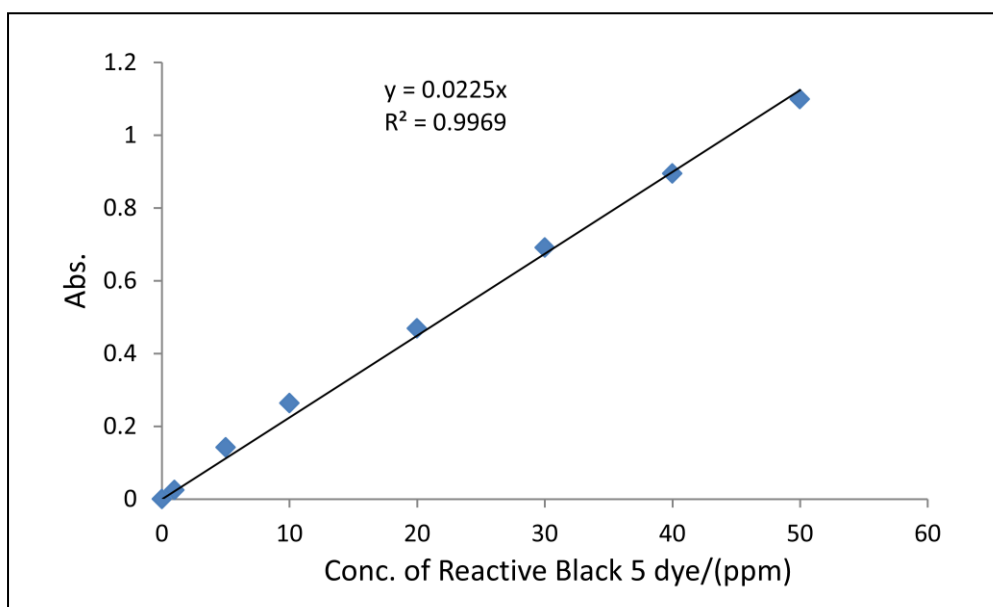
Figure 2-7: Calibration curve at different concentration of RB5 dye.

2.5.2 Kinetic studied of photocatalytic decolorization of dye

Photocatalytic decolorization of RB5 in solution has been performed by focusing UV light irradiation on dye solution in presence of photocatalyst.

The rate constant (k_{app}) of photocatalytic decolorization of RB5 dye was measured using Langmuir-Hinshelwood expression for the first order kinetics according the following equations:[32, 103]

$$C_t = C_o \exp^{(-k_{app} \cdot t)} \qquad \qquad \text{... (2-4)}$$

$$\ln(C_o / C_t) = k_{app} \cdot t \qquad \qquad \text{... (2-5)}$$

where: C_t is a concentration of the reactive black 5 dye at t time of irradiation. C_o is an initial concentration of same studied dye at (dark reaction) in 0 min as the time of irradiation.

The photocatalytic decolorization efficiency (PDE) was calculated via the following equation [104,105]:

$$PDE = \frac{(C_o - C_t)}{C_o} \times 100 \qquad \qquad \text{...(2-6)}$$

2.6 Light Intensity Measurement

The light intensity was calculated through Actinometric method[102], which was widely applied to estimate the light flux density. This method deals with the measurement of the standard or reference photochemical reaction, whose quantum yield is accurately known in order to standardize the used light source. The ferrioxalate actinometric solution was the most used to find the light intensity, which applied on the same photocatalytic reactor. Briefly, freshly prepared was done by mixing 40 mL of 0.15 M (3.94gm) of $Fe_2(SO_4)_3$, 50 mL of 0.45 M(3.74gm) of $K_2C_2O_4$ and 10 mL of 0.05 M of H_2SO_4. After that, the actinometric solution was irradiated from outside using mercury lamp UV (A) for (5, 10 and 15) min. Under these conditions, the color solution changed from yellow to the yellowish green color, that indicated to the generated of ferrioxalate complex $K_3[Fe(C_2O_4)_3].3H_2O$ is formed.

The idea of this reaction was recognized to illuminate undergoes simultaneous reduction of Fe^{3+} to Fe^{2+} and oxidation of oxalate to carbon dioxalate. Under light excitation, the potassium ferrioxalate decomposes according to the following equations [102,106]:

$$Fe(C_2O_4)_3^{3-} \xrightarrow{h\nu} Fe^{2+} + C_2O_4^- + 2C_2O_4^{2-} \qquad \text{...(2-7)}$$

$$Fe(C_2O_4)_3^{3-} + C_2O_4^- \xrightarrow{\Delta} Fe^{2+} + 2CO_2 + 3C_2O_4^{2-} \qquad \text{...(2-8)}$$
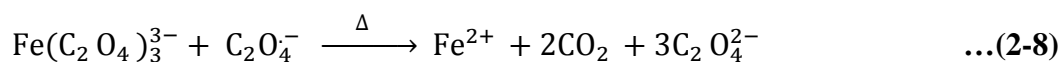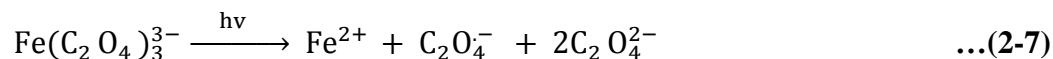
After the passage of irradiation time at (5, 10 and 15) min, exact 2.5mL of the irradiated solution pull it out, and centrifuged at (6000 rpm, for 10 min). After filtration, the 0.5 mL from filtered solution was added to 2.5 mL of 1% from 1, 10-phenanthroline, and a red orange complex (tris-phenanthroline) was occurred.

The quantity of the produced ferrous ions during the irradiation period is monitored by conversion to the colored tris-phenanthroline. The light intensity had been calculated via the following equations [106].

$$I_0 = \frac{A V_1 V_2}{\varepsilon\, t\, Q_\lambda V_2} \qquad \text{...(2-9)}$$

$$I_0 = \frac{1.838 \text{ x } 100 \text{ x } 3}{1045 \text{ x } 1000 \text{ x } 600 \text{ x } 1.2 \text{ x } 0.5} \qquad \text{...(2-10)}$$

$$I_0 = 1.47 \text{X} 10^{-6} \quad \text{Einstein s}^{-1}$$

Where: I_o is light intensity, A is absorbent of ferrous ions tris-phenanthroline at 510 nm, V_1 is volume of solution irradiated (100 cm^3), V_3 is the final volume after complexation with 1, 10-phenonethroline (3 cm^3), ε is molar absorbent coefficient (slope value), t is irradiation time, Q is quantum yield (1.2) and V_2 is the aliquot of the irradiated solution taken for the determination of the ferrous ions (0.5 cm^3).

2.7 Activation Energy

In general, Arrhenius equation [77] played an ideal equation to calculate the activation energy. The equation was plotted in the range of temperatures (283.15 –303.15 K).

$$\text{Ln } k_{app.} = -\frac{Ea}{RT} + \text{Ln } A \qquad \qquad \textbf{... (2-11)}$$

where: k_{app} is apparent rate constant, T is absolute temperature of reaction, Ea is the apparent activation energy, R is the gas constant ($8.314 \text{ J mol}^{-1} \text{ K}^{-1}$), and A is frequency constant

2.8 Thermodynamic Parameters

The thermodynamics parameters such as $\Delta H^{\#}$ and $\Delta S^{\#}$ values were determined by plotting Eyring-Polanyi equation [107]

$$\text{Ln } \frac{k_{app}}{T} = \frac{-\Delta H^{\#}}{RT} + (\text{Ln } \frac{k_B}{h} + \frac{\Delta S^{\#}}{R}) \qquad \qquad \textbf{... (2-12)}$$

Where k_{app} is the apparent rate constant, k_B is Boltzmann's constant, T is the temperature of reaction, R is the gas constant, and h is Plank's constant.

The free energy $\Delta G^{\#}$ [108] was calculated via equation (2-13)

$$\Delta G^{\#} = \Delta H^{\#} - T\Delta S^{\#} \qquad \qquad \textbf{... (2-13)}$$

CHAPTER THREE

RESULTS AND

DISCUSSION

3.1. Characterization of Catalyst
3.1.1. XRD Analysis

The XRD patterns of the ZnS commercial, metalized of ZnS and bare prepared by co-precipitation method are shown in figure 3-1.
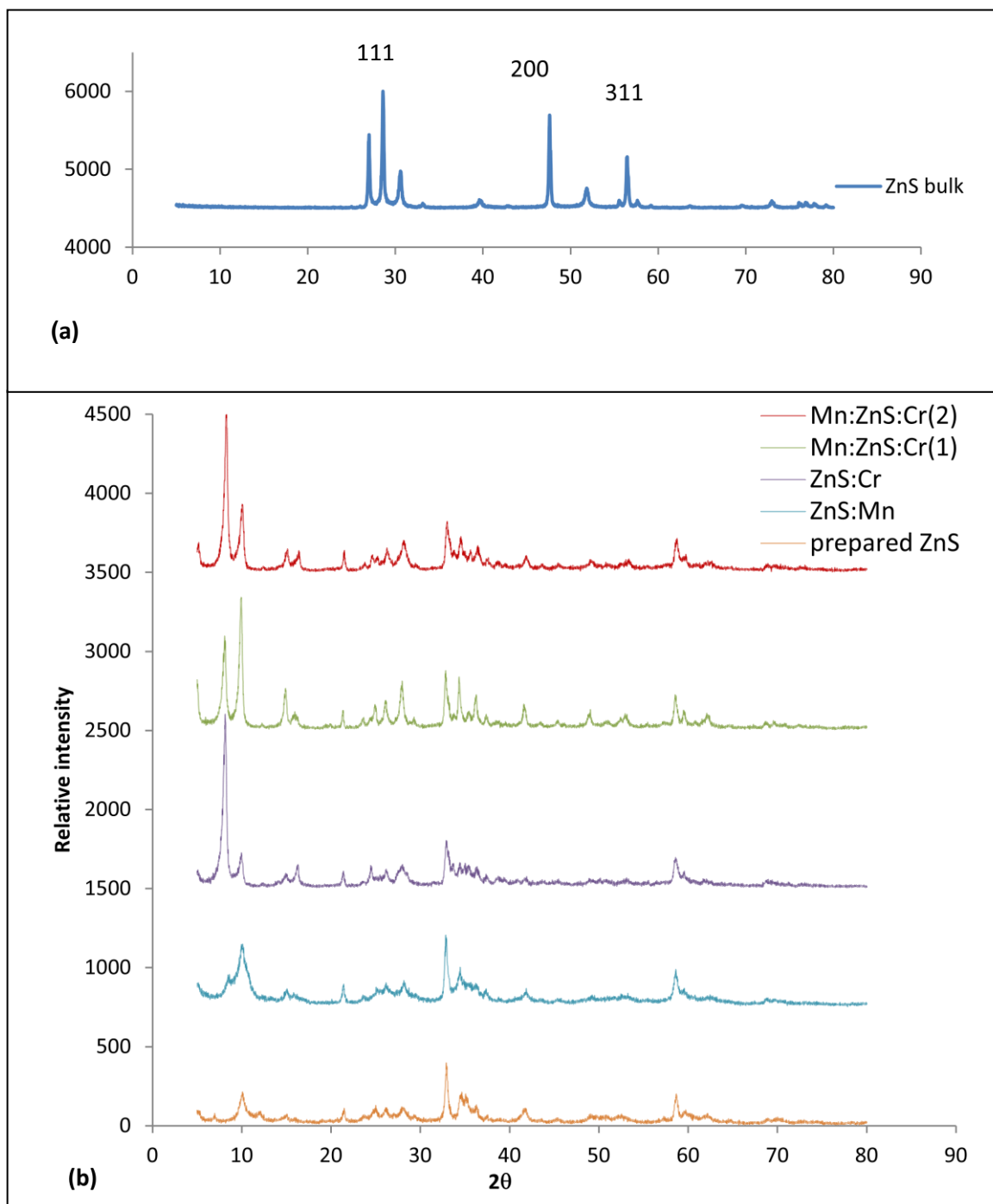
Figure 3-1: (a) XRD patterns for commercial ZnS. (b) XRD patterns for all prepared samples.

3.1.2 Atomic Force Microscopy (AFM)

AFM images were used to measure particle sizes of commercial ZnS, prepared ZnS and metalized as explained in figures 3-2 to 3-7 respectively. Crystallinity index was calculated by depending on particle sizes attained from AFM and mean crystallite sizes obtained from XRD as shown in equation 2-9 and results listed in table 3-1.
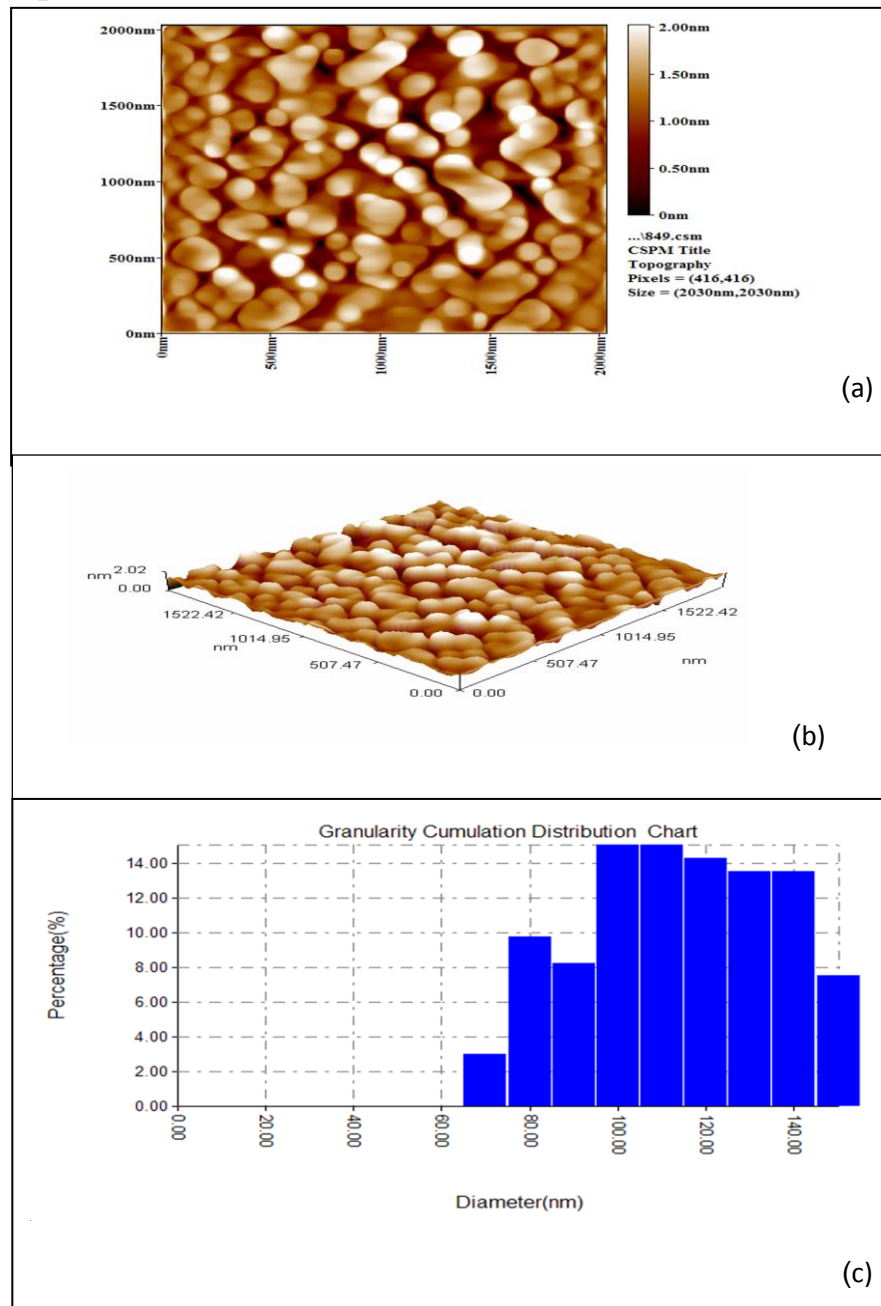
Figure3- 2: AFM Image of commercial ZnS a) 2 - Dimensions Image b) 3- Dimensions Image and c) TheHistogram.
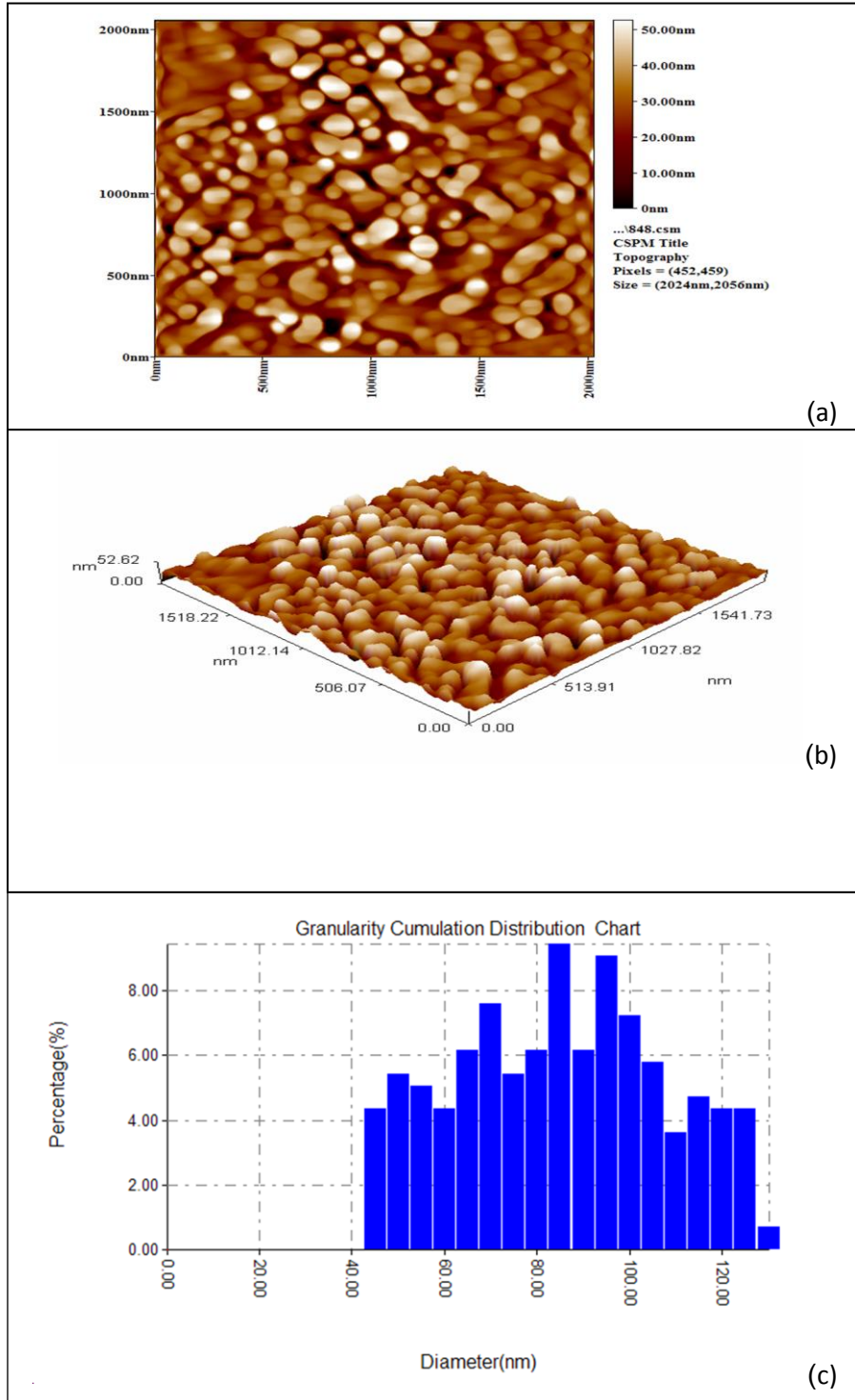
Figure3-3: AFM Image of ZnS :Mn a) 2 - Dimensions Image

b) 3- Dimensions Image and c) TheHistogram.

(a)

(b)

Granularity Cumulation Distribution Chart

(c)
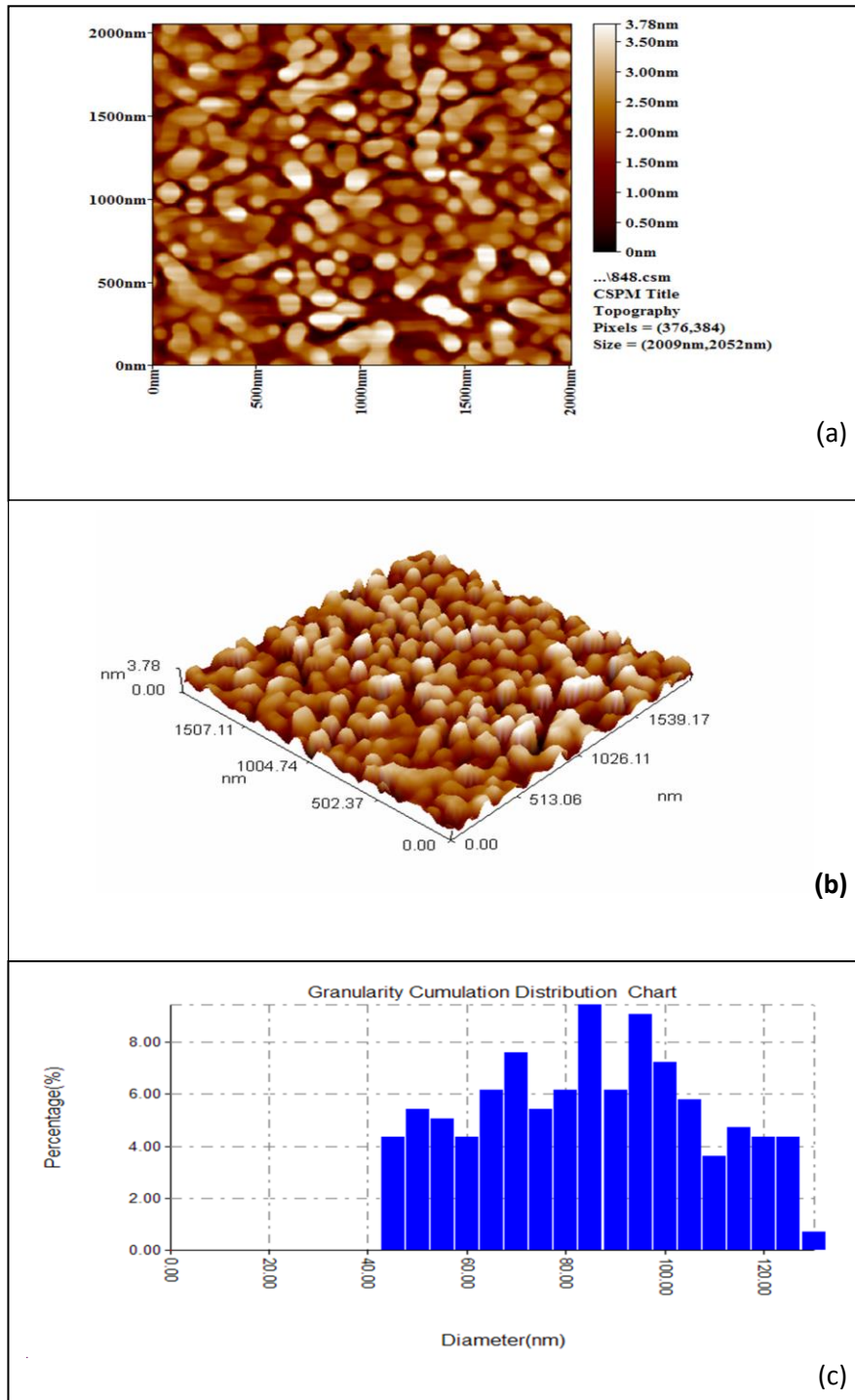
Figure3-4: AFM Image of ZnS: Cr a) 2 - Dimensions Image

b) 3- Dimensions Image and c) TheHistogram.
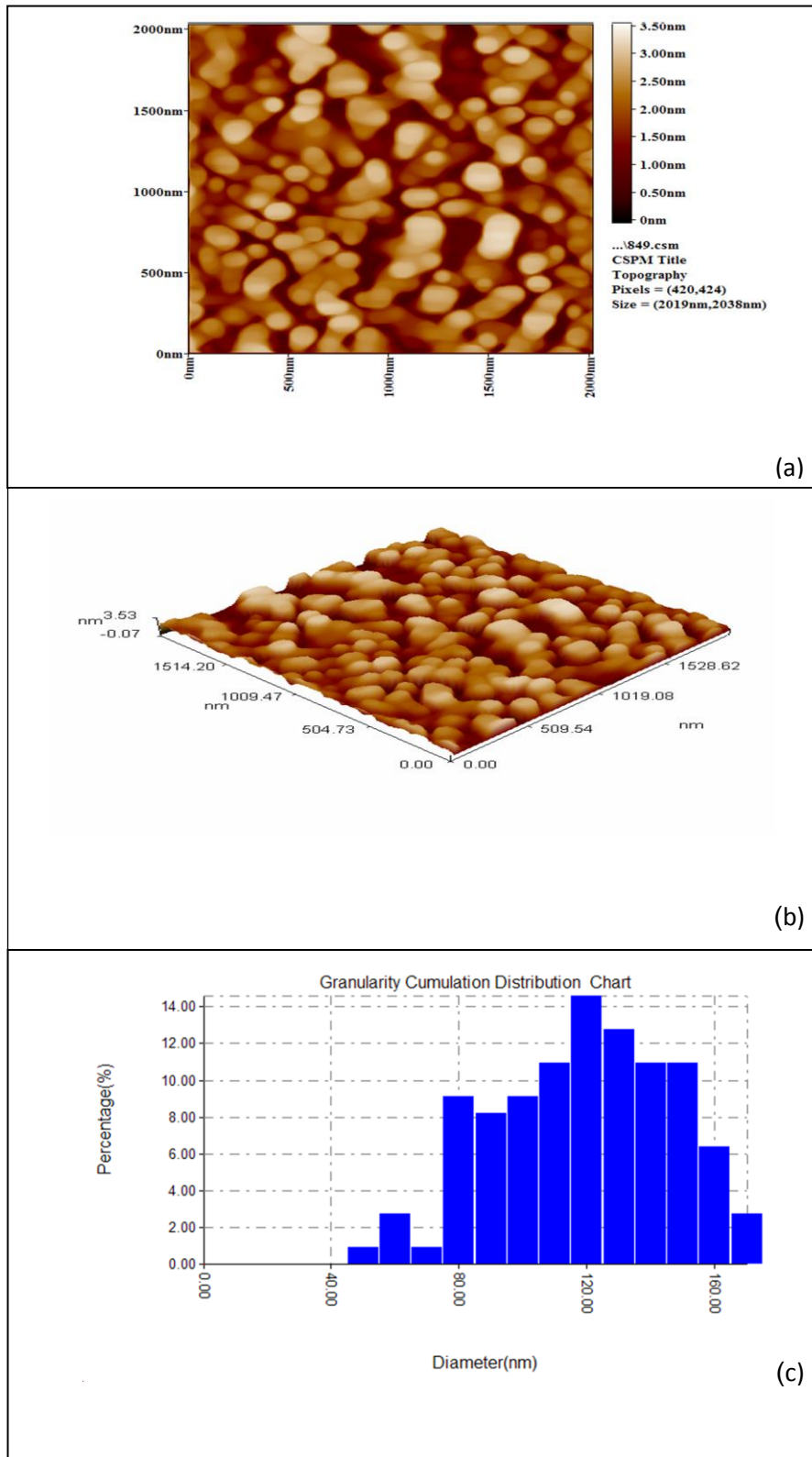
Figure3-5: AFM Image of Mn :ZnS :Cr$_{(1)}$ a) 2 - Dimensions Image

b) 3- Dimensions Image and c) TheHistogram.
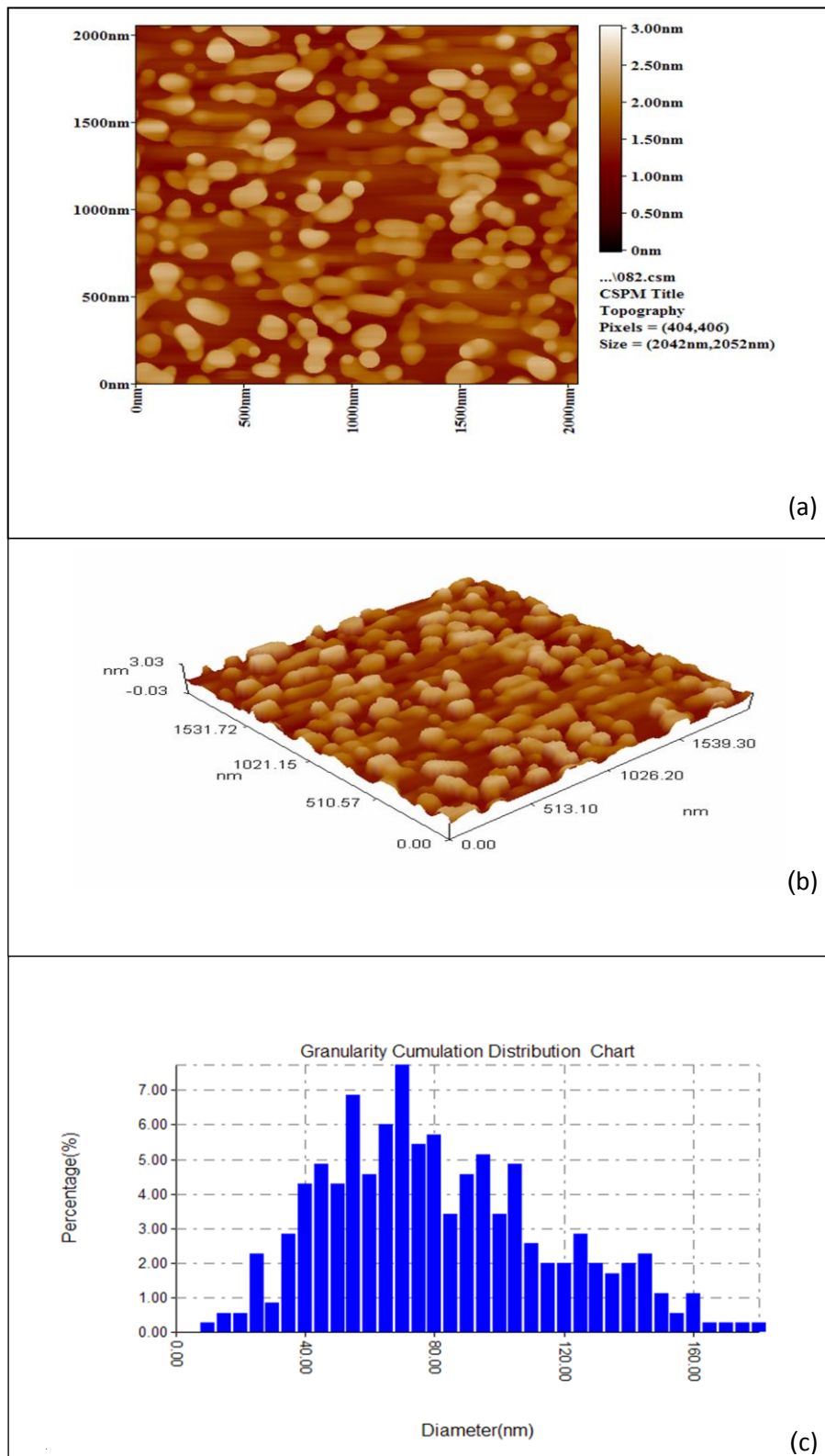
Figure3-6: AFM Image of Mn ZnS :Cr (2) a) 2 - Dimensions Image

b) 3- Dimensions Image and c) TheHistogram.
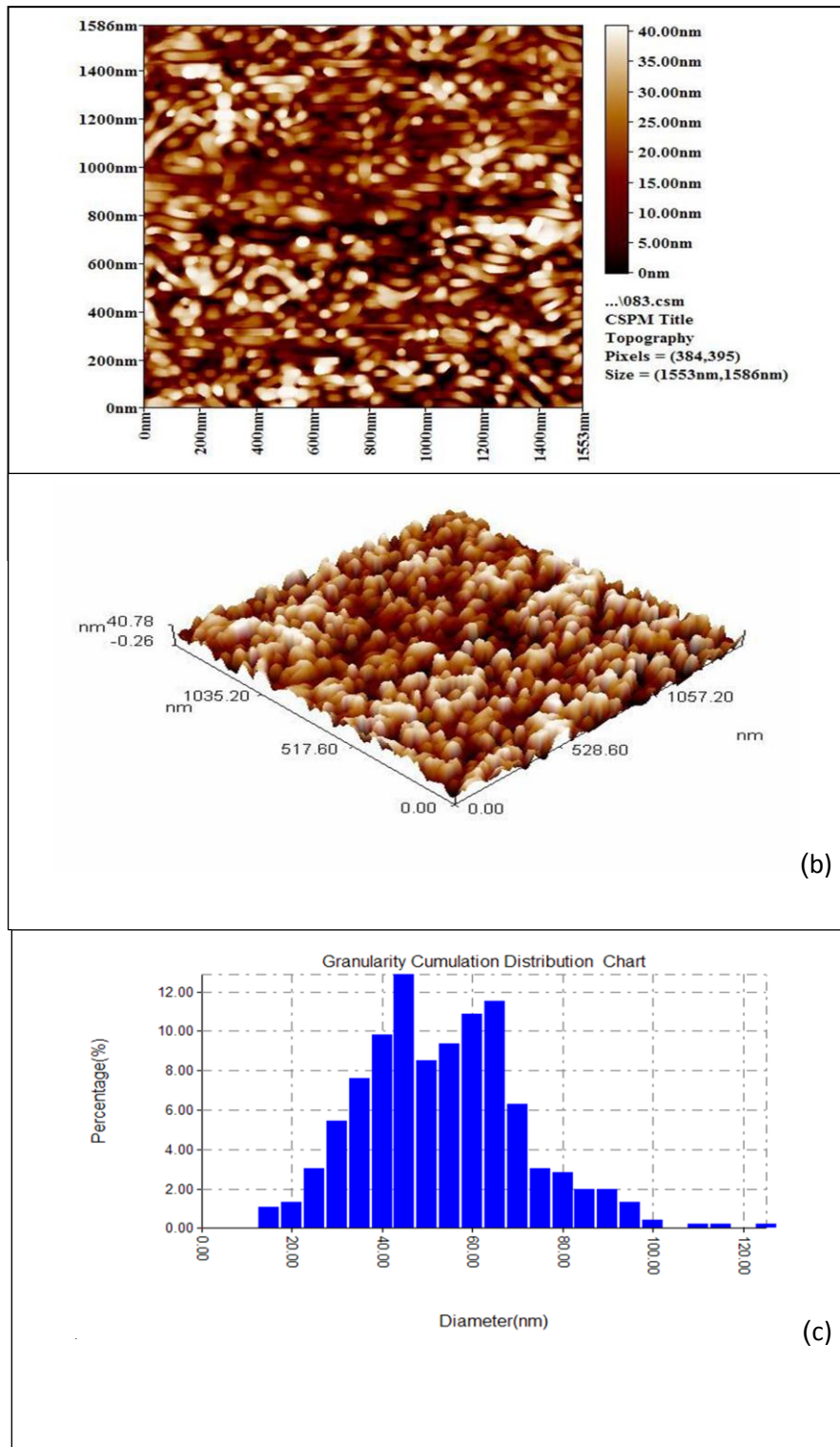
Figure3-7: AFM Image of prepared ZnS bare: a)2 - Dimensions Image b) 3- Dimensions Image and c) TheHistogram.

Table 3-1: Mean Crystallite Sizes and particle sizes of commercial ZnS, prepared ZnS and elements loaded on ZnS.

Sample	Average crystallite size(L)/nm	Particle size /nm	Crystallinty index
commercial ZnS	40.4018	108.870	2.690
ZnS:Mn	15.251	90.250	5.917
ZnS:Cr	16.215	82.330	5.077
Mn:ZnS:Cr$_{(1)}$	18.757	113.880	6.071
Mn:ZnS:Cr$_{(2)}$	17.114	93.740	5.477
Prepared ZnS	19.986	51.020	2.552

3.1.3. Band gap energy measurements

The band gaps for the prepared samples were investigated by measuring the fluorescence spectra in figures 3-8 to 3-13 respectively. The band gaps (Eg) were calculated employing the previous expression in equation 2-10 for optical absorption of the above prepared photo-catalysts and the results are listed in Table 3-2.
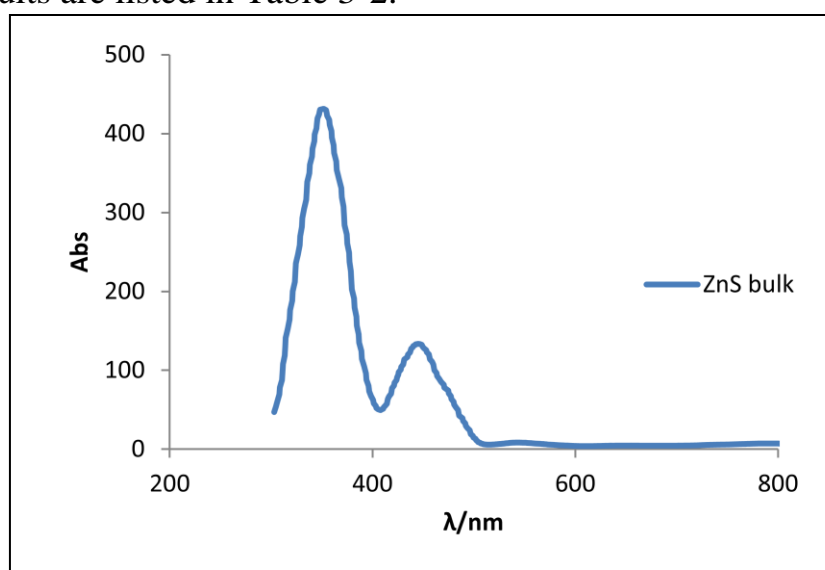
Figure 3-8: Fluorescence spectra of commercial ZnS.
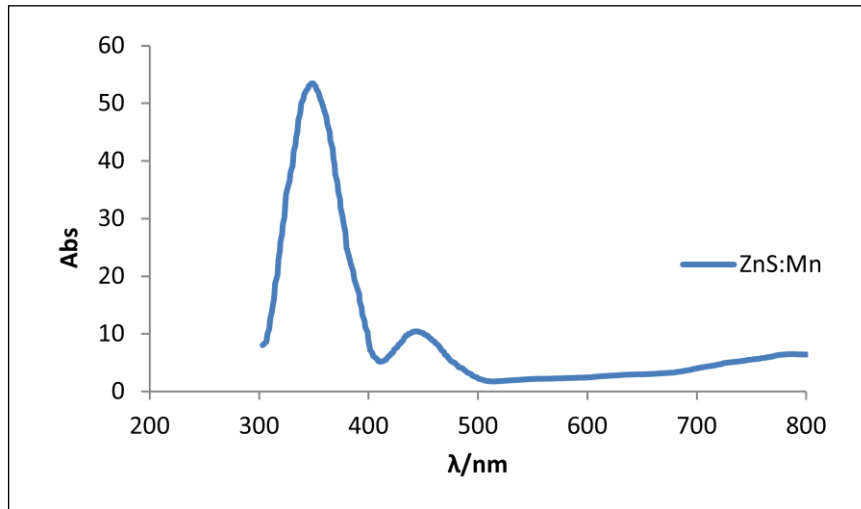
Figure 3-9:   Fluorescence spectra of Mn Loaded on ZnS .
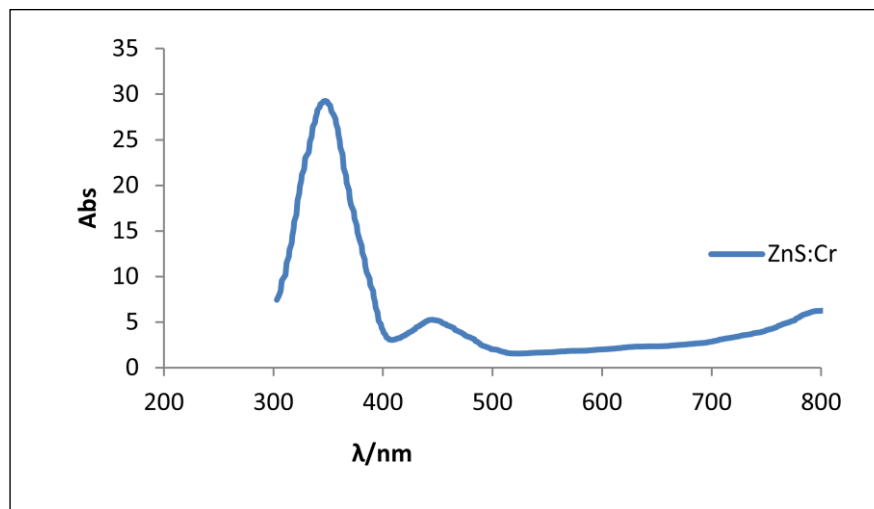
Figure 3-10 : Fluorescence spectra of Cr Loaded on ZnS.
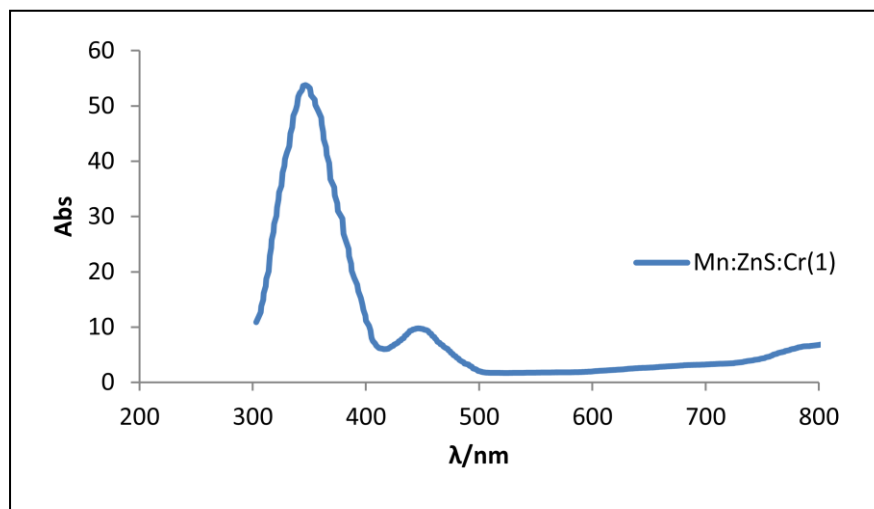
Figure 3-11: Fluorescence spectra of Mn and Cr Loaded on ZnS (1).
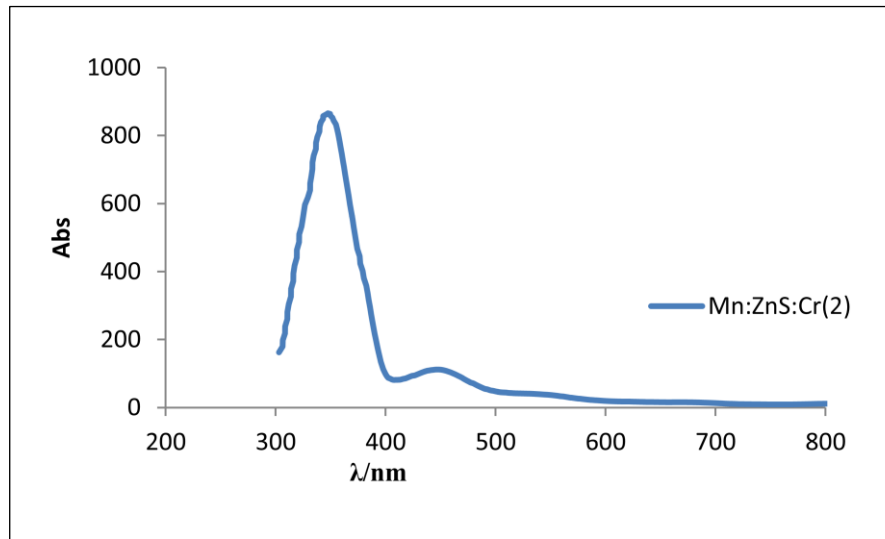
Figure 3-12: Fluorescence spectra of Mn,Cr loaded on ZnS $_{(2)}$.
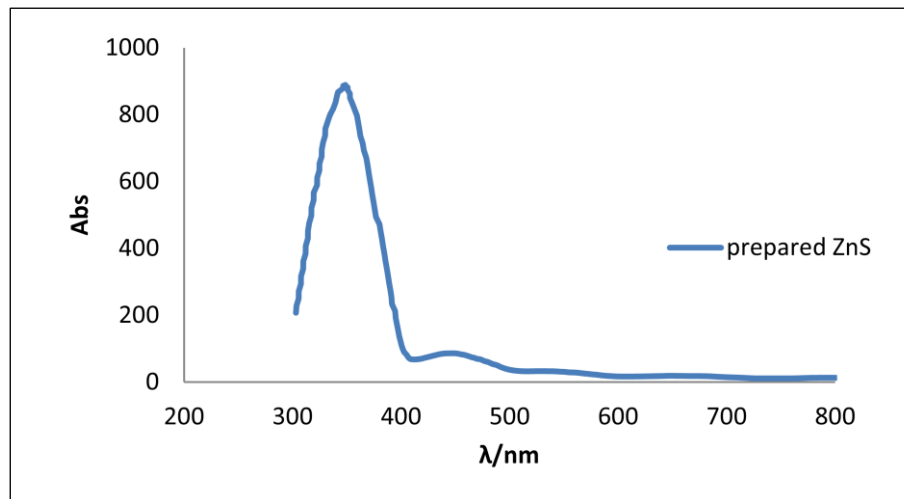
Figure3-13: Fluorescence spectra of prepared ZnS .

Table 3-2: Measured Band gap energy from Fluorescence spectra.

Sample	Commercial ZnS	ZnS:Mn	ZnS:Cr	Mn:ZnS:Cr$_{(1)}$	Mn:ZnS:Cr$_{(2)}$	Prepared ZnS
λ / nm	351.6	348	347.1	346.6	347.5	348.5
E_g / eV	3.526	3.563	3.572	3.577	3.568	3.558

3.1.4 Atomic Absorption Spectrophotometry (A.A)

Atomic absorption spectrometry is an analytical technique that used of the wavelengths of light specifically absorbed by elements to measure

the rest concentrations of elements [109] (Mn, Cr) in solution via loading them on the surface of these samples. The difference between concentrations before and after loading was compared in table 3-3.

Table 3-3: **Loaded Calculations of Mn,Cr on prepared ZnS Surface**

sample	[Cr] /ppm before loaded	[Cr]/ppm After loaded	[Mn]/ppm before loaded	Mn/ppm After loaded
ZnS:Mn	-	-	9895.500	32.003
ZnS:Cr	7916.260	0.0795	-	-
Mn:ZnS:Cr$_{(1)}$	7916.260	0.0341	9895.500	21.317
Mn:ZnS:Cr$_{(2)}$	7916.260	0.0079	9895.500	21.836

3.2 Effect of different parameters on the photocatalytic decolorization of RB5.

3.2.1. Effect of the mass of commercial ZnS

The effect of commercial ZnS dose on the photocatalytic for decolourization of RB5 dye solution that shown in figure 3-14(a), the rates of reaction were found to be directly proportional to the catalyst dosage from 0.5 to 3 g/100 mL. The decolourization rate levels reach maximum at 2.5g/100 mL as optimum catalyst commercial ZnS dosage. The results are listed in tables 3-4 and 3-5 and plotted in figures 3-14(b) and 3-15.

Table 3-4: The change of ln C_o/C_t with irradiation time at different mass of commercial ZnS.

Time of irradiation t/min	Dose/ g	ln C_o/C_t					
		0.5	0.75	1	2	2.5	3
0	0	0	0	0	0	0	0
10		0.110	0.200	0.634	0.598	0.985	0.740
20		0.200	0.247	-	1.161	1.688	1.639
30		0.298	0.414	1.678	1.738	2.123	1.639
40		0.414	0.633	1.752	2.912	-	-
50		0.510	0.807	-	-	-	-
60		-	0.807	1.919	-	-	-
70		0.674	1.032	2.269	-	-	-
80		0.994	1.454	2.336	-	-	-
90		-	1.890	2.525	-	-	-
100		-	-	2.659	-	-	-
k_{app}/min^{-1}		0.010	0.017	0.051	0.066	0.089	0.079

Table 3-5: The change of irradiation time with PDE% on different mass of commercial ZnS.

Time of irradiation t/min	Dose/ g	PDE%					
		0.5	0.75	1	2	2.5	3
0	0	0	0	0	0	0	0
10	10.465	18.160	46.999	45.047	62.681	52.320
20	18.139	21.933	71.333	68.690	81.521	80.590
30	25.813	33.962	81.333	82.428	88.043	90.717
40	33.953	46.933	82.666	-	-	-
50	40	55.424	83.333	-	-	-
60	-	55.424	85.333	-	-	-
70	49.069	64.386	89.666	-	-	-
80	63.023	76.650	90.333	-	-	-
90	-	84.905	92	-	-	-
100	-	-	93	-	-	-

3.2.2. Effect of initial pH of the solution

The most important parameter that influences on the photocatalytic decolourization of dye is the initial pH of solution, the relationship between the rate constant and pH is explained at conducting a series of experiments of dye concentration 25 ppm in 100 mL, dose of ZnS bulk is 2.5 g/100 mL within range pH (3-11), light intensity equal to 1.47×10^{-6} Einstein s^{-1}. The kinetic results listed in tables 3-6 and 3-7 and plotted in figures 3-22 and 3-23. The rate constant of reaction increases with increasing the solution pH up to the maximum level at pH=4.1 and then decrease. The decolorization percentage of BR5 increased with the increase of pH and the maximum of efficiency percentage 92.326% at 25 min.

Table 3-6: The change of ln C_o/C_t with irradiation time at different initial pH of dye by commercial ZnS.

Time of irradiation t/min	pH	ln C_o/ C_t						
		3	4.1	6.3	7	8	9	11
0	0	0	0	0	0	0	0	0
5		0.471	0.672	1.815	0.575	0.449	0.251	0.050
10		0.908	1.319	2.679	1.005	0.787	0.467	0.103
15		1.255	1.813	5.111	1.420	1.070	0.666	-
20		1.509	2.646	5.411	1.536	1.1082	0.793	0.229
25		1.789	2.869	8.117	1.942	-	1.013	0.287

30	1.819	-	8.363	-	1.682	1.188	-
35	2.295	-	8.117	-	2.309	1.332	0.428
40	-	-	-	-	-	-	0.521
50	-	-	-	-	-	-	0.666
55	-	-	-	-	-	-	0.776
65	-	-	-	-	-	-	0.928
70	-	-	-	-	-	-	1.107
k_{app}/min^{-1}	0.068	0.122	0.089	0.082	0.062	0.039	0.014

Table 3-7: The change of irradiation time with PDE%. at different initial pH of dye by commercial ZnS.

Time of irradiation t/min	pH	PDE%						
		3	4.1	6.3	7	8	9	11
0		0	0	0	0	0	0	0
5		37.592	48.936	44.927	43.773	36.217	22.260	4.910
10		59.705	73.286	62.681	63.396	54.487	37.328	9.821
15		71.498	83.687	80.434	75.849	65.705	48.630	
20		77.886	92.907	81.521	78.490	66.987	54.794	20.535
25		83.292	94.326	87.681	85.660	-	63.698	25
30		83.783	-	88.043	-	81.410	69.520	-
35		89.926	-	87.681	-	90.064	73.630	34.821
40		-	-	-	-	-	78.767	40.625
50		-	-	-	-	-	-	48.660
55		-	-	-	-	-	-	54.017
60		-	-	-	-	-	-	59.598
65		-	-	-	-	-	-	60.491
70		-	-	-	-	-	-	66.964

3.2.3. Effect of temperature

The photocatalytic decolorization of RB5 was studied at different temperatures in the range (283.15-303.15) K. Under the determined experimental condition with initial dye concentration equal to 25ppm, ZnS dosage 2.5 g /100mL pH equal to 4.1, light intensity equal to1.47x10^{-6} Einstein. The results indicate that the decolorization efficiency of RB5 decreases with increase of temperature. The results are listed in tables 3-8,3-9 and 3-10 and plotted in figures 4-17. Arrhenius relationship is plotted in figure 3-31(a) to calculate the activation energy of the reaction. Moreover, Eyring equation is plotted in figure 3-31(b) to calculate the change in entropy and change in enthalpy for this photoreaction. The results of the activation energy and the thermodynamics functions are shown in Table 3-11.

Table 3-8: The change of $\ln C_o/C_t$ with irradiation time at different temperature by commercial ZnS.

Time of irradiation t/min	T/°C				
	$\ln C_o / C_t$				
	10	17	20	25	30
0	0	0	0	0	0
5	0.276	0.596	0.257	0.111	0.161
10	0.732	0.985	0.363	0.320	0.403
15	1.203	1.631	0.686	0.405	0.551
20	1.516	1.688	-	0.618	0.460
25	1.878	2.094	1.036	0.728	0.551
30	2.330	-	1.223	0.951	0.809
35	-	-	1.351	1.352	1.013
40	-	-	1.729	-	1.129
k_{app}/min^{-1}	0.076	0.089	0.041	0.033	0.027

Table 3-9: The change of irradiation time with PDE% at different temperature of dye by commercial ZnS.

Time of irradiation t/min	T/°C				
	PDF%				
	10	17	20	25	30
0	0	0	0	0	0
5	24.166	44.927	22.695	10.591	14.939
10	51.944	62.681	30.496	27.414	33.231
15	70	80.434	49.645	33.333	42.378
20	78.055	81.521	-	46.105	36.890
25	84.722	87.681	64.539	51.713	42.378
30	90.277	-	70.567	61.370	55.487
35	-	-	74.113	74.143	63.719
40	-	-	82.269	-	67.682

Table 3-10: Relationship between 1/T with $\ln k_{app}$ and $\ln(k_{app}/T)$.

1/T(K)	$\ln k_{app}$	$\ln(k_{app}/T)$
3.531	-2.570	-8.216
3.446	-2.410	-8.080
3.411	-3.186	-8.867
3.354	-3.405	-9.102
3.298	-3.586	-9.300

Table 3-11: The calculated activation kinetic and thermodynamics parameters for decolourization of RB5 with using commercial ZnS.

Sample	Ea / kJmol^{-1}	$\Delta H^{\#}$ / kJ mol^{-1}	$\Delta S^{\#}$ / J mol^{-1}K^{-1}	$\Delta G^{\#}$ /kJ mol^{-1}
Commercial ZnS	42.350	-44.790	-6.114	-43.018

3.2.4. Effect of addition of K$_2$S$_2$O$_8$

Under the determined experimental condition with 25ppm of studied dye, 2.5 g /100mL of ZnS dosage, best pH at 4.1 and best temperature 290.15 K, light intensity equal to1.47x10^{-6} Einstein. The photocatalytic decolorization rate of RB5 increased with increasing the addition of K$_2$S$_2$O$_8$ and reached to maximum value at 8 mmole/L, and then it decreases that due to K$_2$S$_2$O$_8$ acts as a scavenger for •OH. The results listed in the tables 3-12 and 3-13and plotted in figures 3-38 and 3-39.

Table 3-12: The change of ln C$_o$/C$_t$ with irradiation time at different addition of K$_2$S$_2$O$_8$ for commertial ZnS.

Time of irradiation t/min	K$_2$S$_2$O$_8$/ mmole L^{-1}	0	3	4	5	7	8	9	10
0	0	0	0	0	0	0	0	0	0
0.5	-		-	-	-	-	-	0.378	0.011
1	-		-	-	-	-	0.462	0.697	-
1.5	-		-	-	-	-	-	1.096	0.391
2	-		-	0.354	0.338	0.705	0.871	1.246	0.835
2.5	-		-	-	-	-	-	1.677	1.597
3	-		0.726	-	-	-	1.285	2.147	2.062
3.5	-		-	-	-	-	-	2.448	2.157
4	-		-	0.680	0.606	1.403	1.768	-	-
5	0.596		-	-	-	-	2.138	-	-
6	-		0.861	0.922	0.912	1.853	2.419	-	-
7	-		-	-	-	-	2.895	-	-
8	-		-	1.334	1.304	2.660	-	-	-
9	-		1.319	-	-	-	-	-	-
10	0.985		-	1.674	1.572	3.255	-	-	-
12	-		1.711	2.107	1.786	-	-	-	-
14	-		-	2.513	2.292	-	-	-	-
15	1.631		1.935	-	-	-	-	-	-
18	-		2.127	-	-	-	-	-	-
20	1.688		-	-	-	-	-	-	-
25	2.094		-	-	-	-	-	-	-
k$_{app}$/min^{-1}	0.089		0.130	0.137	0.157	0.327	0.418	0.011	0.009

Table 3-13: The change of irradiation time with PDE% at different addition of $K_2S_2O_8$ for ZnS commercial.

Time of irradiation t/min	$K_2S_2O_8$ / mmole L^{-1}	PDE%							
		0	3	4	5	7	8	9	10
0	0	0	0	0	0	0	0	0	0
0.5	-	-	-	-	-	-	-	31.54	1.156
1	-	-	-	-	-	-	37.01	50.23	-
1.5	-	-	-	-	-	-	-	66.58	32.36
2	-	-	-	29.87	28.72	50.602	58.17	71.26	56.64
2.5	-	-	-	-	-	-	-	81.30	79.76
3	-	-	51.624	-	-	-	72.35	88.31	87.28
3.5	-	-	-	-	-	-	-	91.35	88.43
4	-	-	-	49.36	45.47	75.421	82.93	-	-
5	32.857	-	-	-	-	-	88.22	-	-
6	-	-	57.761	60.25	59.84	84.337	91.10	-	-
7	-	-	-	-	-	-	94.47	-	-
8	-	-	-	73.67	72.87	93.012	-	-	-
9	-	-	73.285	-	-	-	-	-	-
10	52.285	-	-	81.26	79.25	96.144	-	-	-
12	-	-	81.949	87.84	83.24	-	-	-	-
14	-	-	-	91.89	89.89	-	-	-	-
15	67.714	-	85.559	-	-	-	-	-	-
18	-	-	88.086	-	-	-	-	-	-
20	72.000	-	-	-	-	-	-	-	-
21	-	-	89.891	-	-	-	-	-	-
25	78.857	-	-	-	-	-	-	-	-
30	87.142	-	-	-	-	-	-	-	-
35	92.571	-	-	-	-	-	-	-	-

3.3 Effect of different parameters on the photocatalytic decolorization of RB5 dye for Cr: ZnS

3.3.1. Effect of the mass of Cr: ZnS

These experiments were carried out at different doses of in the ranged 0.5 g to 2 g/100mL of Cr: ZnS at pH 6.3 and temperature 290.15 K light, intensity equal to$1.47x10^{-6}$ Einstein. The results are given in tables 3-14 and 3-15 and plotted in figures 3-16and 3-17. The photo-decolorization efficiency with using Cr :ZnS was increment with the increasing of the dosage of catalyst and the maximum value was found at 1g/100mL.

Table 3-14: The change of ln C_o/C_t with irradiation time at different mass of ZnS :Cr.

Time of irradiation t/min	Dose/ g	$ln\ C_o/C_t$			
		0.5	0.75	1	2
0	0		0	0	0
5	0.101		0.010	0.229	0.038
10	0.188		0.036	0.391	0.093
20	-		0.155	0.459	0.102
30	-		0.250	0.875	0.127
40	-		0.305	1.210	0.135
50	0.655		0.312	1.373	0.110
60	-		0.497	1.438	0.144
70	0.935		0.642	-	0.127155
80	1.134		0.713	-	0.188
90	1.225		0.756	-	0.179
100	1.315		-	2.105	0.045
110	1.425		-	2.187	0.282
120	1.501		-	2.277	0.253
130	1.512		-	2.607	0.263
140	1.789		1.260	2.698	0.188
150	1.661		1.530	2.798	
155	-		-	-	0.282
160	1.688		1.578	2.852	-
170	-		2.176	-	0.225
180	-		2.559	-	-
185	-		-	-	0.272
200	-		-	-	0.515
215	-		-	-	0.541
k_{app}/min^{-1}	0.012		0.011	0.019	0.002

Table 3-15: The change of irradiation time with PDE% at different mass of ZnS :Cr.

Time of irradiation t/min	Dose/ g	PDE %			
		0.5	0.75	1	2
0	0		0	0	0
5	9.620		1.030	20.512	3.731
10	17.21		3.608	32.371	8.955
20	42.025		14.432	36.858	9.701
30	41.265		22.164	58.333	11.940
40	47.848		26.288	70.192	12.686
50	48.101		26.804	74.679	10.447

60	46.582	39.175	76.282	13.432
70	60.759	47.422	85.897	11.940
80	67.848	51.030	86.538	17.164
90	70.632	53.092	86.858	16.417
100	73.164	52.061	87.820	4.477
110	75.949	56.185	88.782	24.626
120	77.721	59.793	89.743	22.388
130	77.974	67.525	92.628	23.134
140	83.291	71.649	93.269	17.164
150	81.012	78.350	93.910	-
155	-	-	-	24.626
160	81.518	79.381	94.230	-
170	-	88.659	-	20.149
180	-	92.26804	-	-
185	-	-	-	23.880
200	-	-	-	40.298
215	-	-	-	41.791

3.3.2. Effect of initial pH of the solution

Initial pH of 25 ppm solution of RB5was investigated when control the pH ranges of (3-11), using 1g of Cr: ZnS at 290.15 K, light intensity equal to1.47x10^{-6} Einstein. The practically data explain in tables 3-16 and 3-17, and drawn in figures 3-24and 3-25 The best photocatalytic decolorization of studied dye occurred at pH 4.1.

Table 3-16: The change of $\ln(C_o/C_t)$ with irradiation time at different initial pH of dye by Cr: ZnS.

Time of irradiation t/min	pH	$\ln C_o/C_t$						
		3	4.1	6.3	7.1	8	9	11
0	-	-	0	0	0	0	0	0
2	-	-	0.016	-	-	-	-	-
4	-	-	0.045	-	-	-	-	-
5	-	0.17768	-	0.229	0.049	0.075	0.043	0.016
6	-	-	0.057	-	-	-	-	-
8	-	-	0.081	-	-	-	-	-
10	-	-	0.088	0.391	-	0.188	0.088	0.044
12	-	-	0.131	-	-	-	-	-

14	-	0.171	-	-	-	-	-
16	-	0.184	-	-	-	-	-
18	-	0.225	-	-	-	-	-
20	-	0.269	0.459	0.013	-	0.189	0.069
25	-	0.419	-	-	-	-	-
30	-	0.566	0.875	-	-	-	0.085
35	-	0.649	-	-	-	-	-
40	-	0.727	1.210	-	-	-	0.105
45	-	0.825	-	-	-	-	-
50	-	0.891	1.373	-	-	-	0.151
60	-	-	1.438	0.710	0.463	-	0.217
70	-	-	-	0.719	0.545	-	-
75	0.978	-	-	-	-	-	0.314
80	1.009	-	-	0.746	0.604	-	-
85	-	2.046	-	-	-	-	-
90	1.110	-	-	0.853	0.740	-	0.384
100	1.122	-	2.105	0.927	0.641	-	-
105	-	-	-	-	-	-	0.468
110	1.394	-	2.187	0.905	0.693	0.649	-
115	-	-	-	-	-	-	-
120	1.492	-	2.277	0.949	0.991	0.659	0.579
130	1.545	-	2.607	1.031	1.000	0.790	-
135	-	-	-	-	-	-	0.70415
140	1.6017		2.698	1.056	1.125	0.844	
145	-	-	-	-	-	-	-
150	-	-	2.798	1.081	1.177	0.876	-
155	-	-	-	-	-	-	0.855
160	-	-	2.852	-	-	0.955	-
170	-	-	-	-	-	1.057	1.023
180	-	-	-	-	-	1.136	-
185	-	-	-	-	-	-	1.288
190	-	-	-	-	-	1.259	-
k_{app}/min^{-1}	0.012	0.020	0.009	0.007	0.007	0.006	0.005

Table 3-17: Change of irradiation time with PDE% at different initial pH of dye by Cr: ZnS.

Time of irradiation t/min	pH	PDE %						
		3	4.1	6.3	7.1	8	9	11
0	0	0	0	0	0	0	0	0
2		-	1.685	-	-	-	-	-
4		-	4.494	-	-	-	-	-
5	16.279		-	20.512	4.782	7.2847	4.244	1.642

6	-	5.617	-	-	-	-	-
8	-	7.865	-	-	-	-	-
10	36.434	8.426	32.371	-	17.218	8.488	4.379
12	-	12.359	-	-	-	-	-
14	-	15.730	-	-	-	-	-
16	-	16.853	-	-	-	-	-
18	-	20.224	-	-	-	-	-
20	52.325	23.595	36.858	1.304	29.801	17.241	6.751
25	-	34.269	-	-	-	-	-
30	55.426	43.258	58.333	15.652	37.417	24.137	8.211
35	-	47.752	-	-	-	-	-
40	-	51.685	70.192	22.173	39.072	29.177	10.036
45	-	56.179	-	-	-	-	-
50	58.914	58.988	74.679	47.826	40.728	33.952	14.051
55	59.302	60.674	-	-	-	-	-
60	62.015	61.235	76.282	50.869	37.086	-	19.525
65	-	61.797	-	-	-	-	-
70	62.403	62.921	85.897	51.304	42.052	-	-
75	-	66.853	-	-	-	-	27.007
85	-	87.078	-	-	-	-	-
90	67.054	-	86.858	57.391	52.317	-	31.934
100	67.441	-	87.820	60.434	47.350	-	-
105	-	-	-	-	-	-	37.408
110	75.193	-	88.782	59.565	49.999	47.745	-
120	77.519	-	89.743	61.304	62.913	48.275	43.978
130	78.682	-	92.628	64.347	63.245	54.641	-
135	-	-	-	-	-	-	50.547
140	79.844	-	93.269	65.217	67.549	57.029	-
150	-	-	93.910	66.086	69.205	58.355	-
155	-	-	-	-	-	-	57.481
160	-	-	94.230	-	-	61.538	-
170	-	-	-	-	-	65.252	64.051
180	-	-	-	-	-	67.904	-
185	-	-	-	-	-	-	72.445
190	-	-	-	-	-	71.618	-
200	-	-	-	-	-	73.740	80.291
210	-	-	-	-	-	75.862	-

3.3.3. Effect of temperature

The figures 4-23 and 4-24 note that the photocatalytic decolorization of RB5 dye on ZnS:Cr by keeping all other experimental conditions constant at different temperature was raised with decreasing temperature. This behavior indicates the reaction is exothermic. The values of apparent

activation energy and $\Delta H^{\#}, \Delta S^{\#}$ by Erying equation were shown in tables from 3-18 to 3-21 and plotted in figures 3-32 and 3-33.

Table 3-18: Relationship between 1/T with lnk$_{app}$ and ln(k$_{app}$/T).

1/T(K)	ln k$_{app}$	ln(k$_{app}$/T)
3.531	-4.350	-9.996
3.470	-4.500	-10.239
3.446	-4.585	-10.255
3.411	-4.767	-10.436

Table 3-19: The calculated activation kinetic and thermodynamics parameters for decolourization of RB5 with using Cr: ZnS.

Sample	Ea /kJ mol^{-1}	$\Delta H^{\#}$ /kJ mol^{-1}	$\Delta S^{\#}$ /J mol^{-1}K^{-1}	$\Delta G^{\#}$ /kJmol^{-1}
Cr:ZnS	27.954	-29.230	-5.550	-27.625

Table 3-20: The change of lnC$_o$/C$_t$ with irradiation time at different temperature by Cr: ZnS.

Time of irradiation t/min	T/°C	ln C_o/ C_t			
		10	15	17	20
0	0	0	0	0	0
5		0.165	0.135	0.071	0.119
10		0.202	0.188	0.171	0.187
15		-	-	0.221	-
20		0.249	0.262	0.267	0.195
30		0.375	0.395	-	-
40		0.525	0.553	0.333	0.395
50		0.559	0.662	-	0.509
60		0.757	0.760	-	0.521
70		0.965	0.766	-	0.525
80		1.054	0.796	-	0.655
90		1.129	-	0.755	0.727
100		-	-	0.782	0.826
110		-	-	0.884	1.006
120		-	-	0.945	1.118

130	-	1.361	1.009	1.081
140	-	-	-	1.163
k_{app}/min^{-1}	0.012	0.010	0.010	0.008

Table 3-21: The change of irradiation time with PDE% at different temperature of dye by Cr:ZnS .

Time of irradiation	T/°C	PDE %			
		10	15	17	20
0	0	0	0	0	0
5		15.288	12.676	6.882	11.298
10		18.295	17.183	15.789	17.067
15		-	-	19.838	-
20		22.055	23.098	23.481	17.788
30		31.328	32.676	27.530	14.903
40		40.852	42.535	28.340	32.692
50		42.857	48.450	29.149	39.903
60		53.132	53.239	29.554	40.625
70		61.904	53.521	39.271	40.865
80		65.162	54.929	50.202	48.076
90		67.669	55.211	53.036	51.682
100		77.694	55.492	54.251	56.25
110		78.696	62.253	58.704	63.461
120		-	67.887	61.133	67.307
130		-	74.366	63.562	66.105
140		-	74.929	63.967	68.75

3.3.4. Effect of addition of $K_2S_2O_8$

Under the determined experimental conditions with 25ppm of dye concentration,1 g /100mL from Cr:ZnS dosage, initial pH equal to 4.1 and temperature at 290.15K, light intensity equal to1.47x10^{-6} Einstein.. The rate of photocatalytic decolorization of RB5 was raised with increasing the addition of $K_2S_2O_8$ and reached to maximum value at 7mmole/L, after that the rate was decreased. The measured results listed in the tables 3-22 and 3-23and plotted in figures 3-40and 3-41.

Table 3-22: The change of $\ln C_0/C_t$ with irradiation time at different addition of $K_2S_2O_8$ for Cr: ZnS.

Time of irradiation t/min	$K_2S_2O_8$ / mmole L^{-1} — $\ln C_o/C_t$						
	0	3	4	7	8	9	10
0	0	0	0	0	0	0	0
2	-	-	-	-	0.094	-	-
4	-	-	-	-	0.160	-	-
5	0.229	0.050	0.140	0.419	-	0.186	0.129
10	0.391	0.202	-	0.874	-	0.730	0.894
15	-	0.371	0.381	2.456	1.795	1.591	-
20	0.459	0.530	0.706	2.967	2.984	-	1.972
25	-	0.887	0.922	4.066	-	-	2.493
30	0.875	1.939	-	5.164	-	-	2.730
35	-	2.034	2.246	-	-	-	-
40	1.210	-	-	-	-	-	-
50	1.373	-	-	-	-	-	-
60	1.438	-	-	-	-	-	-
100	2.105	-	-	-	-	-	-
110	2.187	-	-	-	-	-	-
120	2.277	-	-	-	-	-	-
130	2.607	-	-	-	-	-	-
140	2.698	-	-	-	-	-	-
150	2.798	-	-	-	-	-	-
160	2.852	-	-	-	-	-	-
k_{app}/min^{-1}	0.039	0.048	0.048	0.159	0.123	0.091	0.094

Table 3-23: The change of irradiation time with PDE% at different addition of $K_2S_2O_8$ for Cr:ZnS.

Time of irradiation t/min	$K_2S_2O_8$/ mmole L^{-1} — $PDE\%$						
	0	3	4	7	8	9	10
0	0	0	0	0	0	0	0
2	-	-	-	-	9.025	-	-
4	-	-	-	-	14.801	-	-
5	20.512	4.901	13.141	34.28	-	17.03	12.173
6	-	-	-	-	23.465	-	-
8	-	-	-	-	25.992	-	-
10	32.371	18.300	16.666	58.28	42.960	51.85	59.130
15	-	31.045	31.730	91.42	83.393	79.62	-
20	36.858	41.176	50.641	94.85	94.945	83.70	86.086
25	-	58.823	60.256	98.28	96.028	85.55	91.739

30	58.333	85.620	75.320	99.42	-	-	93.478
35	-	86.928	89.423	-	-	-	-
40	70.192	92.156	-	-	-	-	-
45	-	95.424	-	-	-	-	-
50	74.679	-	-	-	-	-	-
60	76.282	-	-	-	-	-	-
70	85.897	-	-	-	-	-	-
80	86.538	-	-	-	-	-	-
90	86.858	-	-	-	-	-	-
100	87.820	-	-	-	-	-	-
110	88.782	-	-	-	-	-	-
120	89.743	-	-	-	-	-	-
130	92.628	-	-	-	-	-	-
140	93.269	-	-	-	-	-	-
150	93.910	-	-	-	-	-	-
160	94.230	-	-	-	-	-	-

3.4 Effect of different parameters on the photocatalytic decolorization of RB5 dye for Mn:ZnS:Cr$_{(2)}$

3.4.1. Effect of the mass of Mn:ZnS:Cr$_{(2)}$

Under experimental condition, the effect of Mn:ZnS:Cr $_{(2)}$ dose on decolourization of RB5 dye solution was done. The rates of reaction were found to be directly proportional to the catalyst dose and the maximum value was obtained at 1.5 g/100 mL. While with increases of Mn: ZnS:Cr$_{(2)}$ dosage more than 1.5 g/100 mL the rate of decolourization is decreased. The results were recorded in tables3-24 and 3-25 and plotted in figures 3-18 and 3-19.

Table 3-24: The change of ln C$_o$/C$_t$ with irradiation time at different mass of Mn:ZnS :Cr$_{(2)}$

Time of irradiation t/min	Dose/ g	$ln\ C_o/\ C_t$			
		0.5	1	1.5	2
0	0	0	0	0	0
5		0.080	0.059	0.180	0.209
10		0.088	-	0.373	
20		0.161	-	0.428	0.251
30		0.225		0.522	0.191
40		0.250	-	0.591	0.320
50		0.286	-	0.727	0.504
60		0.347	0.454	0.786	0.517
70		0.401	0.550	1.027	0.594
80		0.519	0.592	1.036	0.730

90	-	0.598	1.062	0.770
100	-	0.724	-	0.954
110	-	0.454	-	0.963
120	-	-	-	-
130	-	0.867	-	0.916
150	-	0.952	-	0.993
170	-	1.085	-	1.121
180	-	1.225	-	-
k_{app}/ min^{-1}	0.006	0.006	0.013	0.007

Table 3-25: The change of irradiation time with PDE% at different mass of MnCr: ZnS$_{(2)}$

Time of irradiation t/min	Dose/ g	PDE%			
		0.5	1	1.5	2
0	0	0	0	0	
5	7.711	5.802	16.513	18.888	
10	8.457	4.095	31.192	20.370	
20	14.925	5.119	34.862	22.222	
30	20.149	-	40.672	17.407	
40	22.139	9.556	44.648	27.407	
50	24.875	16.040	51.681	39.629	
60	29.353	36.518	54.434	40.370	
70	33.084	42.320	64.220	44.814	
80	40.547	44.709	64.525	51.851	
90	-	-	65.443	53.703	
100	67.661	45.051	66.360	61.481	
110	71.890	51.535	70.336	61.851	
120	70.646	44.368	73.394	52.592	
130	72.636	58.0-20	-	60	
140	74.129	48.122	-	60.740	
150	74.875	61.433	-	62.962	
160	75.870	61.092	-	63.703	
170	-	66.211	-	67.407	
180	-	70.648	-	-	

3.4.2. Effect of initial pH of the solution

In order to study the effect of pH on this reaction, the range of initial pH was applied from 3.1 to 11 at 25 ppm dye concentration, 1.5 g/100mL catalyst and light intensity equal to1.46x10^{-6} Einstein s^{-1}. The initial pH of the solution is adjusted before irradiation and it is not controlled during the reaction, but at decolorization the pH reaches to neutral. The kinetic

results listed in tables 3-26 and 3-27 and plotted in figures 3-26 and 3-27. The rate constant of reaction increases with the increase of the pH of solution up to the maximum level at pH=6.3 and then decrease.

Table 3-26: The change of lnC$_o$/C$_t$ with irradiation time at different initial pH of dye by Mn:ZnS:Cr$_{(2)}$.

Time of irradiation t/min	pH	$\ln C_o/C_t$					
		3	4.1	6.3	7.1	9	11
0	0	0	0	0	0	0	0
5		0.012	0.100	0.180		0.011	0.041
10		0.025	0.122	0.373	0.054	0.007	0.064
20		0.102	0.309	0.428	0.130	0.053	0.072
30		0.111	0.131	0.522	0.221	0.057	0.094
40		0.120	0.144	0.591	0.295	0.061	-
50		0.253	0.319	0.727	0.353	0.153	-
60		0.418	0.358	0.786	0.364	0.207	0.140
70		0.424	0.498	1.027	0.280	0.293	0.142
80		0.392	0.492	1.036	0.432	0.543	0.193
90		0.450	0.505	1.062	-	0.590	-
100		0.437	0.819	-	-	-	0.218
110		0.562	0.838	-	0.493	-	-
120		0.585	0.865	-	-	-	-
130		0.592	0.885	-	-	-	0.384
170		-	-	-	-	-	0.653
180		-	-	-	-	-	0.771
195		-	-	-	-	-	0.956
210		-	-	-	-	-	1.0376
240		-	-	-	-	-	1.134
k$_{app}$/min^{-1}		0.004	0.006	0.013	0.005	0.005	0.004

Table 3-27: The change of irradiation time with PDE% at different initial pH of dye by Mn:ZnS:Cr$_{(2)}$.

Time of irradiation t/min	pH	PDF%					
		3	4.1	6.3	7.1	9	11
0	0	0	0	0	0	0	0
5		1.265	9.523	16.513	11.450	1.123	4.020
10		2.531	11.507	31.192	5.343	0.749	6.281
20		9.704	26.587	34.862	12.213	5.243	7.035
30		10.548	12.301	40.672	19.847	5.618	9.045

40	11.392	13.492	44.648	25.572	5.992	12.311
50	22.362	27.380	51.681	29.770	14.23	9.799
60	34.177	30.158	54.434	30.534	18.726	13.065
70	34.599	39.285	64.220	24.427	25.468	13.316
80	32.489	38.888	64.525	35.114	41.947	17.587
90	36.286	39.682	65.443	25.572	44.569	19.598
100	35.443	55.952	66.360	31.297	55.056	19.598
110	43.037	56.746	70.336	38.931	56.179	21.105
120	44.303	57.936	73.394	20.610	58.052	27.638
130	44.725	58.730	-	37.786	56.928	31.909
140	-	-	-	38.167	58.426	38.190
150	-	-	-	-	-	40.954
160	-	-	-	-	-	42.964
170	-	-	-	-	-	47.989
180	-	-	-	-	-	53.768
195	-	-	-	-	-	61.557
210	-	-	-	-	-	64.572
240	-	-	-	-	-	67.839

3.4.3. Effect of temperature

The photocatalytic declolzation of RB5 was performed at different temperatures in the range (283.15-293.15)K. Under the determined experimental condition with initial dye concentration equal to 25ppm, Mn: Zns:$Cr_{(2)}$ dosage 1.5 g /100mL pH equal to 6.3, light intensity equal to1.46x10^{-6} Einstein s^{-1}. The results indicate that the decolorization efficiency of RB5 increases with increase of temperature, and the reaction is endothermic by using this photocatalyst. The results are listed in tables 3-28 and 3-29 and plotted in figure 3-34. Arrhenius and Erying relationship are plotted in figure 3-35 .The results of the activation energy and the thermodynamics functions are shown in table 3-30 and 3-31.

Table 3-28: The change of lnC_o/C_t with irradiation time on different temperatures by Mn:ZnS:$Cr_{(2)}$.

Time of irradiation t/min	T/°C	ln C_o/ C_t			
		10	15	17	20
0	0	0	0	0	0
5	-		0.010	0.022	0.095
10	-		0.085	0.130	0.125
20	-		0.121	0.156	0.153
30	0.200		0.183	0.182	0.214
35	-		-	0.1957	
40	0.225		0.278	0.223	0.276

45	-	-	0.251	-
50	0.266	-	0.280	0.368
55		-	0.310	-
60	0.342	-	0.474	0.549
65	-	-	0.567	-
70	0.444	0.541	0.607	0.643
80	0.450	0.553	-	0.702
90	-	0.565	-	0.714
100	-	0.707	-	0.811
110	-	0.722	-	0.818
120	0.653	0.767	-	0.825
130	0.794	0.782	-	0.926
140	0.812	0.806	-	0.950
150	0.908	0.925	-	1.039
160	0.928	1.029	-	1.092
170	1.036	1.091	-	1.138
180	1.222	1.157	-	1.148
190	-	-	-	1.258
k_{app}/min^{-1}	0.006	0.006	0.007	0.007

Table 3-29: The change of irradiation time with PDE% at different temperatures of dye by Mn:ZnS:Cr$_{(2)}$.

Time of irradiation t/min	T/°C	PDF%			
		10	15	17	20
0	0		0	0	0
5	9.677		1.071	2.222	9.063
10	12.499		8.214	12.222	11.782
20	17.338		11.428	14.444	14.199
30	18.145		16.785	16.666	19.335
35	-		-	17.777	-
40	20.161		24.285	20	24.169
45	-		-	22.222	-
50	23.387		37.499	24.444	30.815
55	-		-	26.666	
60	29.032		41.071	37.777	42.296
65	-		-	43.333	-
70	35.887		41.785	45.555	47.432
75	-		-	51.111	
80	36.290		42.499	65.555	50.453
90	37.096		43.214	-	51.057
100	37.499		50.714	-	55.589
110	41.532		51.428	-	55.891
120	47.983		53.571	-	56.193
130	54.838		54.285	-	60.422
140	55.645		55.357	-	61.329
150	59.677		60.357	-	64.652
160	60.483		64.285	-	66.465

170	64.516	66.428	-	67.975
180	70.564	68.571	-	68.277
190	-	69.285	-	71.601

Table 3-30: Relationship between 1/T with lnk$_{app}$ and ln(k$_{app}$/T).

1/T(K)	ln k$_{app}$	ln(k$_{app}$/T)
3.531	-5.099	-10.745
3.470	-5.051	-10.714
3.446	-4.933	-10.604
3.411	-4.919	-10.600

Table 3-31: The calculated activation kinetic and thermodynamics parameters for decolourization of RB5 with using Mn: ZnS:Cr$_{(2)}$.

Sample	Ea /kJ mol^{-1}	$\Delta H^{\#}$ /kJ mol^{-1}	$\Delta S^{\#}$ /J mol^{-1}K^{-1}	$\Delta G^{\#}$ /kJmol^{-1}
Mn:ZnS:Cr(2)	13.420	11.026	-3.590	1.044

3.4.4. Effect of addition of K$_2$S$_2$O$_8$

In addition of K$_2$S$_2$O$_8$ to solution of RB5 dye using Mn:ZnS:Cr $_{(2)}$ as photocatalyst at experimental condition constant, the rates of reaction were found to be directly proportional with increasing of K$_2$S$_2$O$_8$.The maximum value was produced at 8 mmole/L. And then, at more than that concentration of K$_2$S$_2$O$_8$ the rate of decolourization decreased. The results were recorded in tables 3-32 and 3-33 and plotted in figures 3-42and 3-43.

Table 3- 32: The change of $\ln C_o/C_t$ with irradiation time at different additions of $K_2S_2O_8$ for Mn::ZnS:Cr $_{(2)}$.

Time of irradiation t/min	$K_2S_2O_8$/ mmole L^{-1}	$\ln C_o/C_t$					
		0	3	4	7	8	10
0	0	0	0	0	0	0	0
2	-	-	-	-	0.410	0.573	-
4	-	-	-	-	0.788	1.062	-
5	0.180	0.271	0.374	-	-	0.714	
6	-	-	-	-	0.940	1.556	-
8	-	-	-	-	1.424	1.832	-
10	0.373	0.565	0.579	2.140	1.979	1.721	
12	-	0.548	0.789	2.397	2.358	-	
14	-	0.600	0.959	2.523	2.726	-	
15	-	-	-	-	-	2.626	
16	-	0.945	0.805	2.833	-	-	
18	-	1.267	1.164	-	-	-	
20	0.428	1.320	0.729	-	-	-	
22	-	1.436	1.422	-	-	-	
24	-	1.566	1.652	-	-	-	
25	-	-	-	-	-	4.360	
26	-	1.893	1.770	-	-	-	
28	-	1.926	2.058	-	-	-	
30	0.522	2.069	2.383	-	-	-	
40	0.591	-	-	-	-	-	
50	0.727	-	-	-	-	-	
60	0.786	-	-	-	-	-	
70	1.027	-	-	-	-	-	
80	1.036	-	-	-	-	-	
90	1.0625	-	-	-	-	-	
k_{app}/min^{-1}	0.013	0.065	0.084	0.186	0.206	0.173	

Table 3-33: The change of irradiation time with PDE% at different additions of $K_2S_2O_8$ for Mn:ZnS:Cr$_{(2)}$.

Time of irradiation t/min	$K_2S_2O_8$/ mmole L^{-1}	PDE %					
		0	3	4	7	8	10
0	0	0	0	0	0	0	0
2	-	-	-	-	33.689	43.636	-
4	-	-	-	-	54.545	65.454	-
5	16.513	23.786	31.205	-	-	-	51.063
6	-	-	-	-	60.962	78.909	-
8	-	-	-	-	75.93583	84	-
10	31.192	43.203	43.971	88.235	86.181	82.127	
12	-	42.233	54.609	90.909	90.545	-	
14	-	45.145	61.702	91.978	93.454	-	
15	-	-	-	-	-	92.765	
16	-	61.165	55.319	94.117	-	-	
18	-	71.844	68.794	-	-	-	
20	34.862	73.300	51.773	-	-	-	
22	-	76.213	75.886	-	-	-	
24		79.126	80.851				
25	-	-	-	-	-	98.723	
26	-	84.951	82.978	-	-	-	
28	-	85.436	87.234	-	-	-	
30	40.672	87.378	90.780	-	-	-	
40	44.648	-	-	-	-	-	
50	51.681	-	-	-	-	-	
60	54.434	-	-	-	-	-	
70	64.220	-	-	-	-	-	
80	64.525	-	-	-	-	-	
90	65.443	-	-	-	-	-	
100	66.360	-	-	-	-	-	
110	70.336	-	-	-	-	-	
115	-	-	-	-	-	-	
120	73.394	-	-	-	-	-	

3.5 Effect of different parameters on the photocatalytic decolorzation of RB5 dye for prepared ZnS .

3.5.1. Effect of the mass of prepared ZnS

The relationship between the photodecolorzation efficiency of RB5 and concentration of photocatalyst was performed by conducting experiments at different doses of the ranged (0.5- 2.5) g of prepared ZnS, pH 6.3 and the temperature was 288.15 K light intensity equal to1.46x10^{-6} Einstein s^{-1}. The results are given in tables 3-34,3-35 and plotted in figures 3-20 and 3-21. The best dosage of prepared bare ZnS was found at 1g/100mL.

The photo-decolorization efficiency increased with the increasing of the dosage of catalyst up to a maximum value at 1gm/100mL.

Table 3-34: The change of lnC$_o$/C$_t$ with irradiation time at different mass of prepared ZnS .

Time of irradiation t/min	Dose/ g	ln C_o/ C_t				
		0.5	1	1.5	2	2.5
0	0	0	0	0	0	0
5		0.089	0.011	0.028	0.010	0.028
10		0.093	0.017	0.038	0.058	0.033
20		0.114	0.046	0.057	0.058	0.049
30		-	0.052	0.043	0.075	0.060
40		0.146	0.061	0.092	0.102	0.084
50		0.155	0.080	0.112	0.143	0.096
60		0.195	0.133	0.158	0.162	0.125
70		-	0.172	0.151	0.191	0.135
80		-	0.225	0.194	0.265	0.110
90		-	0.193	0.239	0.300	0.142
100		-	0.218	-	0.328	0.147
110		0.346	-	-	0.284	0.207
115		-	0.281	-	-	-
120		0.370	-	-	0.356	0.254
130		0.398	0.428	-	0.325	0.229
140		0.458	-	-	0.365	0.266
145		-	0.675	-	-	-
150		0.482	-	0.719	0.410	0.371
160		0.557	0.891	-	-	0.380
165		-	-	-	0.457	-
170		-	-	-	-	0.419
175		0.704	1.290	-	-	-
180		-	-	-	0.483	0.460
190		0.904	1.570	-	-	-
205		1.053	2.050	-	-	0.502
210		-	-	-	0.602	-
215		-	-	-	-	0.506
220		-	-	-	0.948	0.593
k$_{app}$/min^{-1}		0.003	0.006	0.003	0.003	0.002

Table 3-35 : The change of irradiation time on different at mass of prepared ZnS with photocatalytic Decolourization efficiency

Time of irradiation	Dose/ g	PDE %				
		0.5	1	1.5	2	2.5
0	0	0	0	0	0	0

5	8.582	1.188	2.816	1.014	2.838
10	8.955	1.782	3.822	5.679	3.275
20	10.820	4.554	5.633	5.679	4.803
30	2.985	5.148	4.225	7.302	5.895
40	13.619	5.940	8.853	9.736	8.078
50	14.365	7.722	10.663	13.387	9.170
60	17.723	12.475	14.688	15.010	11.790
70	-	15.841	14.084	17.444	12.663
80	-	20.198	17.706	23.326	10.480
90	-	17.623	21.327	25.963	13.318
100		19.603	-	27.991	13.755
110	29.291	-	-	24.746	18.777
115	30.970	24.554	-	-	-
120	32.835	-	-	30.020	22.489
130	36.753	34.851	-	27.789	20.524
140	38.246	-	-	30.628	23.362
145	42.723	49.108	-	-	-
150	-	-	51.307	33.671	31.004
160	-	59.009	-	-	31.659
165	-	-	-	36.713	-
170	-	-	-	-	34.279
175	50.559	72.475	-	-	-
180	-	-	-	38.336	36.899
190	59.514	79.207	-	-	-
195	-	-	-	34.077	-
205	65.111	87.128	-	-	39.519
210	-	-	-	45.233	-
215	-	-	-	-	39.738
240	-	-	-	61.257	-
245	-	-	-	-	44.759
275	-	-	-	-	53.711
290	-	-	-	-	75.982
305	-	-	-	-	79.694

3.5.2. Effect of initial pH of the solution

The effect of pH on decolonization was studied by keeping all other experimental conditions constant and changing the value of initial pH solution from 3.1 to 9 and results are illustrated in figures 3-28 and 3-29 and listed in tables 3-36 and 3-37. The rate constant increased with increasing in pH and the maximum value at pH 6.3, after that the values decreased with increasing of pH.

Table 3-36: The change of ln C_o/C_t with irradiation time at different initials pH of dye by prepared ZnS .

Time of irradiation t/min	pH	ln C_o/C_t				
		3.1	4.1	6.3	7	9
0	0		0	0	0	0
5	0.037		0.006	0.011	0.008	0.037
10	-		0.040	0.017	0.019	0.074
20	-		0.087	0.046	0.038	0.117
30	0.134		0.117	0.052	0.076	0.176
40	0.163		0.146	0.061	0.119	0.178
50	0.188		0.153	0.080	0.188	0.253
60	0.231		0.173	0.133	0.224	0.264
70	0.244		0.218	0.172	0.245	0.323
80	-		0.277	0.225	0.294	0.391
90	0.359		0.300	0.193	0.305	0.520
100	0.367		0.328	0.218	0.337	0.458
110	0.373		0.340	-	0.361	0.464
115	-		-	0.281	-	-
120	0.410		0.355	-	0.398	0.467
130	0.465		0.361	0.428	0.442	-
135	-		-	-	-	-
140	0.515		0.395	-	0.455	-
145	-		-	0.675	-	-
150	0.594		0.446	-	-	-
160	-		-	0.891	-	-
165	0.806		0.482	-	-	0.641
175	-		-	1.290	-	-
180	0.820		0.762	-	-	0.718
190	1.02303		-	1.570	-	-
195	-		-	-	0.744	-
205	-		-	-	-	-
210	1.191		-	-	0.871	0.995
225	-		-	-	-	-
240	-		-	-	1.286	-
250	-		-	-	1.574	-
270	-		-	-	-	-
285	-		-	-	-	-
k_{app}/min^{-1}	0.003		0.003	0.006	0.004	0.004

Table 3-37: The change of irradiation time with PDE% at different initials pH of dye by prepared ZnS .

Time of irradiation t/min	pH	PDE %				
		3.1	4.1	6.3	7	9
0	0	0	0	0	0	
5	3.719	0.627	1.188	0.836	3.697	
10	9.504	3.974	1.782	1.882	7.218	
20	12.190	8.368182	4.554437	3.765	11.091	
30	12.603	11.087	5.148	7.322	16.197	
40	15.082	13.598	5.940575	11.29705	16.373	
50	17.148	14.225	7.722	17.154	22.359	
60	20.661	15.899	12.475	20.083	23.239	
70	21.694	19.665	15.841	21.757	27.640	
80	29.752	24.267	20.198	25.523	32.394	
90	30.165	25.941	17.623	26.359	40.598	
100	30.785	28.033	19.603	28.661	36.795	
110	31.198	28.870	-	30.334	37.147	
115	-	-	24.554	-	-	
120	33.677	29.9163	-	32.845	37.323	
130	37.190	30.334	34.851	35.774	-	
135	-	-	-	-	37.852	
140	40.289	32.635	-	36.61087	-	
145	-	-	49.108	-	-	
150	44.834	35.983	-	-	40.669	
160	-	-	59.009	-	-	
165	55.371	38.284	-	-	47.359	
175	-	-	72.475	-	--	
180	55.991	53.347	-	-	51.232	
190	64.049	-	79.207	-	-	
195	-	-	-	52.510	-	
205	-	-	87.128	-	-	
210	69.628	63.598	-	58.158	63.028	
225	-	69.246	-	-	-	
240	-	-	-	72.384	67.957	
250	-	-	-	79.288	-	
270	-	-	--	--	80.633	
285	-	-	-	-	86.443	

3.5.3. Effect of temperature

The photocatalytic declolzation of RB5 was determined at different ranges of temperature the (283.15-293.15) K. The experimental condition with initial dye concentration equal to 25ppm, dosage of prepared ZnS 1 g /100mL and pH equal to 6.3, light intensity equal to1.46x10^{-6} Einstein s^{-1}. The results show that the decolorization efficiency of RB5 increases with increase of temperature. That ensured this reaction is endothermic. The results are registered in tables 3-38 and 3-39 and plotted in figures

3-36 and 3-37. The activation energy for photocatalytic and the thermodynamics functions are shown in table 3-40 and 3-41.

Table 3-38: The change of ln C_o/C_t with irradiation time at different temperatures by prepared ZnS.

Time of irradiation t/min	T/°C	ln C_o/C_t			
		10	15	17	20
0		0	0	0	0
5		0.021	0.008	0.011	0.018
10		0.043	0.017	0.017	0.025
20		0.051	0.063	0.046	0.050
30		0.085	-	0.052	0.069
40		0.111	-	0.061	0.096
50		0.114	-	0.080	0.114
60		0.117	-	0.133	0.145
70		0.138	-	0.172	0.171
80		0.159	0.102	0.225	0.195
90		0.184	0.252	0.245	0.212
100		0.200	-	0.268	-
105		-	0.295	-	0.249
110		0.219	-	-	-
115		-	-	0.281	-
120		0.226	0.331	-	0.284
130		0.291	-	0.428	-
135		-	0.382	-	0.321
140		0.316	-	-	-
145		-	-	0.675	-
150		0.356	0.462	-	-
155		-	-	-	0.340
160		-	-	0.891	-
165		0.375	-	-	-
175		-	-	1.290	-
180		0.434	0.505	-	-
190		-	-	1.570	-
205		-	-	-	-
210		0.593	0.540	-	-
220		-	-	-	0.590
240		0.747	1.049	-	-
250		-	-	-	0.833
255		-	-	-	-
260		-	-	-	-
270		-	-	-	-
300		-	-	-	-
k_{app}/min^{-1}		0.002	0.003	0.006	0.003

Table 3-39: The change of irradiation time with PDE% at different temperatures of dye by prepared ZnS.

Time of irradiation t/min	T/°C	PDE %			
		10	15	17	20
0		0	0	0	0
5		2.105	0.882	1.188	1.801
10		4.2105	1.764	1.782	2.477
20		5.000	6.176	4.554	4.954
30		8.157	-	5.148	6.756
40		10.526	4.117	5.940	9.234
50		10.789	6.764	7.722	10.810
60		11.052	8.823	12.475	13.513
70		12.894	9.411	15.841	15.765
80		14.736	9.705	20.198	17.792
90		16.842	22.352	21.782	19.144
100		18.157	-	23.564	-
105		19.736	25.588	-	22.072
115		-	-	24.554	-
120		20.263	28.235	-	24.774
130		25.263	-	34.851	-
135		-	31.764	-	27.477
140		27.105	-	-	-
145		-	-	49.108	-
150		30	37.058	-	-
155		-	-	-	28.828
160		-	-	59.009	-
165		31.315	-	-	-
175		-	-	72.475	33.108
180		35.263	39.705	-	-
190		-	-	79.207	36.261
205		-	-	87.128	-
210		44.736	41.764	-	-
220		-	-	-	44.594
240		52.631	65	-	-
250		-	-	-	56.531
255		65	-	-	-
260		-	-	-	73.198
270		-	68.823	-	-
300		-	71.470	-	-

Table 3-40: Relationship between 1/T with $\ln k_{app}$ and $\ln(k_{app}/T)$.

1/T(K)	$\ln k_{app}$	$\ln(k_{app}/T)$
3.531	-5.991	-11.637
3.470	-5.744	-11.408
3.446	-5.099	-10.769
3.411	-5.914	-11.595

Table 3-41: The calculated activation kinetic and thermodynamics parameters for decolourization of RB5 with using prepared ZnS.

Sample	E_a /kJ mol^{-1}	$\Delta H^{\#}$ /kJ mol^{-1}	$\Delta S^{\#}$ /J mol^{-1}K^{-1}	$\Delta G^{\#}$ /kJmol^{-1}
Prepared ZnS	20.760	18.366	-3.302	19.323

3.5.4. Effect of addition of $K_2S_2O_8$

The influence of addition $K_2S_2O_8$ on the rate of decolorization was studied at 25 ppm of RB5 dye solution, 1g of prepared ZnS, pH 6.3 and temperature ranges (288.15-290.15) K, light intensity equal to 1.46×10^{-6} Einstein s^{-1}. The photocatalytic decolorization of RB5 was increased with increasing the addition of $K_2S_2O_8$ and the maximum value reaches at 8mmole/L and after then decreases. The result listed in the tables 3-42 and 3-43 and plotted in figures 3-44and 3-45.

Table 3-42: The change of $\ln C_o/C_t$ with irradiation time at different additions of $K_2S_2O_8$ with prepared ZnS .

Time of irradiation t/min	$K_2S_2O_8$/ mmole L^{-1}	$\ln C_o/C_t$				
		0	3	7	8	10
0	0	0	0	0	0	0
2		-	-	0.019	0.006	0.018
4		-	-	0.060	0.074	0.067

5	0.011	0.057	-	-	-
6	-	-	0.087	0.106	0.122
8	-	-	0.104	0.139	0.168
10	0.017	0.081	0.129	0.228	0.229
15	-	0.127	0.186	-	-
20	0.046	0.177	0.244	-	-
25	-	0.220	0.313	-	1.449
30	0.052	0.313	-	1.941	2.231
35	-	0.427	-	3.392	2.853
40	0.061	-	-	-	-
45	-	-	-	-	-
50	0.080	-	-	-	-
60	0.133	-	-	-	-
70	0.172	-	-	-	-
80	0.225	-	-	-	-
90	0.245	-	-	-	-
100	0.268	-	-	-	-
115	0.281	-	-	-	-
130	0.428	-	-	-	-
145	0.675	-	-	-	-
160	0.891	-	-	-	-
175	1.290	-	-	-	-
180	-	-	-	-	-
190	1.570	-	-	-	-
k_{app}/min^{-1}	0.006	0.010	0.012	0.077	0.069

Table 3-43: The change of irradiation time with PDE% at different additions of $K_2S_2O_8$ for prepared ZnS.

Time of irradiation t/min	$K_2S_2O_8$/ mmole L^{-1}	PDE %				
		0	3	7	8	10
0	0	0	0	0	0	0
2	-	-	-	1.909	0.672	1.789
4	-	-	-	5.902	7.174	6.560
5	1.188	5.583	-	-	-	-
6	-	-	-	8.333	10.089	11.530
8	-	-	-	9.895	13.004	15.506
10	1.782	7.868	12.152	20.403	20.477	
15	-	11.928	17.013	28.923	33.002	
20	4.554	16.243	21.701	39.237	53.280	

25	-	19.796	26.909	57.623	76.540
30	5.148	26.903	35.243	85.650	89.264
35	-	34.771	-	96.636	94.234
40	5.940	-	65.798	-	-
45	-	-	83.333	-	-
50	7.722	-	-	-	-
60	12.475	-	-	-	-
70	15.841	-	-	-	-
80	20.198	-	-	-	-
90	21.782	-	-	-	-
100	23.564	-	-	-	-
115	24.554	-	-	-	-
130	34.851	-	-	-	-
145	49.108	-	-	-	-
160	59.009	-	-	-	-
175	72.475	-	-	-	-
190	79.207	-	-	-	-

3.6. Characterization of Catalyst

3.6.1. XRD Analysis

From XRD data for all studied samples are observed that the essential peaks are occurred at miller indexes (111), (200) and (311) at (26.44 ^{o} - 27.76 ^{o}), 32.98 ^{o} and 58.6 ^{o} (JCPDS Card No 65-9585) respectively [110-112]. In fact, the diffraction peaks of miller index (111) at 26.44 for ZnS prepared is slightly shift to large angles (2θ) at range (26.92^o-27.6^o) for dispersed Mn &Cr ions in ZnS matrix. This behavior may be assigned to the small ionic radii of Cr^{3+} (0.63 Å) & Mn^{2+} (0.81Å) that interaction with Zn^{2+} (0.74 Å) in ZnS matrix [113,114]. The new peaks for organic moiety of (PEG) which used as capping agent are observed as small and broading peaks at range13^o-26° [115].

3.6.2 Atomic Force Microscopy (AFM)

From the results in AFM images, which indicates to all samples are semispherical grains. The particle sizes for all samples are more than the mean crystal size, that is beyond to the particles could be formed from several crystal size [116] and particle sizes contain from 2.5-6crystals.

3.6.3. Band gap energy (Bg) measurements

The results of measured Bg of the most samples were obtained, that the values of band gaps increased with decreased mean crystal size. But, the Bg of prepared bare & metalized ZnS were found, that the Bg of prepared ZnS was small value (3.558 eV) and had a large mean crystal size 19.986 nm. This behavior is obeyed the reported in nanofield [117]. From other hand, the Bg of most metalized prepared samples were shifted to large values with decreasing the mean crystal sizes for them [118].

3.6.4 Atomic Absorption Spectrophotometry

The atomic absorption technique was employed to ensure if all the addition amounts of Mn & Cr loading on ZnS surface. The activity of Cr:ZnS was more than the activity of Mn:ZnS That attitude to the work functions for these metals compared with work function for ZnS. The work functions for the (111) crystal plane for Cr and Mn are 4.5 eV and 4.1 eV, whereas, the work function of Zn in ZnS have a high work

function 4.22 eV[119]. In fact, the interaction for the metal which have a high work function is best, hence, the Cr loaded on prepared ZnS leads to improve the photo catalytic effect [45].

3.7 Effect of different parameters on the photocatalytic decolorization of RB5 dye

3.7.1 Effect of Mass of catalysts.

3.7.1.1 Effect of Mass of commercial ZnS catalysts on studied dye.

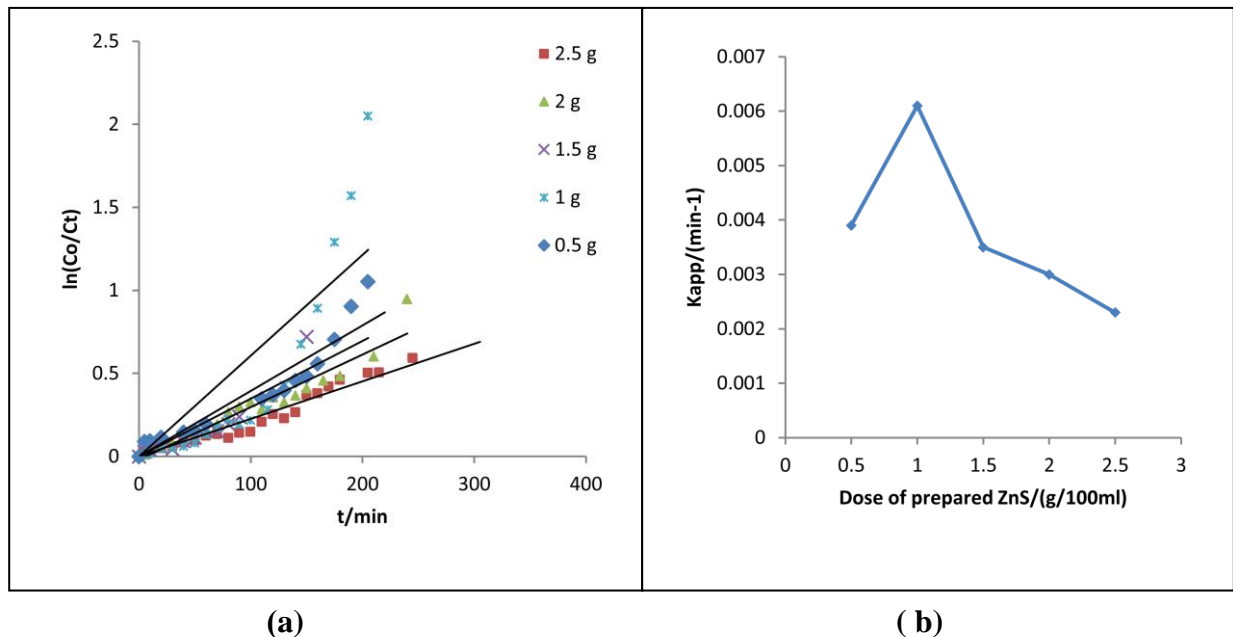(a)   (b)
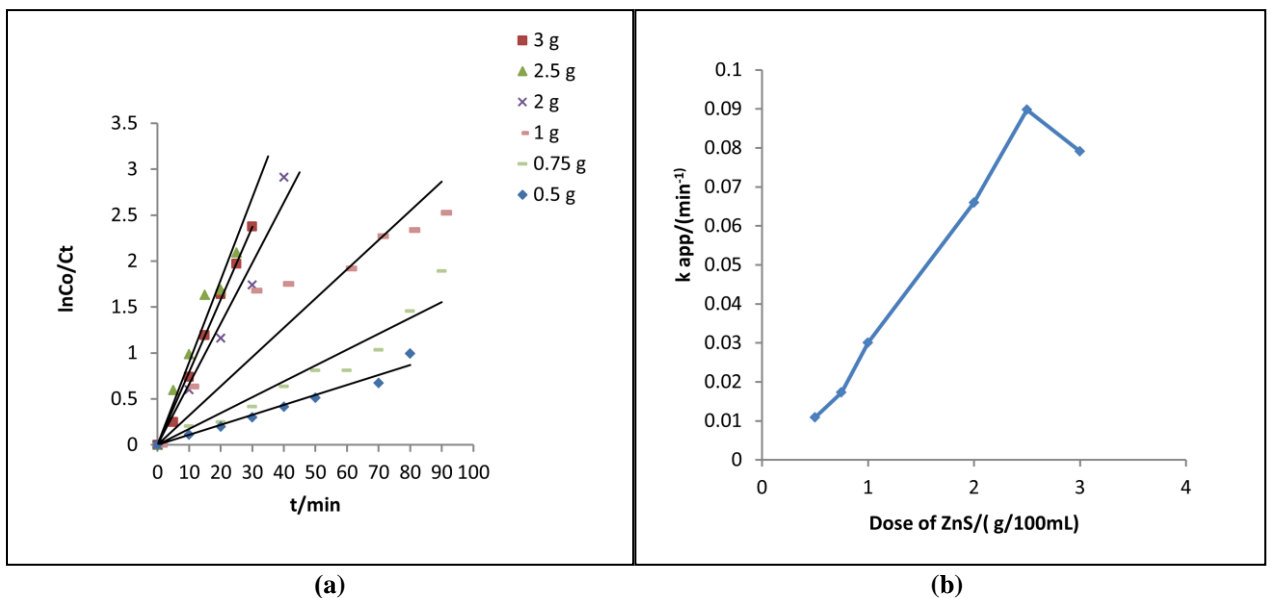
Figure 3-14: (a) The change of ln C_0/C_t with Irradiation time at different mass of commercial ZnS. (b) Relationship between apparent rate constant and different mass commercial ZnS .
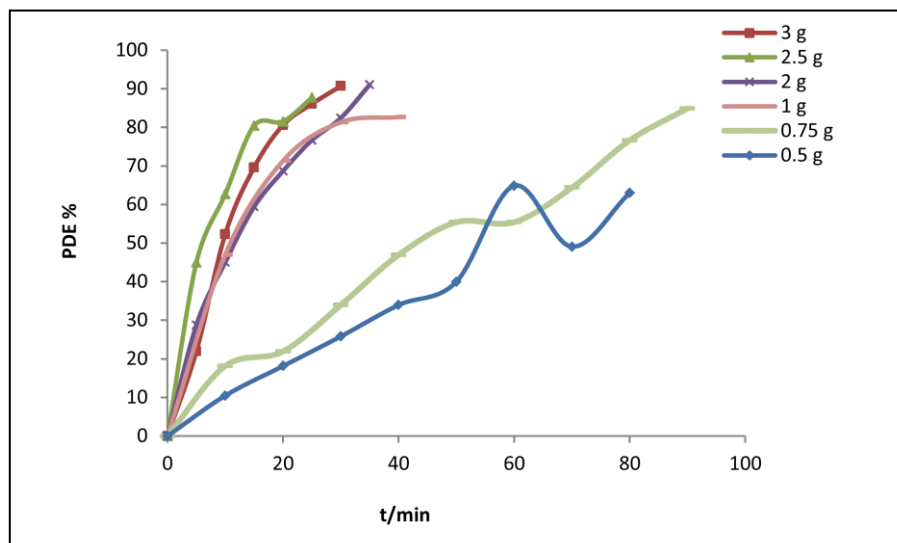
Figure 3-15: Effect of different mass of commercial ZnS on

photodecolorization efficiency.

Based on the above results in figure 3-14 $_{(a,b)}$, the rate of reaction increase with increasing the amount of ZnS, and the maximum rate constant value is obtained at 2.5 g of commercial ZnS. Then the rate constant depresses, this behavior is beyond to screening effect[45,94].The highest PDE% for photodecolorization of studied dye reaches to 87.681 % at 25 min in figure 3-15.

3.7.1.2 Effect of Mass of Cr: ZnS catalysts on studied dye

(a)　　　　　　　　　　　　　　　**(b)**
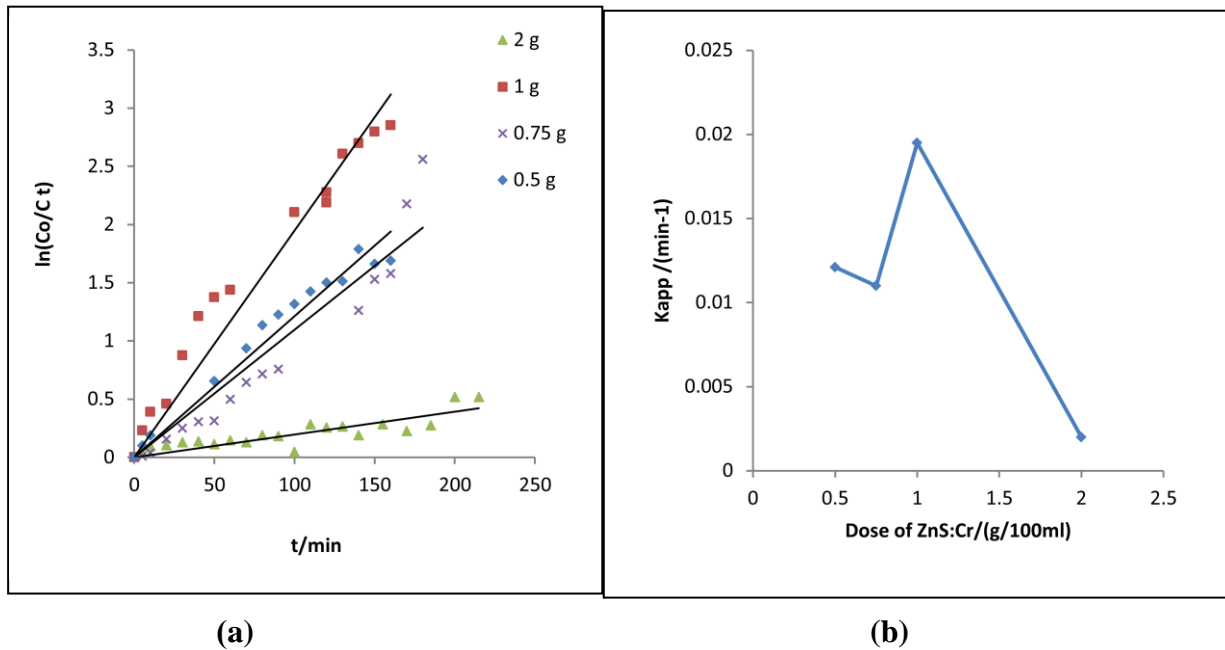
Figure 3-16: (a) The change of ln C_o/C_t with Irradiation time at different mass of Cr: ZnS. (b) Relationship between apparent rate constant and different mass of Cr: ZnS.
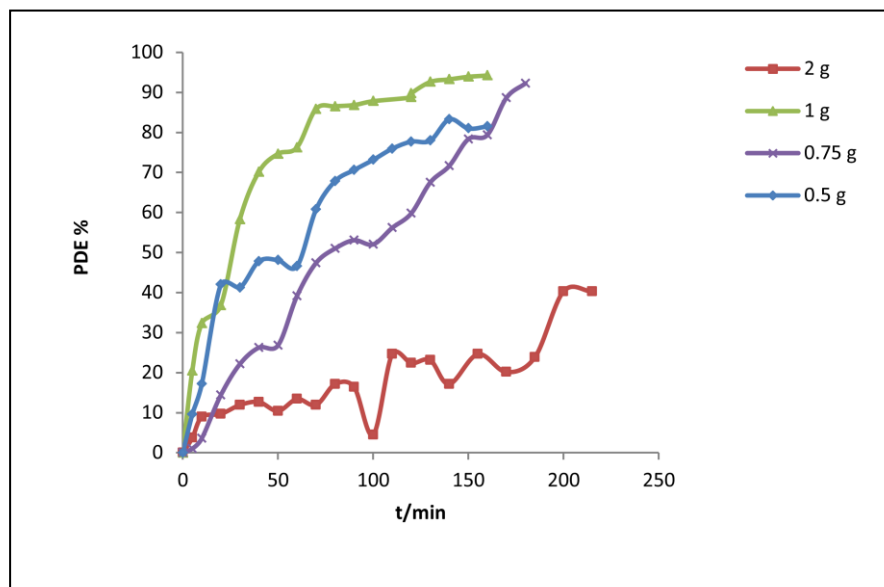
Figure 3-17: Effect of different mass of Cr:ZnS on photodecolorization

efficiency.

3.7.1.3 Effect of Mass of Mn:ZnS:C$_{(2)}$ catalysts on studied dye.
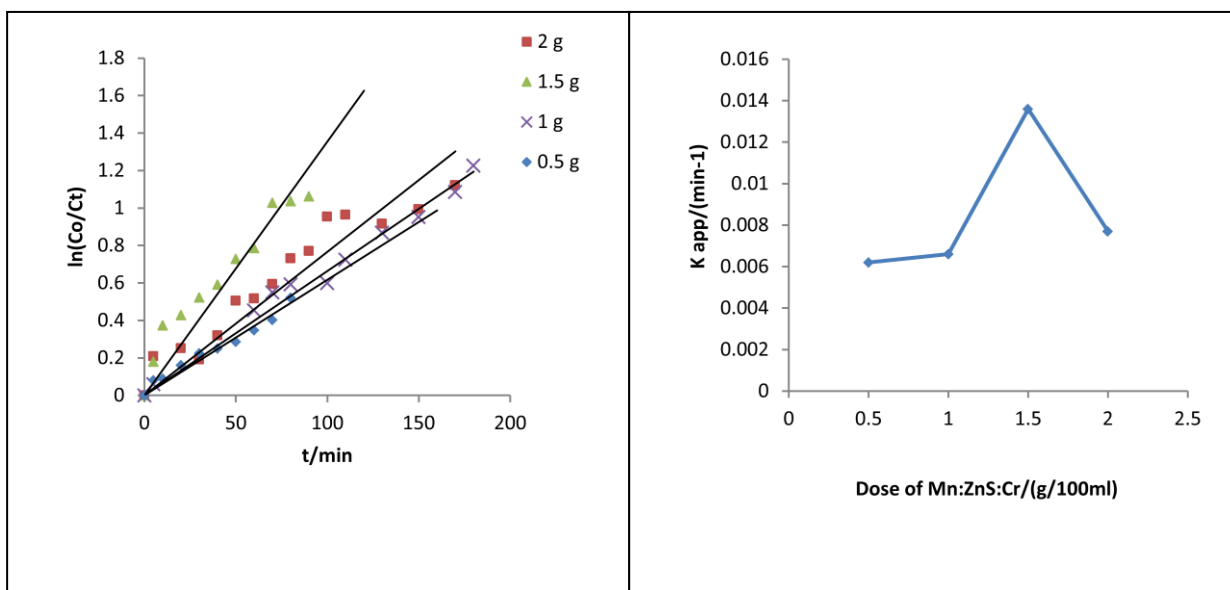
(a)   (b)

Figure 3-18: (a) The change of ln C$_o$/C$_t$ with Irradiation time at different mass of Mn:ZnS:Cr$_{(2)}$. b)Relationship between apparent rate constant and different mass of Mn:ZnS:Cr$_{(2)}$
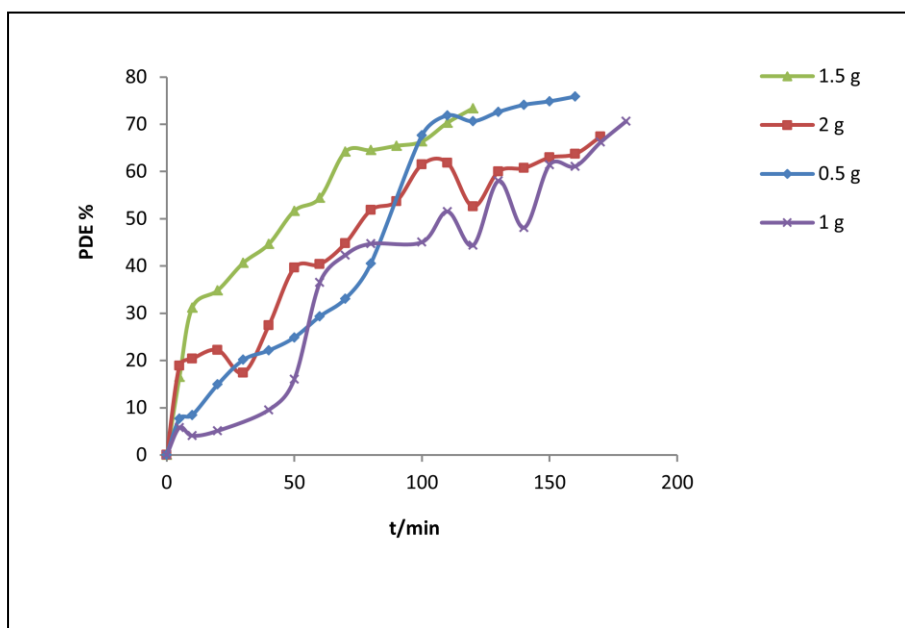
Figure 3-19: Effect of different mass of Mn:ZnS:Cr$_{(2)}$ on photodecolorization efficiency.

3.7.1.4. Effect of Mass of prepared ZnS catalysts on studied dye.

(a)   **(b)**

Figure 3-20: (a) The change of ln C_0/C_t with Irradiation time at different mass of (b) Relationship between apparent rate constant and different prepared ZnS mass of prepared ZnS.
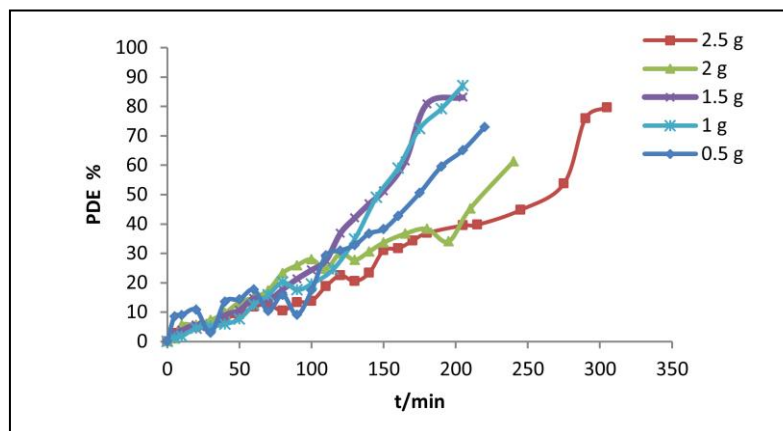
Figure 3-21: Effect of different mass of prepared ZnS onphotodecolorization

efficiency.

From figures $3\text{-}16_{(a,b)}, 3\text{-}18_{(a,b)}$ and $3\text{-}20_{(a,b)}$,The rates of reaction for prepared Cr:ZnS, Mn:ZnS:Cr$_{(2)}$ and ZnS are equal to 89.743,73.349 and 34.851 at 120 min respectively in figures (3-17),(3-19) and (3-21) that refer to improvement the rates of reaction with loaded metals and the maximum value of rate of reaction is obtained by using Cr:ZnS. From the other hand, the best doses of prepared photocatalysts are 1 g, 1.5 g and 1

g for prepared Cr: ZnS, Mn:ZnS:Cr$_{(2)}$ and prepared ZnS respectively. These weights are regarded economic compared with using 2.5 g of commercial ZnS.

3.7.2. Effect of initial pH

3.7.2.1 Effect of initial pH of the solution dye for commercial ZnS
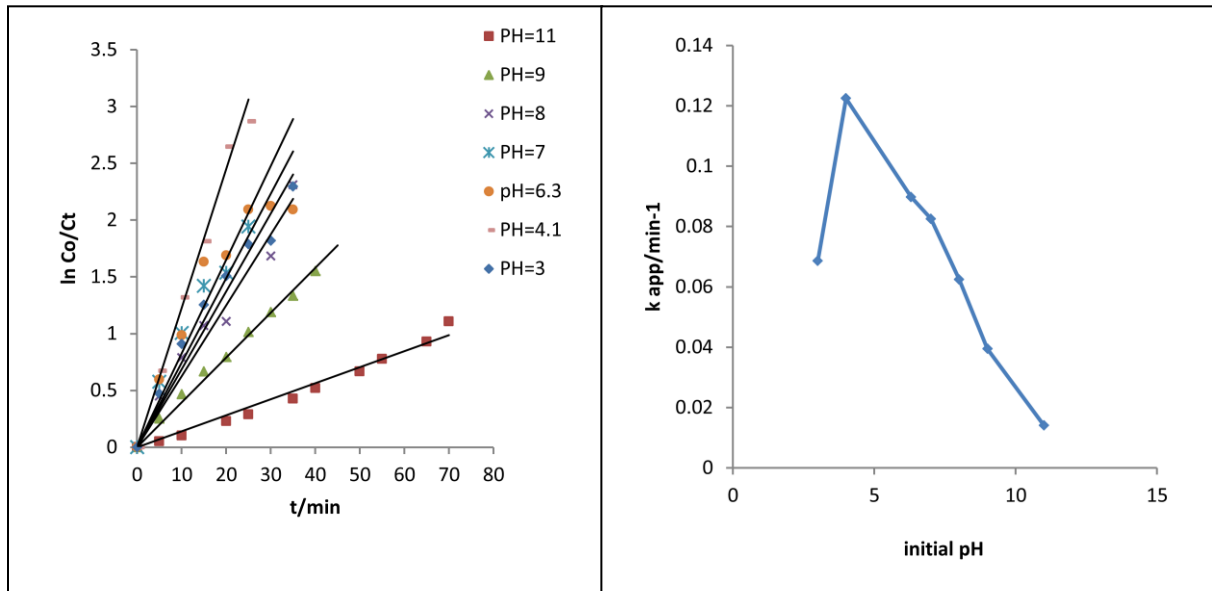
(a)   (b)

Figure 3-22: (a) The change of ln C$_o$/C$_t$ with Irradiation time at different initial pH of dye solution for commercial ZnS .(b) Relationship between apparent rate constant and different initial pH of dye solution for commercial ZnS.
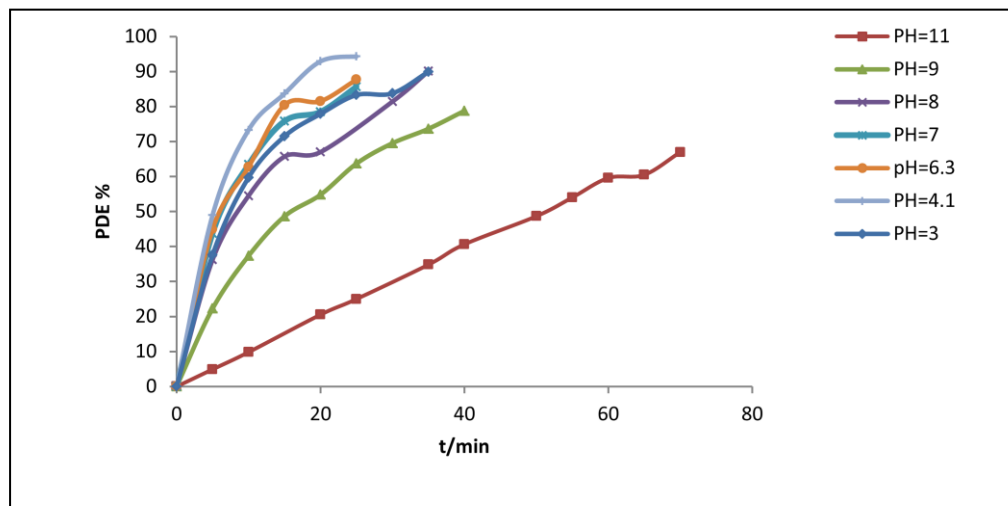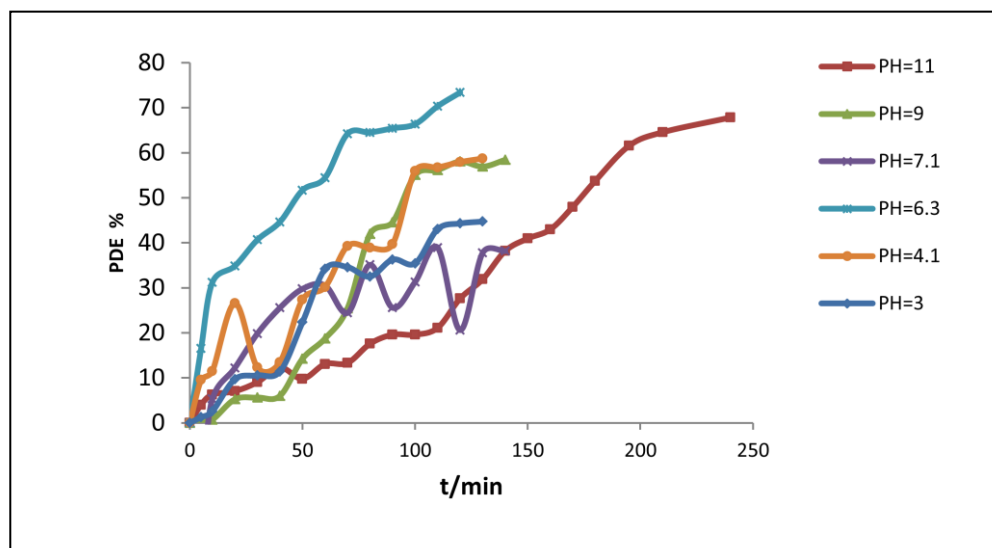

Figure3-23: Effect of different initial pH of dye solution on photodecolorization

efficiency for commercial ZnS.

The pH of solution is an important parameter to improve the value rate of reaction and efficiency percentage, hence, the optimum value of pH value is equal to 4.1, and the PDE% raised from 87.681 % to 94.396% at 25 min and 2.5g, see figures 3-22$_{(a,b)}$ and 3-23.

3.7.2.2. Effect of initial pH of the solution dye for Cr: ZnS.

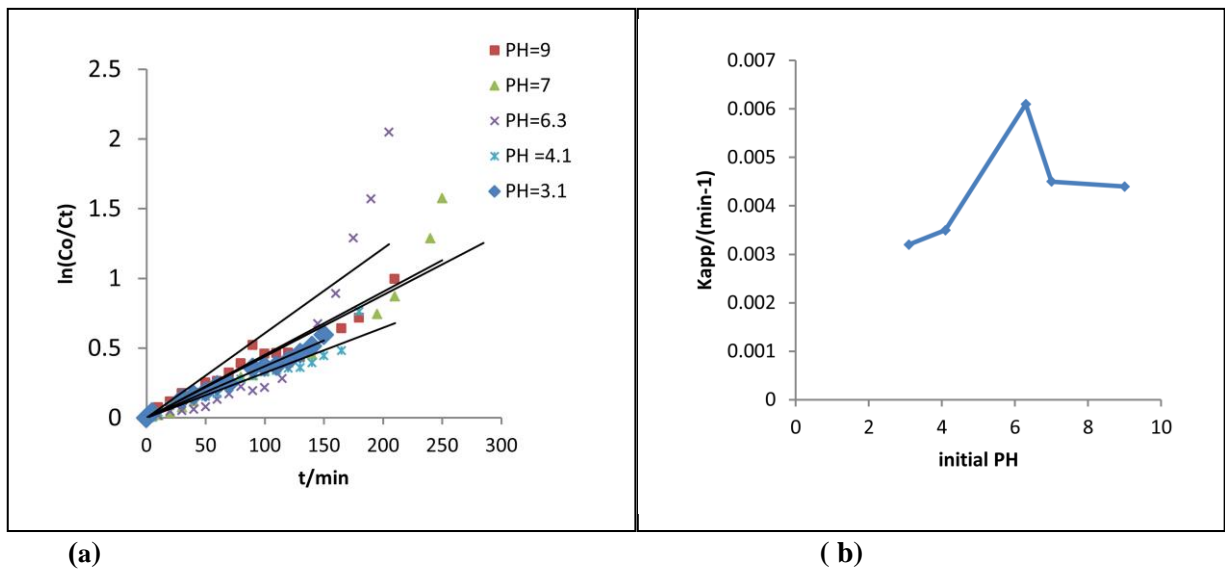(a)   (b)
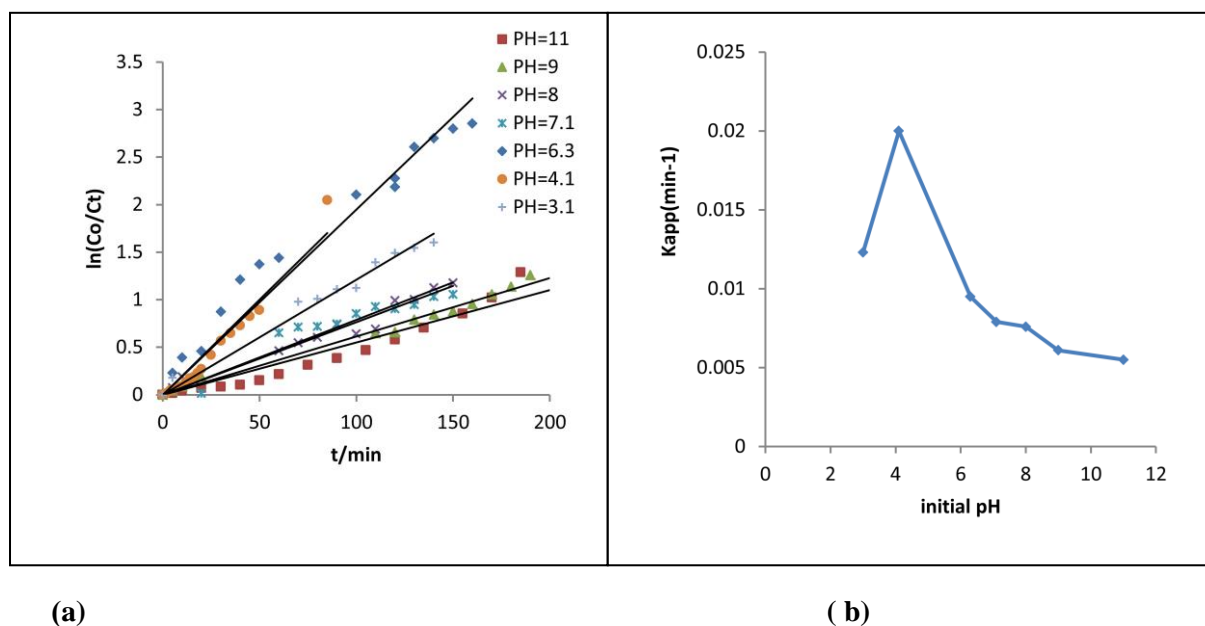
Figure 3-24: (a) The change of ln C$_0$/C$_t$ with Irradiation time at different initial pH of dye solution for Cr: ZnS .(b) Relationship between apparent rate constant and different initial pH of dye solution for Cr: ZnS.
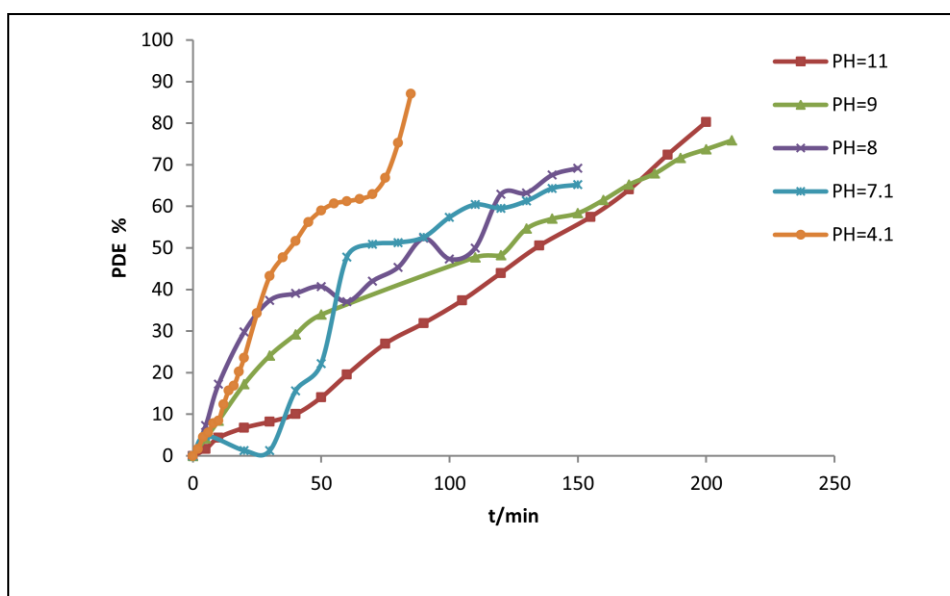
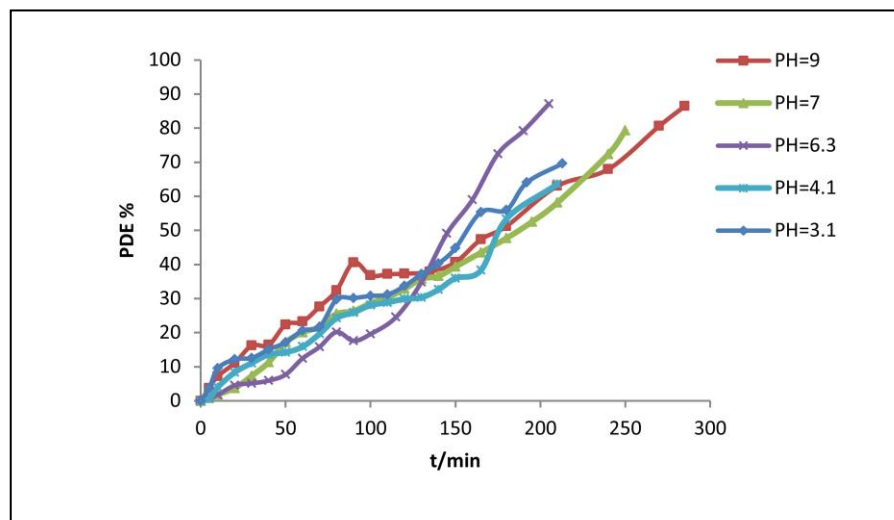**Figure3-25: Effect of different initial pH of dye solution on photodecolorization**

efficiency for Cr: ZnS.

3.7.2.3. Effect of initial pH of the solution dye for Mn:ZnS:Cr$_{(2)}$.
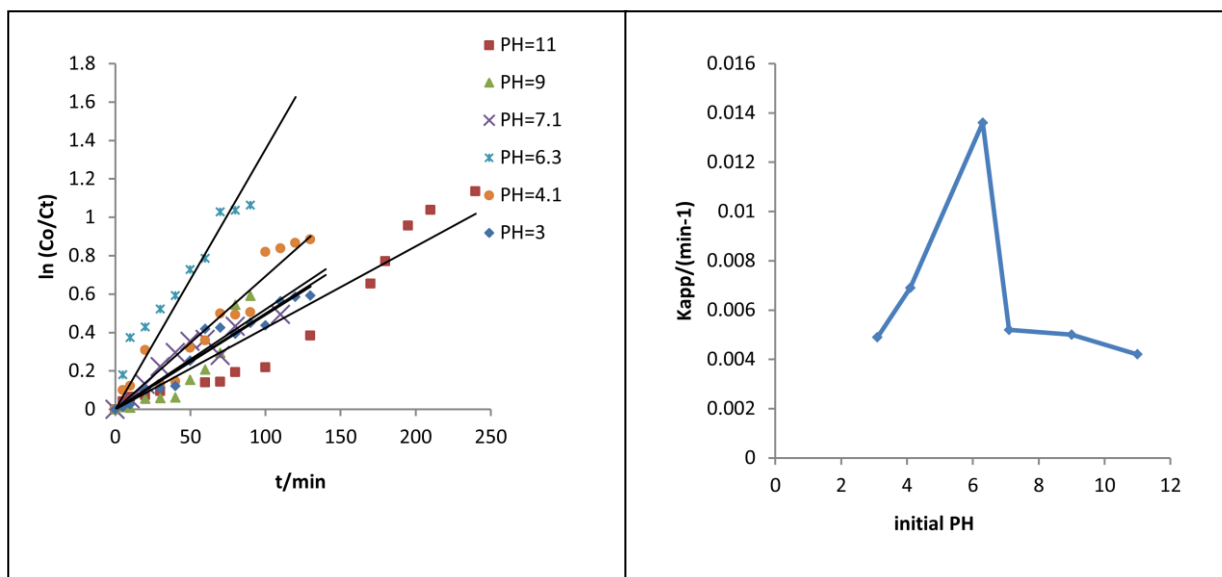
(a)   (b)

Figure 3-26: (a) The change of ln C$_o$/C$_t$ with Irradiation time at different initial pH of dye solution for Mn:ZnS:Cr$_{(2)}$.(b) Relationship between apparent rate constant and different initial pH of dye solution for Mn:ZnS:Cr$_{(2)}$.

Figure 3-27: Effect of different initial pH of dye solution on photodecolorization efficiency for Mn:ZnS:Cr$_{(2)}$.

3.7.2.4. Effect of initial pH of the solution dye for prepared ZnS .

(a) (b)

Figure 3-28: (a) The change of ln C_o/C_t with Irradiation time at different initial pH of dye solution for prepared ZnS .(b) Relationship between apparent rate constant and different initial pH of dye solution for prepared ZnS

Figure3-29: Effect of different initial pH of dye solution on photodecolorization efficiency for prepared ZnS.

Depending on the figures 3-24$_{(a,b)}$,3-26$_{(a,b)}$ 3-28 $_{(a,b)}$, the results explain the optimum values of initial pH for using prepared Cr:ZnS, Mn:ZnS:Cr$_{(2)}$ and prepared ZnS as photocatalysts are 4.1, 6.3 and 6.3 respectively. From figures 3-25,3-27 and 3-29, the PDE % for prepared catalysts are 86.538, 64.525 and 20.198 at 80 min, for prepared Cr:ZnS, Mn:ZnS:Cr$_{(2)}$ and prepared ZnS respectively, whereas, with increasing the time of

irradiation the PDE% increases also to be 87.078 at 85 min for Cr:ZnS ,
but for Mn:ZnS:Cr$_{(2)}$ is 73.394 at 120 min and be 87.128 at 205 min for
prepared ZnS.

3.7.3. Effect of temperature

3.7.3.1Effect of temperature of the solution dye for commercial ZnS .
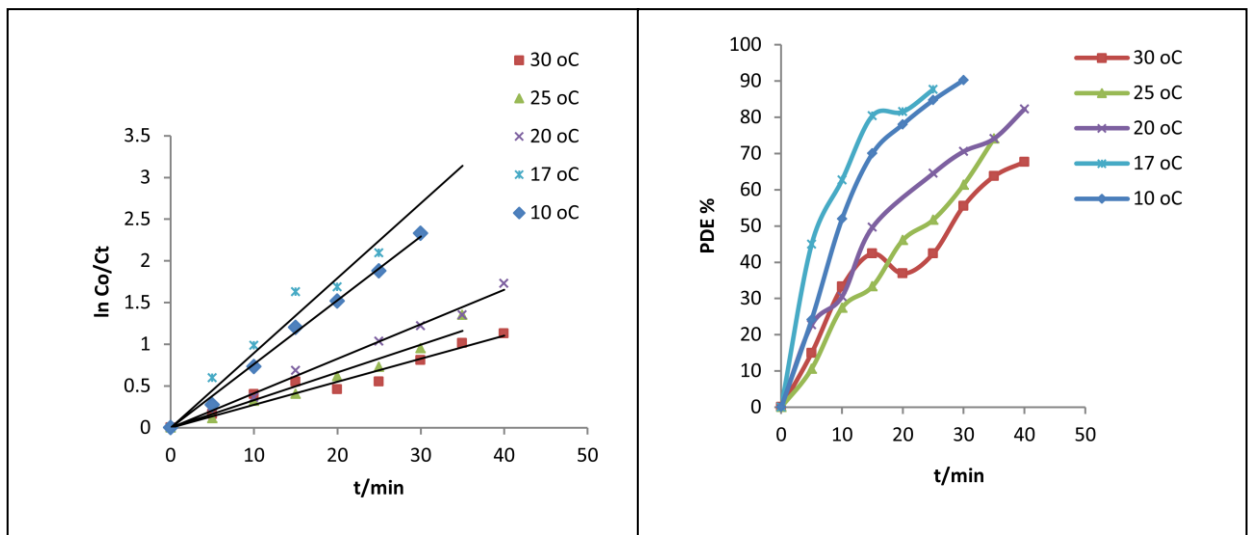

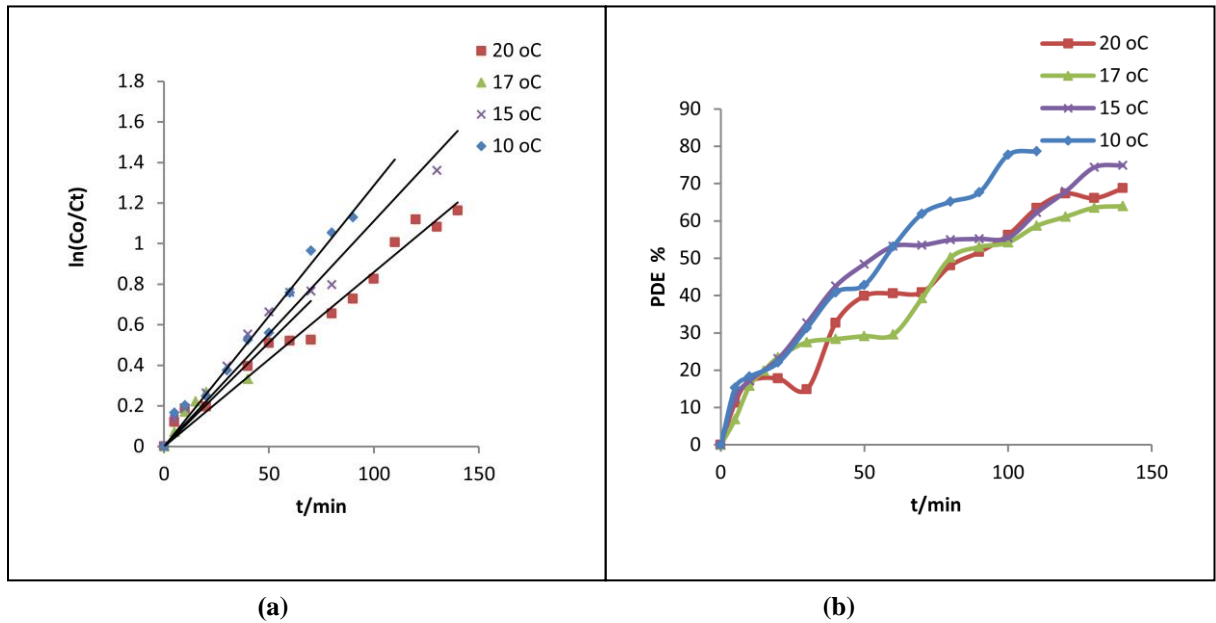(a)   (b)

**Figure 3-30: (a) The change of ln C$_o$/C$_t$ with Irradiation time at different
temperatures of dye solution for commercial ZnS .(b) Effect of different
temperatures of dye solution on photodecolorization efficiency by commercial
ZnS.**

(a)   (b)
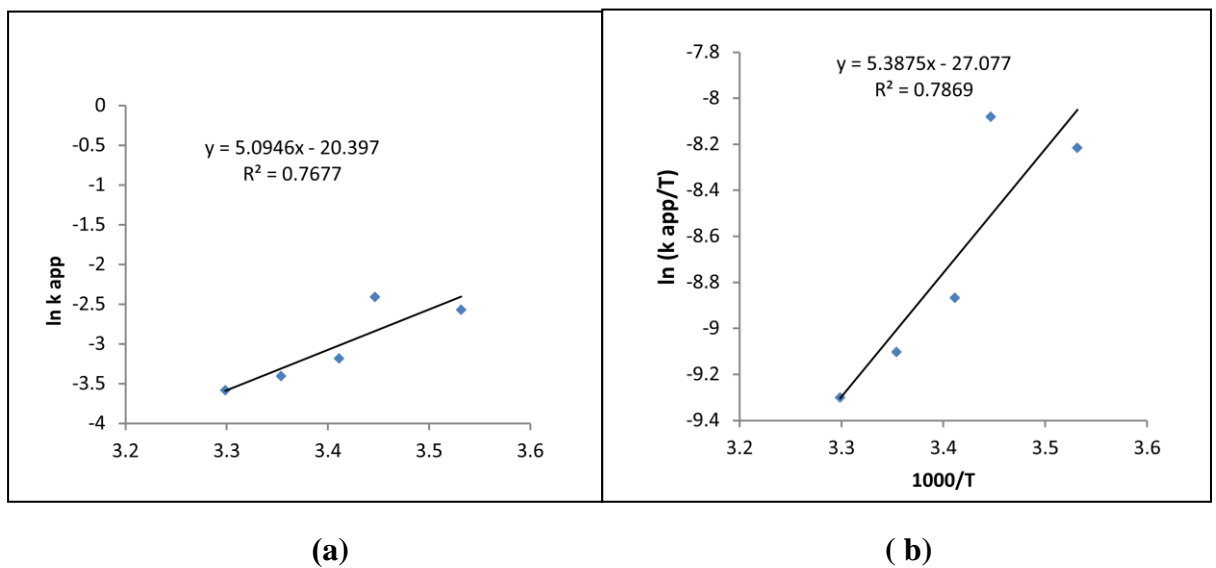
**Figure 3-31: (a) Arrhenius plot by commercial ZnS(b) Eyring–Polanyi plot
ln (k$_{app}$/T) VS.1000/T**

The rate of reaction decreases with increasing temperature during used commercial ZnS as agreement with the results that reported in ref.[3]. The best temperature for this reaction is 17°C and given PDE% 87.681 at 25 min, that noted in figures 3-30(a,b),figures 3-31(a,b)and the results listed in table 3-13, that found the reaction is exothermic, less random and spontaneous. From the other hand, the value of apparent activation energy is low, so, the reaction is fast at optimum conditions.

3.7.3.2Effect of temperature of the solution dye for Cr:ZnS .

(a)   (b)

Figure 3-32: (a) The change of ln C_o/C_t with Irradiation time at different temperatures of dye solution for Cr:ZnS .(b) Effect of different temperature of dye solution on photodecolorization efficiency by Cr:ZnS.
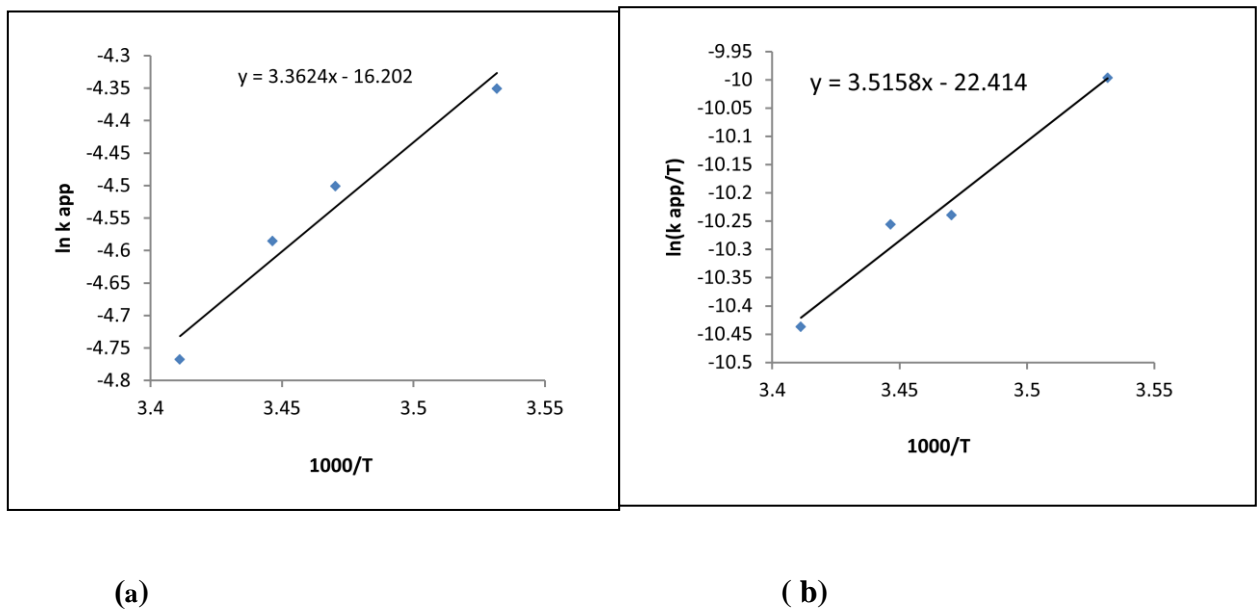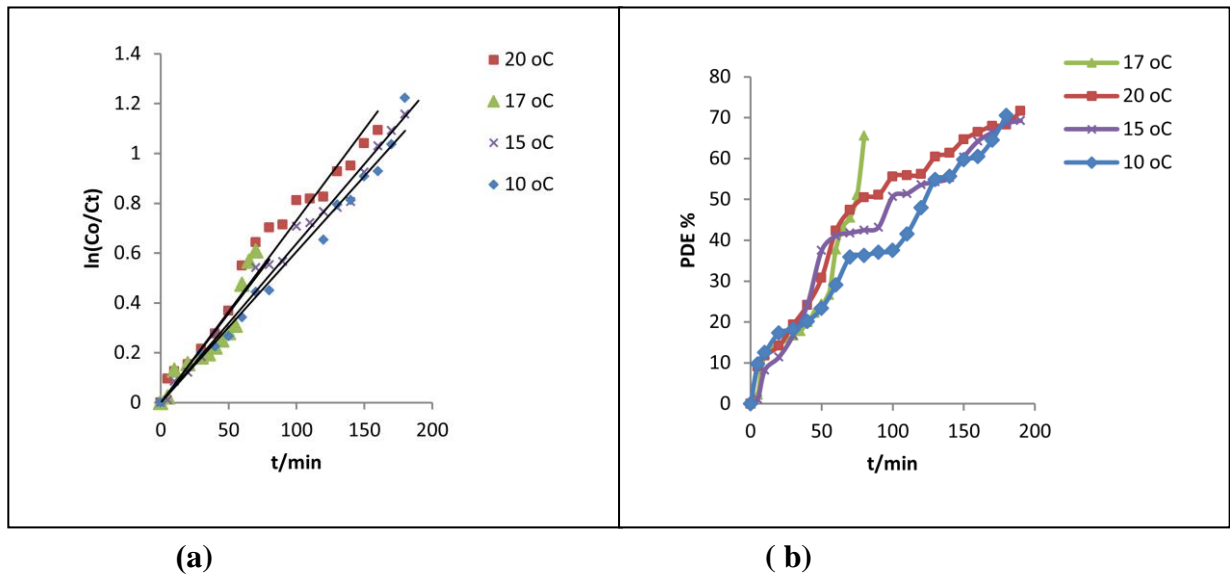

(a)   (b)

Figure 3-33: (a) Arrhenius plot by Cr:ZnS . (b) Eyring–Polanyi plot ln ($k_{app.}/T$) VS.1000/T .

3.7.3.3 Effect of temperature of the solution dye for Mn:ZnS:Cr$_{(2)}$.

(a)   (b)

Figure 3-34: (a) The change of ln C$_o$/C$_t$ with Irradiation time at different temperatures of dye solution for Mn:ZnS:Cr$_{(2)}$.(b) Effect of different temperatures of dye solution on photodecolorization efficiency by Mn:ZnS:Cr$_{(2)}$.
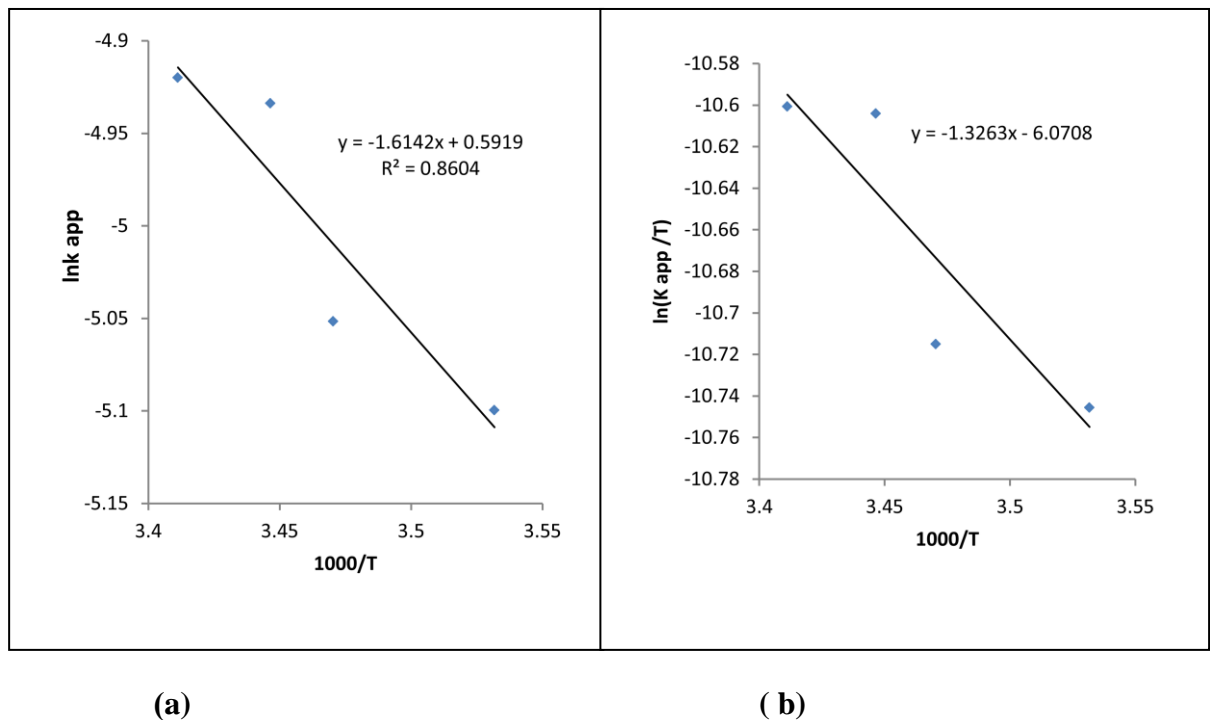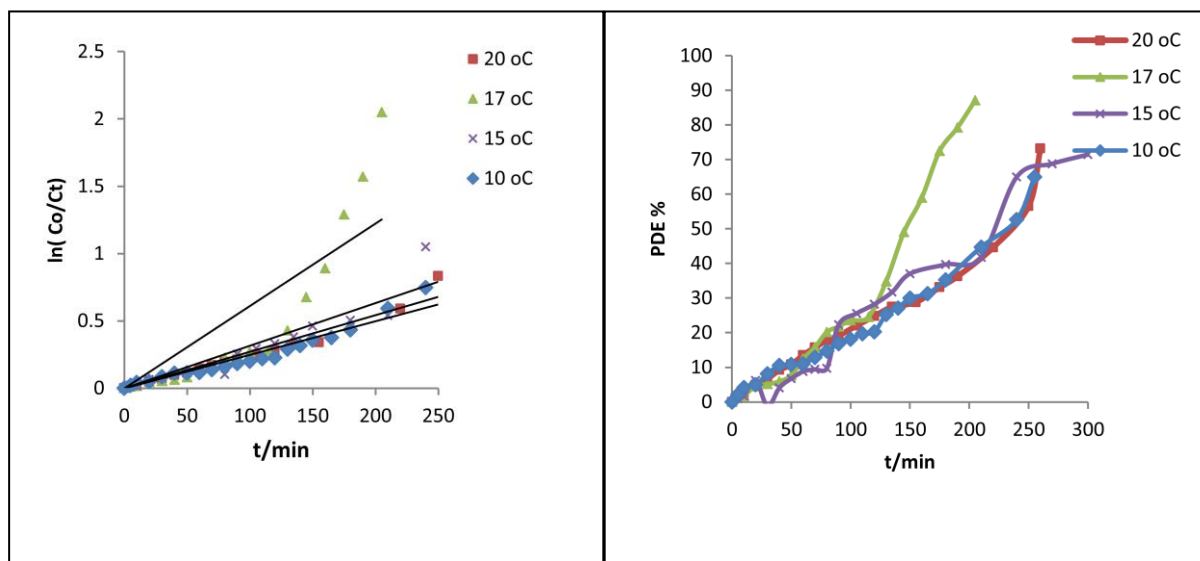

(a)   (b)

Figure 3-35: (a) Arrhenius plot by Mn:ZnS:Cr$_{(2)}$ (b) Eyring–Polanyi plot ln (k$_{app}$ /T)
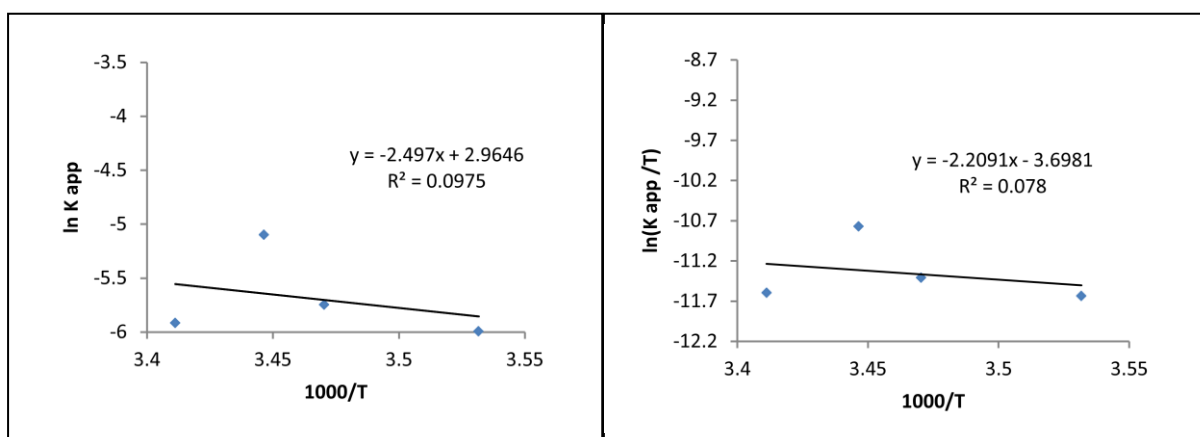
3.7.3.4. Effect of temperature of the solution dye for prepared ZnS.

(a)　　　　　　　　　　　　　(b)

Figure 3-36: (a) The change of ln C_o/C_t with Irradiation time at different temperatures of dye solution for prepared ZnS (b) Effect of different temperatures of dye solution on photodecolorization efficiency by prepared ZnS.


(a)　　　　　　　　　　　　　(b)

Figure 3-37: (a) Arrhenius plot by prepared ZnS (b) Eyring–Polanyi plot ln (k_{app} /T) VS.1000/T.

All results are reported in figures $3\text{-}32_{(a,b)}$ -$3\text{-}37_{(a,b)}$, and tables (3-21)-(3-43). The reactions that using prepared ZnS & Mn:ZnS:Cr$_{(2)}$ are endothermic and nonspontaneous, that referred to dominate the change in entropy on the direct of photoreaction[120]. While by using prepared Cr:ZnS as photocatalyst, the reaction is exothermic and spontaneous

[121], that indicated the changes in entropy & enthalpy are dominated on the push the reaction. In general, values for all prepared photocatalysts are having a low values for activation energies, this behavior is ensured the activities for these catalysts in photoreaction after control on the optimum condition.

3. 7.4. Effect of $K_2S_2O_8$

3.7.4.1 Effect of addition $K_2S_2O_8$ on the solution dye for commercial ZnS.
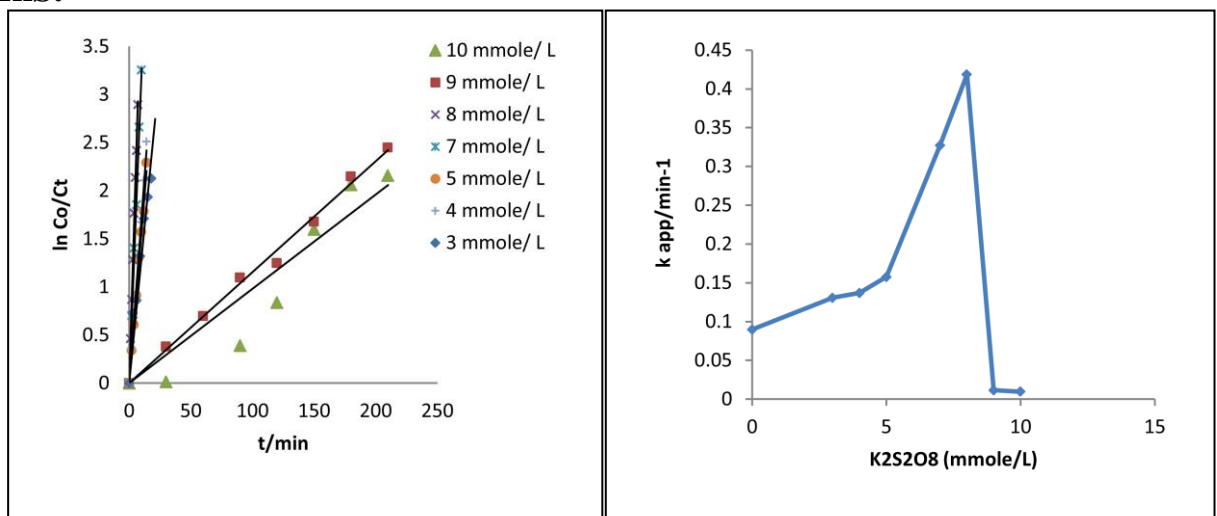
(a)   (b)

Figure 3-38: (a) The change of ln C_o/C_t with Irradiation time at different additions $K_2S_2O_8$ for commercial ZnS. (b) Relationship between apparent rate constant and different additions $K_2S_2O_8$.
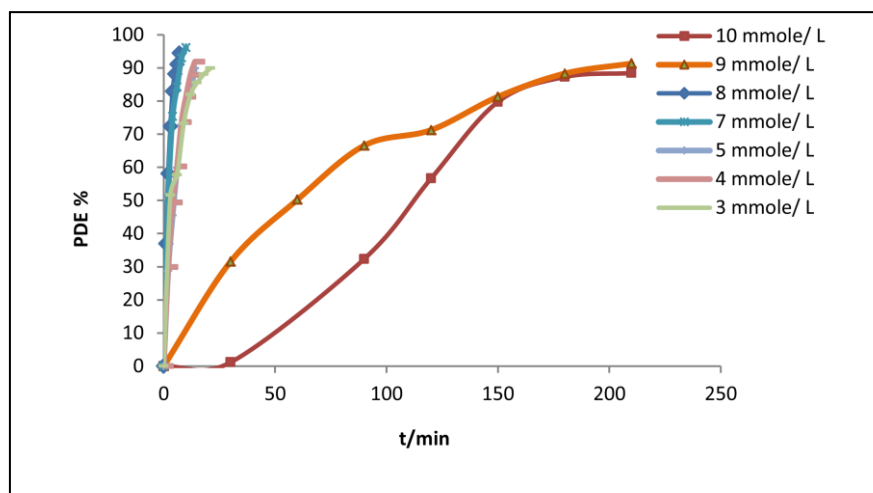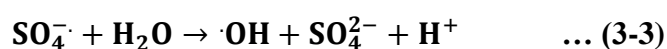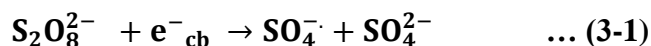

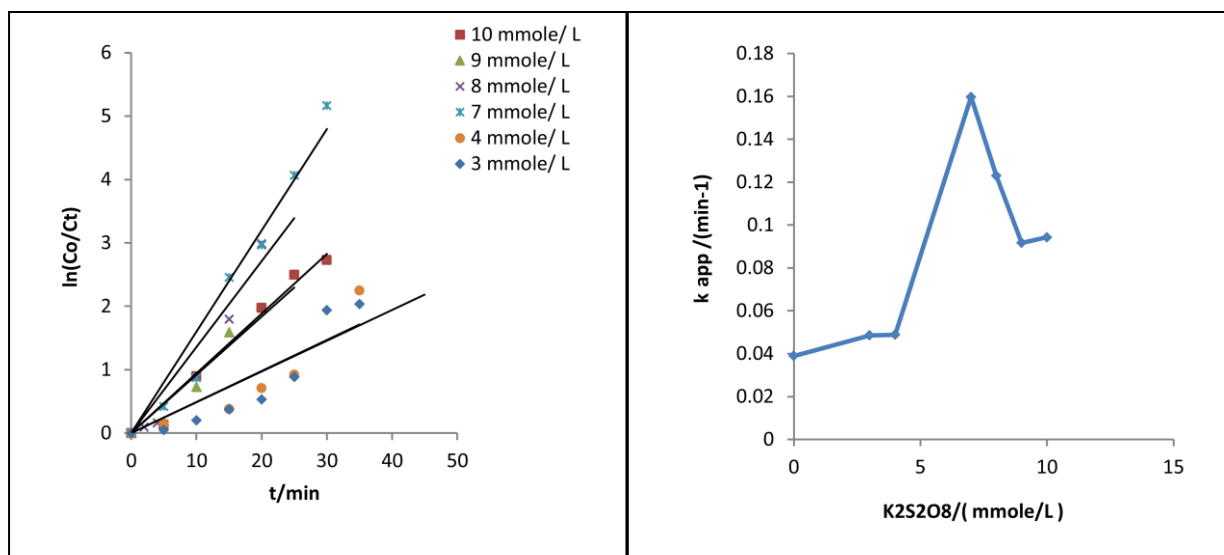Figure3-39: Effect of different additions $K_2S_2O_8$ for commercial ZnS on photodecolorization efficiency.

The used of oxidant agent like $K_2S_2O_8$ is plays a vital role to improve the rate of reaction and the efficiency percentage. The figures $3\text{-}38_{(a,b)}$ & 3-39 show, that the rate constant increases with increasing the concentration of $K_2S_2O_8$ and gives a maximum value equal to 8 mmole/L at 7 min with PDE % 94.471%. The raise in rate of reaction depended upon formed hydroxyl radical [102].

$$S_2O_8^{2-} + e^-{}_{cb} \rightarrow SO_4^{-\cdot} + SO_4^{2-} \qquad \text{... (3-1)}$$

$$SO_4^{-\cdot} + e^-{}_{cb} \rightarrow SO_4^{2-} \qquad \text{... (3-2)}$$

$$SO_4^{-\cdot} + H_2O \rightarrow {}\cdot OH + SO_4^{2-} + H^+ \qquad \text{... (3-3)}$$

While, with increasing of $K_2S_2O_8$, which leads to depress the rate of reaction due to the oxidant reagent acts as scavenger for hydroxyl radical [102].

$$SO_4^{2-} + h_{vb}^+ \rightarrow SO_4^{-\cdot} \qquad \text{... (3-4)}$$

$$SO_4^{2-} + {}\cdot OH \rightarrow SO_4^{-\cdot} + OH^- \qquad \text{... (3-5)}$$

3.7.4.2. Effect of addition $K_2S_2O_8$ on the solution dye for Cr :ZnS.

(a)   (b)

Figure 3-40: (a) The change of ln C_o/Ct with Irradiation time at different additions $K_2S_2O_8$ for Cr :ZnS . (b) Relationship between apparent rate constant and different additions $K_2S_2O_8$ for Cr :ZnS
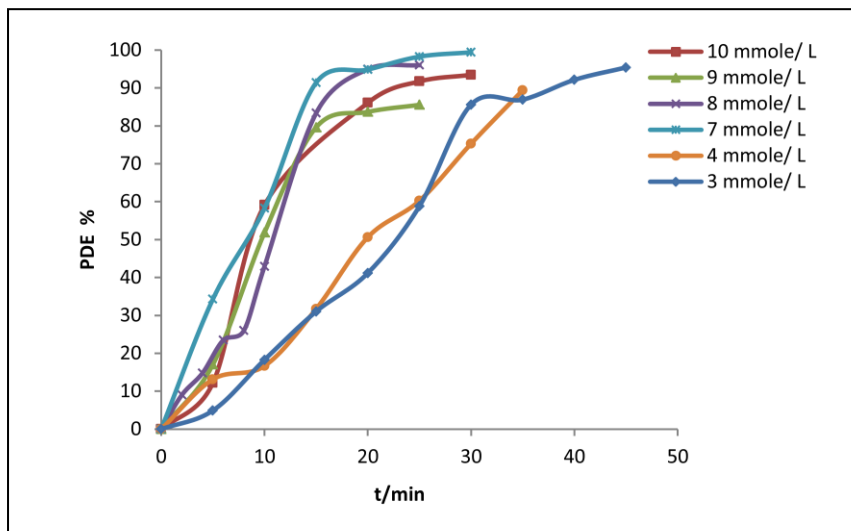
Figure 3-41: Effect of different additions K$_2$S$_2$O$_8$ for Cr:ZnS on photodecolorization efficiency.

3.7.4.3. Effect of addition K$_2$S$_2$O$_8$ on the solution dye for Mn:ZnS:Cr$_{(2)}$.

(a)   (b)

Figure 3-42: (a) The change of ln C$_o$/C$_t$ with Irradiation time at different additions K$_2$S$_2$O$_8$ for Mn:ZnS:Cr$_{(2)}$. (b) Relationship between apparent rate constant and different additions K$_2$S$_2$O$_8$ for Mn:ZnS:Cr$_{(2)}$.

Figure 3-43: Effect of different additions K$_2$S$_2$O$_8$ for Mn:ZnS:Cr$_{(2)}$

on photodecolorization efficiency.

3.7.4.4 Effect of addition K$_2$S$_2$O$_8$ on the solution dye for prepared ZnS.

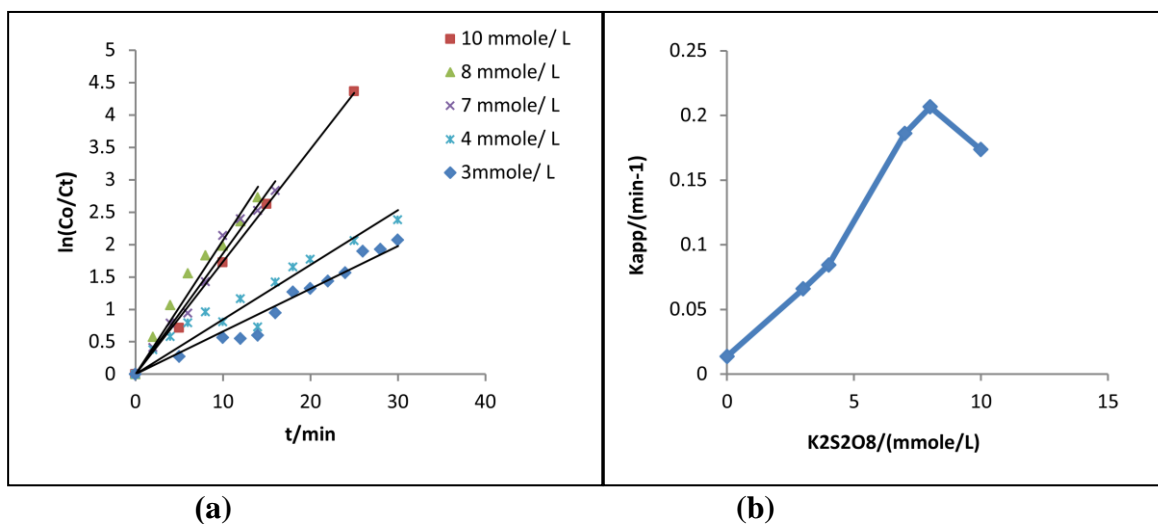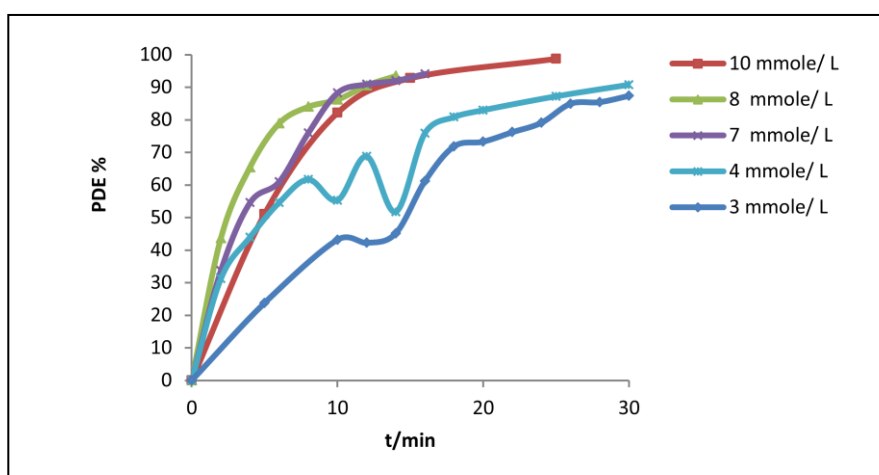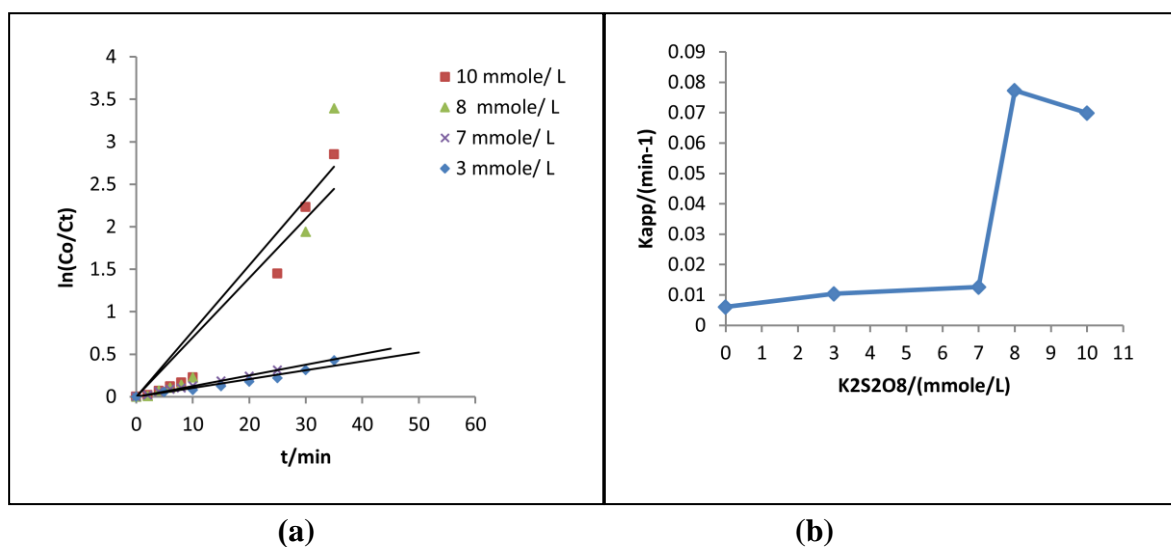**(a)**   **(b)**

Figure 3-44: (a) The change of ln C$_o$/C$_t$ with Irradiation time at different additions K$_2$S$_2$O$_8$ for prepared ZnS. (b) Relationship between apparent rate constant and different addition K$_2$S$_2$O$_8$ for prepared ZnS.
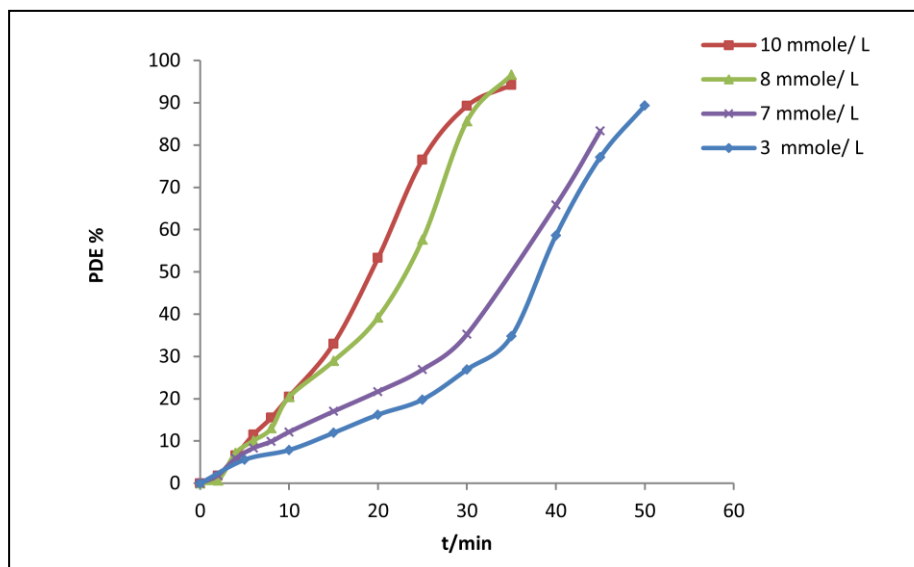
Figure 3-45: Effect of different additions K$_2$S$_2$O$_8$ for prepared ZnS

on photodecolorization efficiency.

The figures 3-40 (a,b)- 3-45 obtain that the best addition of oxidation agent are 7 mmole /L at 30 min, PDE% 99.428 %for Cr:ZnS nanopowder ,but 8 mmole /L at 14 min % PDE 93.450 % for Mn:ZnS:Cr$_{(2)}$ nanopowder and 8 mmole /L at 45 min PDE% 83.333% for prepared ZnS nanopowder.

CHAPTER FOUR
CONCLUSIONS AND RECOMMENDATIONS

4.1: Conclusions

The main conclusions in this work can be summarized to:

1. The photodecolorization of RB5 dye from aqueous solution by using commercial ZnS and the prepared samples was obeyed the pseudo first order.
2. All the prepared samples are having a nano size, that proved by XRD and AFM analysis.
3. XRD data were proved that the Cr & Mn are really loaded on prepared ZnS.
4. Atomic absorption analysis was indicated the loading Cr & Mn on prepared ZnS.
5. AFM images for all samples obtained the shapes for studied samples are semi-spherical and the particles sizes contain from 2.5-6 crystals.
6. Band gap for Cr: ZnS is more than the band gap for prepared ZnS, and equal to 3.572 eV and 3.558 eV respectively.
7. The dose of prepared photocatalysts that used to deoclorize RB5 dye are less amounts than that used by commertial ZnS.
8. The best pH for reaction is occurred at acidic medium 4.1 for commercial ZnS& prepared Cr:ZnS and the reactions for both are exothermic. While, the optimum pH for prepared Mn:ZnS:Cr $_{(2)}$ & prepared ZnS are 6.3 and the reactions for both are endothermic.
9. The best concentrations of oxidation agent ($K_2S_2O_8$) are ranged from 7 mmole/L to 8 mmole/L for all used samples, and the % PDE values increased in ranged from 83.333% to 99.428%.

4.2 Recommendations:

Future studies can be completed:

1. A study the loaded of other metals like Pt, Pd, Au and Ag on ZnS surface in different methods such as photodeposition, hydrothermal, and microwave method.
2. The BET analysis can be used to explore the properties of surface area and the EDX analysis can be employed to find out the amount of metals loaded on the surface.
3. Study the photo decolorization of these prepared samples with different type of dyes.

REFERENCES

References:

1. W. Xiaoning, J. Jia & Y. Wang, "Enhanced Photocatalytic-Electrolytic Degradation of Reactive Brilliant Red X-3B in The Presence of Water Jet Cavitation", *Ultrasonic Sonochemistry*, vol.23, no.1, 2015, pp. 93-99.

2. T. Robinson, G. McMullan, R. Marchant & P. Nigam, "Remediation of Dyes in Textiles Effluent: A critical Review on Current Treatment Technologies with A proposed Alternative", *Bioresource Technol,* vol. **77,** no.3, 2001, pp. 247-255.

3. E. K. Goharshadi, M. Karimi, M. Hadadian & H.A.Toupkanloo, "Photocatalytic Degradation of Reactive Black 5 Azo Dye by Zinc Sulfide Quantum Dots Prepared by A sonochemical Method", *Materials Science in Semiconductor Processing*, vol.16, no.4, 2013, pp.1109-1116.

4. K.V. Radha, V. Sridevi & K. Kalaivani, "Electrochemical Oxidation for The Treatment of Textile Industry Wastewater", *Bioresource Technology*, vol.100, no.2, 2009, pp.987-990.

5. S. A. Paul, S. K. Chavan & S. D. Khambe ,"Studies on Characterization of Textile Industrial Waste water in Solapur City", *International Journal of Chemical* Sciences, vol.10, no.2, 2012, pp.635-642.

6. D. Rajkumar, B.J. Song & J.G. Kim, "Electrochemical Degradation of Reactive Blue 19 in Chloride Medium for The Treatment of Textile Dyeing Wastewater with Identification of Intermediate Compounds", *Dyes Pigments,* vol.72, no.1, 2007, pp. 1-7.

7. G. N. P. Kumar & K. B. Sumangala, "Decolorization of Azo Dye Red 3BN by Bacteria", *International Research Journal of Biological Sciences*, vol.1, no.5, 2012, pp. 46-52.

8. A. K. Verma, R. R. Dash & P. Bhunia,"A review on Chemical Coagulation/Flocculation Technologies for Removal of Colour

from Textile Wastewaters", *Journal of environmental management*, vol. 93, no.1, 2012, pp.154-168.

9. S. Khan & A. Malik, "Environmental and Health Effects of Textile Industry Wastewater", *Environmental Deterioration and Human Health*, A. Malik, E. Grohmann, R.Akhtar (Ed.), ISBN:978-94-007-7889-4 Springer Dordrecht Heidelberg London New York Netherlands, 2014.P. 55-71.

10. L. Ahmad, S. W. Puasa & M. M. D. Zulkali, "Micellar-Enhanced Ultrafiltration for Removal of Reactive Dyes from an Aqueous Solution", *Desalination,* vol. 191, issue 1-3, 2006, pp. 153-161.

11. M.T. Amin, A. A. Alazba & M. Shafiq, "Adsorptive Removal of Reactive Black 5 from Wastewater Using Bentonite Clay: Isotherms, Kinetics and Thermodynamics", *Sustainability,* vol. 7, no.1, 2015, pp.15302-15318.

12. M. Farnane, H. Tounsadi, A. Machrouhi, A. Elhalil, F. Z.Mahjoubi‹M. Sadiq, M. Abdennouri, S. Qourzal & N. Barka," Dye removal from AqueousSolution by Raw Maize Corncob and H_3PO_4Activate Maize Corncob", *Journal of Water Reuse and Desalination*,vol.8,no.2,2018pp.214-
224.

13. M. S. Zuraida, C. R. Nurhaslina & H. Ku Halim, "Removal of Synthetic Dyes from Wastewater by Using Bacteria, Lactobacillus delbruckii ", *International Refereed Journal of Engineering and Science,* vol. 2, no. 5, 2013, pp. 01-07.

14. M. Shafiq, A.A. Alazba & M.T. Amin," Removal of Heavy Metals from Wastewater using Date Palm as a Biosorbent: A Comparative Review", *Sains Malaysiana,* vol.47*,* no.1,2018, pp.3549.

15. L. M. Ahmed, F.T. Tawfeeq, M. H. Abed Al-Ameer, K. Abed Al Hussein & A. R. Athaab, "Photo-degradation of Reactive Yellow 14 Dye (A Textile Dye) Employing ZnO as Photocatalyst", *Journal of Geoscience and Environment Protection*, vol. 4, no.1, 2016, pp. 34-44.

16. L. M. Ahmed, Q. M. Mahdi, F. S. Mahmoud, M. J. Mahammed & N. S. Ahmed, "Kinetic study for The Decolorization of

Dispersive Blue 26 dye from Suspension Solution of Commercial ZnO", *Journal of Kerbala University., the Fifth Scientific Conference of the College of Science University of Kerbala,* 2017, pp. 127-136.

17. B. A.Mahammed & L.M. Ahmed," Enhanced Photocatalytic Properties of Pure and Cr-Modified ZnS Powders Synthesized by Precipitation Method" „*Journalof Geoscience and Environment Protection* ,vol.5, no.1, 2017, pp.101-111.

18. R. M. Mohamed, N. M. Nanyan, N. Abdul Rahman, N. M. A. Kutty & A.H. Kassim, "Colour Removal of Reactive Dye from Textile Industrial Wastewater using Different Types of Coagulants ", *Asian Journal of Applied Sciences*, vol. 2 , no. 5, 2014, pp.650-657.

19. M. Qiu, J. Shou, P. Ren & K. Jiang, " A comparative Study of The Azo Dye Reactive Black 5 Degradation by UV/TiO_2 and Photo-Fenton Processes ", *Journal of Chemical and Pharmaceutical Research*, vol. 6, no. 7, 2014, pp. 2046-2051.

20. N. M. Hilal, "Treatment of Reactive Dyeing Wastewater by Different Advanced Oxidation Processes", *Der Chemica Sinica,* vol. 2, no. 4, 2011, pp. 262-273.

21. B. P. Dojčinović, G. M. Roglić, B. M. Obradović, M. M. Kuraica, T. B. Tosti, M. D. Marković & D. D. Manojlović, "Decolorization of Reactive Black 5 Using Adielectric Barrier Discharge in The presence of Inorganic Salts", *Journal of the Serbian Chemical Society,* vol. 77, no. 4, 2012, pp. 535–548.

22. C. R. Holkar, A. J. Jadhav, D. V. Pinjari, N. M. Mahamuni &A. B. Pandit, "A critical Review on Textile Wastewater Treatments: Possible Approaches", *Journal of environmental management* ,vol.182, no.1,2016, pp. 351-366. And references there in.

23. H. A. Begum, A. K. Mondal & T. Muslim,"Adsorptive Removal of Reactive Black 5 from Aqueous Solution Using Chitin Prepared from Shrimp Shells", *Journal Bangladesh Pharmaceutical*, vol.15, no.2, 2012, pp.145-152. And references there in.

24. S. Atalay & G. Ersöz, "Novel Catalysts in Advanced Oxidation of Organic Pollutants",1[st]ed., Springer International Publishing, AG Switzerland,2016, CH3:Advanced Oxidation Processes, P. 23-34.

25. A.S. Stasinakis,"Use of Selected Advanced Oxidation Processes (AOPs) for Wastewater treatment-a mini review"*, Global Nest Journal*, vol.10, no.3 , 2008, pp.376-385.

26. A. Asghar, A. A. Abdul Raman & W. M. A. W. Daud. "Advanced Oxidation Processes for in-Situ Production of Hydrogen Peroxide/Hydroxyl Radical for Textile Wastewater Treatment: A review", *Journal of cleaner production*, vol. 87, no.1, 2015, pp.826-838.

27. M. A. Hassaan & A. El Nemr, "Advanced Oxidation Processes for Textile Wastewater Treatment," *International Journal of Photochemistry and Photobiology* , vol.2, no.3, 2017, pp. 85-93. And references there in.

28. A. L. N. Mota , L. F . Albuquerque, L. T. C. Beltrame, O. Chiavone-Filho, A. Machulek Jr & C. A. O. Nascimento, "Advanced Oxidation Processes And Their Application In The Petroleum Industry: A Review", *Brazilian Journal of Petroleum and Ga*s, vol. 2, no. 3, pp. 122-142, 2008. And references there in.

29. R.C. Pawar & C. S. Lee*,"Heterogeneous Nanocomposite-photocatalysis for Water Purification*,1st ed., Elsevier, William Andrew, USA, 2015,CH1, p.3.

30. K. T. Al-Rasoul, I. M. Ibrahim, I. M. Ali & R.M.AL-Haddad, "Synthesis, Structure And Characterization Of ZnS Qds And Using It In PhotocatalyticReaction", *International Journal Science and Technology Research,*vol.3. ISSN 2277-8616, 2014, pp. 213-217. And references there in.

31. R.Ameta&S.C.Ameta,"Photocatalysis:Principlesand Applications,1[st]ed., CRC press, Boca Raton, 2017,CH1, p. 1.

32. A. Eyasu,O.P.Yadav & R. K. Bachheti,"Photocatalytic Degradation of Methyl Orange Dye Using Cr-Doped ZnS Nanoparticles Under visible radiation", *International Journal Science and Technology Research,*vol.5, no.4, 2013,pp. 1452-1461.

33. M. R. Khan, T. W. Chuan & A. Yousuf, "Schottky Barrier and Surface Plasmonic Resonance Phenomena Towards The Photocatalytic Reaction: Study of Their Mechanisms to Enhance Photocatalytic Activity", *Catalysis Science & Technology*, vol.5, no.5, 2015, pp.2522-2531.

34. D. Beydoun, R. Amal, G. Low & S. MC. Evoy,"Role of nanoparticles in photocataly-sis", *Journal of Nanoparticle Research*, vol.1, no.4, 1999, pp.439-458.

35. S. Wang, J. H. Yun, B. Luo, T. Butburee, P. Peerakiatkhajohn,S. Thawessak, M. Xiao &L. Wang, "Recent Progress on Visible Light Responsive Heterojunctions for Photocatalytic Applications", *Journal of Materials Science & Technology*, vol.33, no.1, 2017, pp. 1-22.

36. A. M. Smith & S. Nie, "Semiconductor Nanocrystals: Structure, Properties, and Band Gap Engineering", *Accounts of Chemical Research*, vol. 43, no.2 , 2010, pp. 190-200. And references there in.

37. L. Gu, V. Srot, W. Sigle, C. Koch, P. Van Aken & F. Scholz,"Band-gap Measurements of Direct and Indirect Semiconductors Using Monochromated Electrons", *Physical Review B*, vol. 75, no.19, 2007, pp.195-214.

38. M. Fujita, "Silicon Photonics: Nanocavity Brightens Silicon", *Nature Photonics*, vol.7, no.4, 2013, pp.264-265.

39. J. M. Herrmann, "Heterogeneous Photocatalysis: Fundamentals and Applications to The Removal of Various Types of Aqueous Pollutants", *Catalysis today*, vol. 53, no.1, 1999, pp.115-129.

40. S. Ahmed, M. G. Rasul, W. N. Martens, R. Brown & M. A. Hashib, "Heterogeneous Photocatalytic Degradation of Phenols in Wastewater: A review on Current Status and Developments", *Desalination*, vol.26, no.1(1), 2010, pp. 3-18.And references there in.

41. J. Ran, J. Zhang, J. Yu & M. Jaroniec,"Earth-abundant Cocatalysts for Semiconductor-based Photocatalytic Water Splitting", *Chemical Society Reviews*, vol.43, no.22, 2014, pp. 7787-7812.

42. U. Jabeen, S. M. Shah & S. U. Khan, "Photo Catalytic Degradation of Alizarin Red S Using ZnS and Cadmium Doped

ZnS Nanoparticles under Unfiltered Sunlight", *Surfaces and Interfaces*, vol. 6, 2017, pp.40-49. And references there in.

43. M. Hoffmann, S. Martin, W. Choi & D. Bahneman, "Environmental Applications of Semiconductor Photo Catalysis", *Chemical Reviews,* vol. 95, no.1,1995, pp. 69-96.

44. P. Sivakumar, G. G. Kumar& S. Renganathan, "Synthesis and characterization of ZnS-Ag nanoballs and its application in photocatalytic dye degradation under visible light", *Journal of Nanostructure in Chemistry*, vol. 4, no.107, 2014, pp.1-9.

45. L. M. Ahmed, I. Ivanova, F. H. Hussein & D. W. Bahnemann, "Role of Platinum Deposited on TiO2 in Photocatalytic Methanol Oxidation and Dehydrogen-ation Reactilces", International Journal of Photoenergy, vol.2014, no.1, 2014, pp. 1-9. And references there in.

46. B.Ohtani,"TitaniaPhotocatalysisbeyondRecombination:Acritical Review", *Catalysts*, vol. 3, no.4, 2013, pp.942-953.

47. Y. Liu, L. Guo, W. Yan & H. Liu, "A composite Visible –light Photocatalyst for Hydrogen Production", *Journal of power Sources*, vol. 159, no.1, 2006, pp. 1300-1304.

48. K. Priya,V. K. Ashith, G. K. Rao &G. Sanjeev,"A comparative Study of Structural, Optical and Electrical Properties of ZnS Thin Films Obtained by Thermal Evaporation and Silar techniques", *Ceramics International*, vol. 43,no.13, 2017, pp.10487-10493.And references there in.

49. K. P. Tiwary, S. K. Choubey & K. Sharma,"Structural and optical properties of ZnS Nanoparticles Synthesized by Microwave Irradiation method", *Chalcogenide Letters*, vol.10, no.9, 2013, pp. 319-23. And references there in.

50. H. Labiadh, B.Sellami, A.Khazi, W.Saidani & S.Khemais,"Optical Properties and Toxicity of Undoped and Mn-doped ZnS Semiconductor Nanoparticles Synthesized through The Aqueous Route", *Optical Materials*, vol. 64, 2017, pp. 179-186. And references there in

51. B. Bodo, D. Prakash & P. K. Kalita,"Synthesis and Characterization of ZnS: Mn Nanopartilces", *International Journal of Applied Physics and Mathematics*, vol 2, no.3, 2012, pp.181-183.

52. A. L. Donne, D. Cavalocli, R. A. Mereu & M. Perani, "Study of The Physical Properties of ZnS Thin Films Deposited by RF Sputtering," *Materials Science in Semiconductor Processing*, vol.71, 2017, pp. 7-11. And references there in.

53. N. Kaur, S. Kaur, J. Singh& M. Rawat,"A Review on Zinc Sulphide Nanoparticles: From Synthesis, Properties to Applications", *J Bioelectron Nanotechnol*, vol.1,no.1, 2016, pp.1-5. And references there in.

54. P. Weide, K.Schulz, S. Kaluza, M. Rohe& R. Beranek,"Controlling the Photocorrosion of Zinc Sulfide Nanoparticles in Water by Doping with Chloride and Cobalt Ions", *Langmuir*, vol. 32, no. 48 , 2016, pp.12641-12649. And references there in.

55. S. Ummartyotin & Y. Infahsaeng,"A comprehensive Review on ZnS: From Synthesis to An approach on Solar Cell", *Renewable and Sustainable Energy Reviews*, vol. 55, no.1 2016, pp. 17-24. And references there in.

56. X. Fang, T. Zhai, U. K. Gautam, L. Li, L. Wu &Y. Bando,"ZnS Nanostructures: From Synthesis to Applications", *Progress in Materials Science* ,vol.56, no.2, 2011, pp.175-287.

57. S. A. Feng, J. H. Zhao& Z. P. Zhu, "The Manufacture of Carbon Nanotubes Decorated with ZnS to Enhance the ZnS Photocatalytic Activity", *New Carbon Materials* , vol.23, no.3, 2008, pp.228-234.

58. D. Ayodhya, M.Venkatesham & A. S. Kumari,"Synthesis, Characterization of ZnS Nanoparticles by Coprecipitation Method Using Various Capping agents-Photocatalytic Activity and Kinetic Study", *Journal of Applied Chemistry*, vol. 6, no.1, 2013, pp.101-109. And references there in.

59. T. Sulistyaningsih, S. J. Santosa & D. Siswanta,"Synthesis and Characterization of Magnetites Obtained from Mechanically and Sonochemically Assissted Co-precipitation and Reverse Co-precipitation Methods", *International Journal of Materials, Mechanics and Manufacturing*, vol.5, no.1, 2017, pp.16-19.

60. C. S. S R. Kumer, Magnetic Nanomaterials, Challa, Nanomaterialsforlifesciece,1st ed.,WilyVCHVerlagGmbH&CoKG

aA,USA,2009,ISBN:978-3-527-32154-4,CH7:Core Magnetic Nanomaterials in medical Dianosis and Therapy, pp.260-261.

61. H. Kumar,S. P. Manisha & P. Sangwan ,"Synthesis and characterization of MnO_2 Nanoparticles Using Co-precipitation Technique", *International Journal of Chemical Engineering*, vol.3,no. 3, 2013, pp.60-155.

62. A. Ali, M. Z. H. Zafar, I.U.Haq, A. R. Phull, J. S. Ali & A. Hussain," Synthesis, Characterization, Applications, and Challenges of Iron Oxide Nanoparticles", *Nanotechnology, Science and Applications*, vol. 9, no.49, 2016, pp.49-67.

63. V. A. Basiuk & E. V. Basiuk,"Green processes for Nanotechnology", 1st ed., Springer, Switzerland, 2015, CH_3, P.77.

64. M. Králik,"Adsorption, Chemisorption, and Catalysis." *Chemical Papers*, vol.68, no. 12, 2014, pp.1625-1638.

65. S. Nethaji, A. Sivasamy & A. B. Mandal. "Adsorption Isotherms, Kinetics and Mechanism for The Adsorption of Cationic and Anionic Dyes onto Carbonaceous Particles Prepared from Juglans regia Shell Biomass", *International Journal of Environmental Science and Technology*, vol.10, no.2, 2013, pp.231-242.

66. J. J. Kipling ,"*Adsorption from Solutions of Non-electrolytes*,1st ed., Academic Press, London, 2017,CH1, pp.1-2

67. A. K. Bajpai & M. Rajpoot,"Adsorption Techniques - A review", *Journal of Scienctific & Industrials Research*, vol.58, no.11, 1999, pp.844-860.

68. V. Bolis, "Fundamentals in Adsorption at the Solid-gas Interface. Concepts and Thermodynamics", *Calorimetry and Thermal Methods in Catalysis*, A. Auroux(Ed), ISBN: 978-3-642-11953-8, Springer Berlin Heidelberg, 2013, pp. 3-50.

69. H. H. Schobert, Chemistry of Fossil Fuels and Biofuels, 1st ed., Cambridge, New York, Melbourne, 2013, ISBN :97,8-0-521-11400-4, pp.210-211.

70. R. Sajar," Essential Chemistry Xii",1st ed. Vptyagi, Virat Bhavne,India,2009, ISBN:978-81-8332-571-4.

71. M. Grätzel," Energy Resources through Photochemistry and Catalysis", 1sted., Academic Press, INC, London, 2012, CH 7, P.244.

72. F. H. Hussein, "Photochemical Treatments of Textile Industries Wastewater," *Asian Journal of Chemistry*, vol.24, no.12, 2012, pp.5427-5434.

73. F. Bebensee, F. Voigts & W. Maus-Friedrichs. "The Adsorption of Oxygen and Water on Ca and CaO Films Studied with MIES, UPS and XPS," *Surface Science,* vol. 602, no.9, 2008, pp. 1622-1630. And references there in.

74. R. Li, L. Wang, Q. Yue, H. Li, S. Xu & J. Liu, "Insights into The Adsorption of Oxygen and Water on Low-Index Pt Surfaces by Molecular Dynamics Simulations." *New Journal of Chemistry*, vol.38, no.2, 2014, pp. 683-692. And references there in.

75. W. Izydorczyk & B. Adamowicz, "Computer Analysis of Oxygen Adsorption at SnO," *Optica Applicata*, vol. 37, no.4, 2007, pp.378-385. And references there in.

76. X. Yu, X. Zhang, H. Wang & G. Feng, "High Coverage Water Adsorption on the CuO (111) Surface," *Applied Surface Science*, vol. 425, 2017, pp. 803-810. And references there in.

77. S.S. Zuafuani & L. M. Ahmed, "Photocatalytic Decolourization of Direct Orange Dye by Zinc Oxide under UV Irradiation," *International Journal of Chemical Sciences*, vol.13, no.1, 2015, pp.187-196. And references there in.

78. M. T. Yagub, T. K. Sen, S. Afroze & H. M. Ang,"Dye and Its Removal From Aqueous Solution by Adsorption: A review". *Advances in colloid and interface science*, vol.209, no.1, 2014, pp. 172-184. And references there in.

79. T. W. Seow & C. K. Lim, "Removal of Dye by Adsorption: A Review." *International Journal of Applied Engineering Research*, vol.11, no.4, 2016, pp. 2675-2679. And references there in.

80. S. K. Chinta & S. V. Kumar, "Technical Facts & Figures of Reactive Dyes Used in Textiles." *International Journal of Engineering and Management Sciences*, vol.4, no.3, 2013, pp. 308-312. And references there in.

81. G. Li, S. Park & B. E. Rittmann, "Degradation of Reactive Dyes in a Photocatalytic Circulating-bed Biofilm Reactor," *Biotechnology and Bioengineering*, vol.109, no.4, 2012, pp. 884-893. And references there in.

82. S. W. Puasa, M. S. Ruzitah & A. S. A. Sharifah,"Competitive Removal of Reactive Black 5/Reactive Orange 16 from Aqueous Solution via Micellar-Enhanced Ultrafiltration, " *International Journal of Chemical Engineering and Applications*, vol 3, no.5, 2012, pp. 354-358.

83. S. H. Lin & C. L. Lai, "Catalytic oxidation of Dye Wastewater by Metal Oxide Catalyst and Granular Activated Carbon", *Environment International*, vol. 25, no.1 1999, pp. 497-504. And references there in.

84. S. Alahiane, S. Qourzal, M. El Ouardi, A. Abaamrane & A. Assabbane, " Factors Influencing the Photocatalytic Degradation of Reactive Yellow 145 by TiO_2-Coated Non-Woven Fibers", *American Journal of Analytical Chemistry*, vol. 5, 2014, pp. 445-454. And references there in.

85. I. A. Bhatti, S. Adeel & M. Abbas, " Effect of Radiation on Textile Dyeing", Textile Dyeing, P. Hauser (Ed.), ISBN 978-953-307-565-5, InTech, CH 1, p.4, 2011.

86. A. I. Ahmed, "Texile Dyer and Printer-Reactive Dyes Development- A Review", *Technology of Textile Processing*, A. A. Shenai (Ed.), SEVAK Publications, Bombay, 400 031, 1995, pp. 19-24.

87. A. H. Mahvi, M. Ghanbarian, S. Nasseri & A. Khairi "Mineralization and Discoloration of Textile WasteWater By TiO_2 Nanoparticles", *Desalination*, vol. 239, 2009, pp. 309–316. And references there in.

88. T. Hadibarata, L. A. Adnan, A. R. M. Yusoff, A. Yuniarto, M. M. F. A. Zubir, A. B. Khudhair... &M.A. Naser ,"Microbial Decolorization of an Azo dye Reactive Black 5 Using White-Rot Fungus Pleurotus Eryngii F032. *Water, Air, & Soil Pollution*, vol. 224, no. 6, 2013, pp.1-9. And references there in.

89. M. Sagarika, N. Dafale & N. Neti Rao,"Microbial decolorization of reactive black-5 in a two-stage anaerobic–aerobic reactor

using acclimatized activated textile sludge", *Biodegradation*, vol.17, no.5, 2006, pp. 403-413.

90. F.H.Hussein, "Photochemical Treatments of Textile Industrie Wastewater", *Advances in Treating Textile Effluent*, Peter J. Hauser (Ed.), ISBN: 978-953-307-704-8, InTech, 2011.

91. M. Mashkour, A. Al-Kaim, L. Ahmed & F. Hussein, "Zinc Oxide Assisted Photocatalytic Decolorization of Reactive Red 2 Dye", *International Journal of Chemistry Science.,* vol. 9, no.3, 2011, pp. 969-979.

92. P. Iranmanesh, S.Saeednia, M. Nourzpoor ," Characterization of ZnS Nanoparticles synthesized by Co-precipitation Method",*Chinese Physics B,*vol.24,no.4,2015,pp. 046104.

93. C.S. Pathak, M.K. Mandal, V. Agarwala ,"Synthesis and Characterization of Zinc sulphide Nanoparticles prepared by Mechanochemicalroute",*SuperlatticesandMicrostructures*,vol.58, no.1,2013,pp.135-143.

94. A.Chandran, N.Francis, T.Jose & K. C. George,"Synthesis, Structural, Characterization and Optical Bandgap Determination of ZnS Nanoparticles",*SBCademic Review*,vol. XVII, No.1&2 ,2010, pp. 17-21.

95. K. Bera, S. Saha , P. C. Jana," Investigation of Structural and Electrical properties of ZnS and Mn doped ZnS nanoparticle", vol.5,no.1,2018, pp.6321–6328.

96. N. Shanmugam, S. Cholan, G. Viruthagiri, R. Gobi & N. Kannadasan, "Synthsis and Characterization of Ce[3+-]doped flower like ZnS nanorods",*Applied of Nanoscience*,vol.4, no.3,2014, pp 359–365.

97. R.C.Silvaa, Li. A. Silvaa, P. L. B. Araújoa, E.S. Araújoa, R. Francisca ,S.Santosa, K. A. S.Aquinoa, "ZnS Nanocrystals as an Additive for GammaIrradiatedPoly(VinylChloride)",*MaterialsResearch*vol.20 ,no.2,2017, pp.851-857.

98. S. Dilpazir, M. Siddiq & A. Iqbal," Synthesis of Zinc Sulphide Nanostructures by Co-precipitation: Effects of Doping on Electro-optical Properties", *Kenkyu Journal of Nanotechnology & Nanoscience*,vol.1,no.1,2015,pp. 34-39.

99. S. A. Sundar & N. J. John, "Synthesis and Studies on Structural and Optical Properties of Zinc Oxide and Manganesedoped Zinc Oxide Nanoparticles. *Nanosystems: Physics, Chemistry, Mathematics*, vol.7, no.6, 2016, pp.1024-1030.

100. X. Pan, I. Medina-Ramirez, R. Mernaughc & J. Liu, "Nano Characterization and Bactericidal Performance of Silver Modified Titania Photocatalyst," *Colloids and Surfaces B: Biointerfaces*, vol.77, no. 1, 2010, pp. 82-89.

101. M. Sugiyama, K. Fujii, and S. Nakamura, Eds., *Solar to Chemical Energy Conversion*. Springer, 2016.

102. S. Ahmed, "Photo Electrochemical Study of Ferrioxalate Actinometry at A glassy Carbon Electrode", *Journal of Photochemistry and Photobiology A: Chemistry*, vol. 161, no.2, 2004, pp. 151-154.

103. M. T. Eesa, A. M. Juda & L. M. Ahmed, " Thermodynamic and kinetic study for Photocatalytic Decolourization Of Light Green SF (Yellowish) Dye Using Commercial Bulk Titania and Commercial Nano Titania ", *International Journal of science and research*, vol. 5 , no. 11, 2016, pp. 1495-1500. And references there in.

104. R. G. Saratale, G. D. Saratale, J. S. Chang & S. P. Govindwar, "Ecofriendly Degradation of Sulfonated Diazo Dye C.I. Reactive Green 19A using Micrococcus Glutamicus NCIM-2168", *Bioresource Technology*, vol. 100, no. 17, 2009, pp. 3897-3905.

105. A. Giwa, P. O. Nkeonye, K. A. Bello, E. G. Kolawole & A. O. Campos," Solar Photocatalytic Degradation of Reactive Yellow 81 and Reactive Violet 1 in Aqueous Solution Containing Semiconductor Oxides, *International Journal of Applied*, vol.2, no.4, 2012, pp.90-105.

106. B. Sivasankar, "Engineering Chemistry",1st ed. ,Tata McGraw–Hill, New Delhi, 2008, CH6, P.196.

107. V. Stavila, J. Volponi, A. M. Katzenmeyer, M. C. Dixon & M. D. Allendorf ,"Kinetics and Mechanism of Metal-Organic Frame Work Thin Film Growth:Systematic Investigation of HKUST-1 Deposition on QCM Electrodes", *Chemical Science*, vol.3 , no.5, 2012, pp.1531-1540.

108. M. Doğan, M. H. Karaoğlu & M. Alkan, "Adsorption kinetics of maxilon yellow 4GL and maxilon red GRL dyes on kaolinite", *Journal of Hazardous Materials*,vol.165, no.1, 2009, pp. 1142-1151.

109. B.N. Paula, S. Chandaa, S. Dasa, P. Singha, B.K. Pandeya & S.S.Girib," Mineral Assay in Atomic Absorption Spectroscopy", *The Beats of Natural Sciences*,vol.1, no.4,2014,pp.1-17.

110. B. Barman & K. C. Sarma, "Synthesis And Optical Properties of ZnS Nanoparticles in PVA Matrix", *Optoelectronics And Advanced Materials – Rapid Communications*, vol. 4, no. 10, 2010, pp. 1594 – 1597.

111. S. Wang, S. B. Mirov, V. V. Fedorov & R. P. Camata, "Synthesis and spectroscopic properties of Cr doped ZnS crystalline thin films",*Proceedings of Spie*, vol. 5332, no.1, 2004, pp. 13-20.

112. A. N. Krasnov, J. P. Bender & W. Y. Kim, "Increase luminance of ZnS/Mn thin-film electroluminescent displays due to Ag Co-doping", *Thin Solid Films*, vol. 467, no .1,2004, pp. 247-252.

113. D. A. Reddy, G. Murali, R.P. Vijayalakshmi & B.K. Reddy, "Room-temperature ferromagnetism in EDTA capped Cr-doped ZnS nanoparticles", *Applid Physics American*.A, vol. 105, no.1, 2011, pp.119–124.

114. M. Bodke, H. Khawal, U. Gawai & B. Dole, "Synthesis and Characterization of Chromium Doped Zinc Sulfide Nanoparticles", *Open Access Library Journal,* vol.2, e1549, 2015, pp. 1-8.

115. K. Shameli, M.B. Jazayeri,S.D. Sedaghat, P. Jahangirian, H. Mahdavi, &M. Y.Abdollahi," Synthesis and Characterization of Polyethylene Glycol Mediated Silver Nanoparticles by the Green Method", *International Journal of Molecular Sciences*,vol.13, no.1, 2012, pp.6639-6650.

116. D. Ozkaya," Particle Size Analysis of Supported Platinum Catalysts by TEM", *Platinum Metals Rev*, vol. 52, no. 1, 2008, pp. 61–62.

117. Y. Shin, Y. Hwang, Y. Um, D. A. Tuan & S. Cho, ″Structural and Optical Properties of Polycrystalline NiO Thin Films

Prepared by Using the Oxidation of the Metallic Ni", *Journal of the Korean Physical Society,* vol.63, no.6, 2013, pp. 1199-1202.

118. R. Koole, E. Groeneveld, D. Vanmaekelbergh, A. Meijerink & C. D.M. Doneg, "Size Effects on Semiconductor Nanoparticles", Nanoparticles, workhorses of nanoscience, de Mello Donega (Ed.), Springer, 2014, ISBN: 978-662-44822-9.

119. H. Skriver & N. Rosengaard, "Surface Energy and Work Function of Elemental Metals", *The American Physical Phenomena*, vol. 46, no. 11, 1992, pp. 7157-7168. And references there in.

120. L.M. Ahmed ,S. I. Saaed, & A.A. Marhoon, " Effect of Oxidation Agents on Photo-Decolorization of Vitamin B_{12} in the Presence of ZnO/UV-A System", *Indonesian Journal of Chemistry,* vol.18, no.2, 2018,pp. 272 - 278.

121. M. T. Jaafar," UV-A Activated ZnO Mediated Photocatalytic Decolorization of Nigrosine (Acid Black 2) Dye in Aqueous Solution", *Journal of Geoscience and Environment Protection*, vol.5, no.1, 2017, pp.138-147.

الخلاصة

يتكون الجزء العملي لهذا العمل من ثلاثة اجزاء. تضمن **الجزء الاول** تحضير كبريتيد الخارصين النانوي ومعدنة سطحه بالمنغنيز والكروم كل على انفراد او معا بطريقة الترسيب المصاحب.

يتضمن **الجزء الثاني** التحقق من خواص كبريتيد الخارصين التجاري والمحضر. حيث استخدمت تقنية الامتصاص الذري اللهبي لتخمين كون الفلزات حملت ام لا على سطح ZnS المحضر. تم الاستفادة من نتائج XRD لحساب معدل الحجم البلوري باستخدام معادلة شرر، اذ وجد تسلسل قيم الحجوم البلورية لكل العينات يتبع التسلسل :

commercial ZnS > prepared ZnS > Mn:ZnS:Cr$_{(1)}$ > Mn:ZnS:Cr$_{(2)}$ > Cr:ZnS>
Mn:ZnS.

اشارت صور تحليل مجهر القوة الذرية الى كون اشكال النماذج المدروسة كانت شبه كرويه وكل جسيمة منها تحتوي تقريبا من 2.5 الى 6 بلورة. استعملت تقنية التفلور لقياس مقدار طاقة الفجوة للنماذج المدروسة، اذ وجد بان طاقة الفجوة تتناقص لأغلب النماذج مع زيادة معدل الحجم البلوري، اذ تقع قيمتها لكل العينات المدروسة ضمن مدى من3.260 الكترون. فولت الى 3.577 الكترون. فولت.

ركز **الجزء الثالث** على دراسة العوامل المختلفة المؤثرة على الازالة اللونية للصبغة الفعالة السوداء 5 من محلولها المائي بوجود العوامل الضوئية المساعدة المدروسة وتشمل العوامل المدروسة: نوع الفلزات ، وكمية العامل المساعد ، الدالة الحامضية الابتدائية للمحلول، درجة الحرارة، العامل المؤكسد (بيرسلفات البوتاسيوم).

وجد ان افضل معدنة تمت على سطح كبريتيد الخارصين المحضر باستخدام الكروم وعند استخدام مزيج من المنغنيز والكروم معا في المزيج الثاني. عينت افضل كمية من كبريتيد الخارصين التجاري و من كبريتيد الخارصين المحضر المجرد و من كبريتيد الخارصين الممعدن بالكروم و من كبريتيد الخارصين الممعدن بمزيج من الكروم والمنغنيز معا فكانت 2.5 غم/100 مليلتر، 1 غم/100 مليلتر، 1غم/100 مليلتر، 1.5 غم/100 مليلتر على التوالي. لعبت عملية استخدام الدالة الحامضية دور فعال في عملية تحسين الازالة اللونية للصبغة، ووجد ان اعلى سرعة للتفاعل عند دالة حامضية لمحاليل الصبغة المحفزة ضوئيا لكبريتيد الخارصين التجاري، وكبريتيد الخارصين المحضر المجرد، وكبريتيد الخارصين المحضر الممعدن بالكروم، وكبريتيد الخارصين المحضر الممعدن بالكروم والمنغنيز معا تساوي الى (6.3,4.1,6.3,4.1) على التوالي.

تم التحقق من تاثير درجة الحرارة ضمن المدى من 283.15 كلفن الى 303.15 كلفن. اذ اشارت النتائج ان قيم طاقات التنشيط لجميع العينات المدروسة تقع ضمن المدى من 13.420كيلوجول لكل مول الى 42.35 كيلوجول لكل مول. علاوة على ذلك فقد حسبت الدوال الثرموديناميكية مثل $ΔH^{#}$, و $ΔS^{#}$ و $ΔG^{#}$ لجميع العينات المدروسة، ووجد ان التفاعلات الضوئية باستخدام كبريتيد الخارصين التجاري وكبريتيد الخارصين المحضر الممعدن بالكروم هو باعث للحرارة، بينما يكون ماص للحرارة بحالة استخدام كبريتيد الخارصين المحضر وكبريتيد الخارصين المحضر والممعدن بمزيج من المنغنيز والكروم.

تعد عملية استخدام العامل المؤكسد مثل بيرسلفات البوتاسيوم مهم جدا في عملية زيادة سرعة التفاعل الضوئي وتقليل زمن التشعيع، لذا وجد ان افضل تركيز مستخدم من بيرسلفات البوتاسيوم يقع ضمن مدى من (7-8) ملي مول /لتر لكل النماذج المدروسة.

اللَّهُ نُورُ السَّمَاوَاتِ وَالْأَرْضِ ۚ مَثَلُ نُورِهِ كَمِشْكَاةٍ فِيهَا مِصْبَاحٌ ۖ الْمِصْبَاحُ فِي زُجَاجَةٍ ۖ الزُّجَاجَةُ كَأَنَّهَا كَوْكَبٌ دُرِّيٌّ يُوقَدُ مِن شَجَرَةٍ مُّبَارَكَةٍ زَيْتُونَةٍ لَّا شَرْقِيَّةٍ وَلَا غَرْبِيَّةٍ يَكَادُ زَيْتُهَا يُضِيءُ وَلَوْ لَمْ تَمْسَسْهُ نَارٌ ۚ نُّورٌ عَلَىٰ نُورٍ ۗ يَهْدِي اللَّهُ لِنُورِهِ مَن يَشَاءُ ۚ وَيَضْرِبُ اللَّهُ الْأَمْثَالَ لِلنَّاسِ ۗ وَاللَّهُ بِكُلِّ شَيْءٍ عَلِيمٌ

سورة النور آية (35)

تحضير وتشخيص الدقائق النانوية لكبريتيد الزنك/كبريتيد الزنك المشوب للتفكك الضوئي للأصباغ

رسالة مقدمة الى

مجلس كلية العلوم / جامعة كربلاء وهي جزء من متطلبات نيل درجة

الماجستير في الكيمياء

تقدمت بها

بدور علي محمد السماوي

بكالوريوس علوم كيمياء جامعة كربلاء/2005

بأشراف

أ. م. د. لمى مجيد أحمد

1439 هـ 2018 م